2013-ENAM-0044

École doctorale n° 432 : Sciences des Métiers de l'Ingénieur

Doctorat ParisTech
T H È S E

pour obtenir le grade de docteur délivré par

l'École Nationale Supérieure d'Arts et Métiers

Spécialité "Génie mécanique – procédés de fabrication"

présentée et soutenue publiquement par

Anna DUPLEIX

le 13 décembre 2013

Faisabilité du déroulage du bois assisté par infrarouge.

Feasibility of wood peeling assisted by infrared.

Directeurs de thèse : **Jean-Christophe BATSALE, Mark HUGHES**

Jury
Mme Dominique BAILLIS-DOERMANN, Professeur, LaMCoS, INSA, Lyon — Présidente
M. Bernard THIBAUT, Directeur de recherche émérite, CNRS, LMGC, Montpellier — Rapporteur
M. Róbert NÉMETH, Professor, Institute of Wood Science, University of West Hungary, Sopron — Rapporteur
M. Jean-Christophe BATSALE, Professeur, I2M, Arts et Metiers ParisTech, Bordeaux — Examinateur
M. Mark HUGHES, Professor, Dept of Forest Products Technology, Aalto University, Finland — Examinateur
M. Patrick ECHEGUT, Directeur de recherche, CNRS, CEMHTI, Orléans — Examinateur
M. Louis-Etienne DENAUD, MCF, LaBoMaP, Arts et Metiers ParisTech, Cluny — Examinateur
M. Eero KONTTURI, Doctor, Dept of Forest Products Technology, Aalto University, Finland — Examinateur
M. Andrzej KUSIAK, MCF, I2M, Université de Bordeaux 1 — Invité
M. Fréderic ROSSI, MCF, LaBoMaP, Arts et Metiers ParisTech, Cluny — Invité

Arts et Métiers ParisTech - Centre de Cluny
LaBoMaP

T
H
È
S
E

Abstract

  'Peeling' is the process of converting a log into a continuous thin (from 0.6 to more than 3 mm) ribbon of green wood termed 'veneer' whose production plays an important role in the manufacture of light-weight packaging, plywood and Laminated Veneer Lumber (LVL) which are amongst the most widely used wood products. Prior to peeling, the round green-wood of most species needs to be heated to temperatures ranging from 30 to 90°C in order to soften the wood and ease cutting. Forming part of a broader programme to develop a system that could be embedded on a peeling lathe, the goal of this PhD thesis was to investigate the technological feasibility of using infrared (IR) to heat green logs and so circumvent many of the economic and environmental disadvantages arising from soaking. The main output of this study was to demonstrate that the penetration depth of IR into green wood is limited to several tens of micrometres and that heat transfers into green wood up to the cutting plane (located several millimetres underneath the surface) is by conduction, which is slow due to the insulating properties of wood. Heating green wood with IR radiation is therefore unsuitable for the high peeling rates currently in use in the industry.

Résumé

  Le déroulage permet de transformer un billon en un ruban continu de bois vert (de 0.6 à plus de 3 mm d'épaisseur) appelé « placage » dont la production joue un rôle important car les placages servent de base à un grand nombre de produits industriels parmi les plus utilisés dans l'industrie du bois (Laminated Veneer Lumber (LVL), contreplaqués, emballages légers, etc.). Pour certaines essences, ce procédé exige un prétraitement, appelé « étuvage » qui consiste à chauffer au préalable le bois vert (saturé en eau) par immersion dans l'eau ou dans la vapeur d'eau chaude (de 30 à 90°C) afin de lui conférer une déformabilité remarquable et faciliter la coupe. Cette pratique présente cependant de nombreux inconvénients industriels et environnementaux. Cette étude vise à remplacer les pratiques d'étuvage par une technologie de chauffe par rayonnement infrarouge (IR) embarquée sur les machines de production. L'apport majeur de cette étude est d'avoir démontré que la pénétration des rayonnements IR dans le bois se limite à quelques dizaines de micromètres. La propagation de la chaleur jusqu'au plan de coupe situé à quelques millimètres sous la surface s'effectue donc par conduction, mode de transfert de chaleur lent dans le cas du bois aux propriétés isolantes remarquables. La chauffe embarquée faisant appel aux IR semble donc inadaptée face aux cadences de déroulage imposées par les industriels.

Préface

Ce document est le résumé d'un travail de recherche débuté en octobre 2010 sous la supervision de Mark Hughes, Rémy Marchal, Jean-Christophe Batsale et encadré par Louis-Etienne Denaud, Andrzej Kusiak et Fréderic Rossi.

Ils m'ont permis de conduire ce travail comme je l'entendais. Je les remercie chaleureusement.

Ce travail a été mené au sein des laboratoires de recherche du Department of Forest Products Technology - School of Chemical Technology de l'Université d'Aalto en Finlande et du LaBoMaP (Laboratoire Bourguignon des Matériaux et Procédés) à Cluny, dans le cadre d'une cotutelle de thèse entre l'Université d'Aalto et l'ENSAM (Ecole Nationale Supérieure d'Arts et Métiers) ainsi qu'au sein des laboratoires I2M (Institut de Mécanique et d'Ingénierie) de Bordeaux et CEMHTI (Conditions Extrêmes et Matériaux : Haute Température et Irradiation) d'Orléans.

Ces travaux de recherche ont été menés en vue des cinq articles qui composent cette thèse.

Ce projet est la réalisation collective de différentes équipes de recherche, et en particulier de:

Fabrice, Jean, Jean-Claude, Laurent, Louis, Michael, Rémy, Robert et Simon ;

Andrzej et Jean-Christophe ;

Domingos et Patrick.

Certains résultats présentés sont également issus du travail de :

Guillaume, Hannu, Olivier, Madeleine, Sid'Ahmed, Tiina et Timo.

Je souhaite remercier les membres des équipes administratives qui permettent la vie quotidienne au sein des laboratoires qui m'ont accueilli et

Octobre 2010.

Assise sur les marches de l'école en face du cinéma de Cluny, je m'apprêtais à reprendre la route sans me présenter à l'ENSAM où l'on m'attendait pour y discuter d'un projet de thèse. Je remercie Lucas et Maman pour m'avoir persuadé au téléphone de me rendre à l'entretien.

Réaliser une thèse était alors un rêve et un défi qui clôturait un parcours entamé en classes préparatoires aux lycées Sainte-Geneviève, Faidherbe et Joffre, et poursuivi à l'école Centrale et à l'Université d'Aalto. Je remercie toutes les personnes qui ont facilité mon apprentissage lors de ces années d'études, et auparavant. Je remercie aussi les personnes qui, au cours de mes premières années de vie professionnelle, m'ont invité à faire de la recherche et à découvrir le matériau bois. En particulier, je pense à Jean-François, Matthieu, Patrick de l'AFTBM (Association Forêt Bois Trièves Matheysine) et Pierre de l'Université d'Auckland ainsi qu'à François et aux entreprises Baufritz et Bouygues.

J'envisageai la thèse comme une construction commune au sein de laquelle j'appréciai assembler les idées et expertises de chacun. C'est animée d'un sentiment d'urgence et rarement sereinement que j'ai mené ce travail. Aujourd'hui, il en serait sans doute tout autrement. Ces travaux de recherche auront donc été particulièrement enrichissants et constructifs - au-delà d'une meilleure compréhension des phénomènes physiques mis en jeu lors de la chauffe infrarouge du bois vert déroulé.

Bien des questions se sont posées au cours de ces trois dernières années sur le plan professionnel mais aussi et tout autant sur le plan personnel. La présence rassurante d'un certain nombre de personnes et la richesse de nos échanges m'ont beaucoup aidée et me permettent aujourd'hui de terminer ce travail. Je pense tout particulièrement à :

Bonne ;

Alexandra, Alp, Annaig, Anne, Antoine, Ariane, Betty, Camille, Catherine, Cécile, Céline, Christine, Emmanuel, Erkki, Etty, Helena, Irma, les jardiniers de l'APSH 34, Jacquot, Jacqueline, Karin, Kristina, Liina, Lucas, Lucie, Maimouna, Maman, Manu, Marion, Michel, Michelle, Minna, Mireille, Monique, Myriam, Nolwenn, Olivier, Outi, Papa, Pascale, Patrick, Pauline, Pierre, Rém, Renaud, Sampsa, Seija, Stéphanie, Stevan, Suvi, Sylvie, Tan, Timo, Tom, Véronique, Viet-Anh et Yannick.

et aux personnes croisées ici et là, récemment et il y a plus longtemps.

J'aimerais pouvoir partager les fruits de ce travail avec chacun.

Novembre 2013.

Preface

The following document sums up research work that started in October 2010 under the supervision of Mark Hughes, Rémy Marchal, Jean-Christophe Batsale and lead by Louis-Etienne Denaud, Andrzej Kusiak and Fréderic Rossi.

They enabled me to conduct this research the way I intended. A warm thank you goes to each and all of them.

This thesis took place at the research labs of the Department of Forest Products Technology - School of Chemical Technology of Aalto University in Finland and LaBoMaP (Laboratoire Bourguignon des Matériaux et Procédés) in Cluny, France, and is a cotutelle between Aalto University and ENSAM (Ecole Nationale Supérieure d'Arts et Métiers). Also, parts of the research work took place at the I2M (Institut de Mécanique et d'Ingénierie) labs in Bordeaux, France and at the CEMHTI (Conditions Extrêmes et Matériaux : Haute Température et Irradiation) labs in Orléans, France.

This research work has been conducted in view of the five publications of which composed this thesis.

The overall project is the result of a collective effort from various research teams and I would like to thank the following people in that respect:

Fabrice, Jean, Jean-Claude, Laurent, Louis, Michael, Rémy, Robert and Simon;

Andrzej and Jean-Christophe;

Domingos and Patrick.

Some of the results and obervations presented here are based on the work of:

Guillaume, Hannu, Olivier, Madeleine, Sid'Ahmed, Tiina and Timo.

I wish to thank also:

October 2010

I was then sitting on the school steps facing the movie theater in Cluny, questioning whether or not to attend a meeting in ENSAM concerning a project of doctoral thesis. I wish to thank Mum and Lucas for talking me over the phone into attending the first interview.

At that time, doing a doctorate was a dream for me and a challenge which concludes an education started in preparatory classes in Sainte-Geneviève, Faidherbe and Joffre high schools, and continued in Ecole Centrale and Aalto University. I wish to thank all the people who were directly or indirectly involved in my apprenticeship during these school years and before. I also wish to thank the people and companies who invited me to take part in research and made me discover wood material, namely Jean-François, Matthieu, Patrick from the AFTBM (Association Forêt Bois Trièves Matheysine), Pierre from Auckland University in New Zealand as well as François and Baufritz and Bouygues companies.

I considered this thesis to be a joint construction in which I liked to organise everyone's ideas and expertise. It is with a sense of emergency and rarely with serenity that I conducted this study. Today, it would no doubt be different. This thesis has been a very rewarding and constructive time - beyond the better understanding of the physical phenomena at stake during infrared heating of green wood achieved through this research,

Many questions were raised during those three years, professionally as well as personally. The reassuring presence of many people and the fruitful interactions we have had empowered me to complete the present body of work. Namely:

Bonne ;

Alexandra, Alp, Annaig, Anne, Antoine, Ariane, Betty, Camille, Catherine, Cécile, Céline, Christine, Emmanuel, Erkki, Etty, Helena, Irma, les jardiniers de l'APSH 34, Jacquot, Jacqueline, Karin, Kristina, Liina, Lucas, Lucie, Maimouna, Maman, Manu, Marion, Michel, Michelle, Minna, Mireille, Monique, Myriam, Nolwenn, Olivier, Outi, Papa, Pascale, Patrick, Pauline, Pierre, Rém, Renaud, Sampsa, Seija, Stéphanie, Stevan, Suvi, Sylvie, Tan, Timo, Tom, Véronique, Viet-Anh et Yannick.

and the people met here and there, recently or a longer time ago.

I would like to share the result of this work among all the people mentioned above.

November 2013.

List of publications

This thesis consists of an overview of the following five publications, which from here on are referred to as Roman numerals in the text:

I   Dupleix A., Denaud L., Bléron L., Marchal R., Hughes M. (2013) The effect of log heating temperature on the peeling process and veneer quality: beech, birch and spruce case studies. *Eur J Wood Prod **71(2)***, 163-171, DOI 10.1007/s00107-012-0656-1.

II Dupleix A., De Sousa Meneses D., Hughes M., Marchal R. (2012) Mid infrared absorption properties of green wood. *Wood Sci Technol **47(6)***, 1231-1241, DOI 10.1007/s00226-013-0572-5.

III Dupleix A., Kusiak A., Hughes M., Rossi F. (2012) Measuring the thermal properties of green wood by the transient plane source (TPS) technique. *Holzforschung **67(4)***, 437-445, DOI 10.1515/hf-2012-0125.

IV Dupleix A., Ould Ahmedou S.-A., Bléron L., Rossi F., Hughes M. (2012) Rational production of veneer by IR-heating of green wood during peeling: Modeling experiments. *Holzforschung **67(1)***, 53-58, DOI 10.1515/hf-2012-0005.

V   Dupleix A., Batsale J.C., Kusiak A., Hughes M., Denaud L. (2013) Experimental validation of green wood peeling assisted by IR heating – some analytical considerations for system design. Submitted.

Author's contribution

I   AD carried out the literature review, executed the experimental plan and wrote the whole manuscript with comments from the co-authors. The design of the experimental plan and interpretation of the results was carried out in collaboration with Rémy Marchal, Louis Denaud and Laurent Bléron.

II   AD carried out the literature review, processed the samples and designed the experimental plan with Rémy Marchal, carried out the experiments with the technical help of Domingos De Sousa Meneses, analysed the results with Domingos De Sousa Meneses and wrote the whole manuscript with the careful review of all co-authors. Figures were designed in collaboration with Domingos De Sousa Meneses.

III   AD was responsible of manufacturing and testing the samples investigated, and writing the manuscript. Interpreting the results was done in collaboration with Andrzej Kusiak.

IV   AD was responsible for running the numerical simulation according to the research needs and interpreting the results with the co-authors. The article manuscript was written in collaboration with Sid'Ahmed Ould'Ahmedou, who designed the numerical model.

V   AD processed the samples, designed the experimental plan with Mark Hughes, wrote the manuscript and interpreted the results with Andrzej Kusiak and Jean-Christophe Batsale.

List of abbreviations and symbols

A	absorptivity
Ac	additional coefficient to take the energy lost during the wetting of the cell wall into account
Amb	ambient spectra
Bp	pressure bar
c	specific heat
c_{water}	specific heat of water
C	heat capacity
CD_i	checking depth of check i
CF	checking frequency
CI	Checking Index
CIn_i	checking interval between checks i and i+1
COV	Coefficient Of Variation
CR	radial heat capacity
CR_i	Checking Ratio for check i
CT	tangential heat capacity
d	depth
D	bolt diameter
e_{nom}	nominal veneer thickness
erfc	complementary error function
E_R	reflected flux

E_T	transmitted flux
f.s.p	fibre saturation point
h	heat transfer coefficient
H	Heaviside function
IR	infrared
L	wavelength
LVL	Laminated Veneer Lumber
m_f	mass of the sample after heating
m_i	mass of the sample before heating
m_{od}	mass of the oven-dried sample
M	reference spectra
MC	moisture content
MC_f	moisture content after heating
MC_i	moisture content before heating
n	vector normal to the boundary
q	IR source heat flux
q_{est}	estimated heat flux
q_{mes}	measured heat flux
R	reflectance
R^2	coefficient of determination
t	time
t_h	heating time
s	peeling speed
SMOF	Système de Mesure de l'Ouverture des Fissures
t	time
t_h	heating time
T	bolt temperature

T_d	temperature attained at depth d
T_{ext}	IR source temperature
Tg	glass transition temperature
T_{init}	initial bolt temperature
Tr	transmittance
T_{surf}	surface temperature
THS	Transient Hot Strip
THW	Transient Hot Wire
TPS	Transient Plane Source
x	arc surface of the log subjected to external infrared heating
x_i	position of the lathe check along the veneer length
Xk	vertical effort applied on the cutting knife
Yk	horizontal effort applied on the cutting knife
α_{surf}^{anal}	analytical values of slopes
α_{surf}^{simul}	numerical values of slopes
ΔMC	difference of MC before and after heating
ε	emissivity of the wood surface
κ	thermal diffusivity
κR	radial thermal diffusivity
κT	tangential thermal diffusivity
λ	thermal conductivity
λ_{air}	thermal conductivity of air
λR	radial thermal conductivity
λT	tangential thermal conductivity
λ_{water}	thermal conductivity of water

ρ   wood density

σ   wavenumber

Table of contents

1. Introduction

In the wood-products industry, 'peeling' is the process of converting a log into a continuous thin ribbon of green wood termed veneer. In this process, the log, or 'bolt', rotates about its longitudinal axis on a lathe, whilst the peeling knife and pressure bar are driven forward and placed in tangential contact with the bolt surface (Fig. 1). The rotation speed of the bolt increases continuously with decreasing bolt radius so as to generate veneer at a constant linear speed at the output of the peeling lathe. Industrial peeling speeds, s, range from 1 to 5 m.s^{-1}.
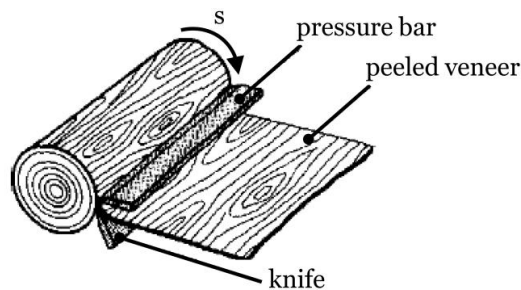
Figure 1 Principle of a rotary peeling lathe

The production of veneer plays an important role in the wood-products industry because plywood and Laminated Veneer Lumber (LVL), which are two of the most widely used Engineered Wood Products, are manufactured from veneers glued and pressed together, with the adjacent plies having their wood grain either crossed at right angles, as in the case of plywood or parallel, as in the case of LVL. Peeling is also widely used to produce material for light weight packaging. Peeling is one of the first steps in the plywood or LVL manufacturing chain, preceded by soaking, debarking and cut-off sawing, and followed by veneer drying, glue spreading, cross-cutting and pressing (Fig. 4a). In the case of almost all hardwood and softwood species it is necessary to heat the green wood prior to peeling in order to 'soften' the wood material for successful veneer production. The purposes

of heating and the physical mechanisms behind it will be reviewed in Section 2.1.1. Industrially, the heating of green wood prior to peeling has traditionally been accomplished by soaking - immersing the whole logs in hot water basins - or by steaming them in vats. In both processes, water, as an integral part of wood, makes an ideal medium for heat transfer into green wood. In the preparation of wood prior to peeling, most of the positive effects resulting from soaking (expressed with ⊕ signs in Fig. 2) come from the action of heating it whilst the utilisation of hot water is a major source of negative effects (expressed with ⊖ signs in Fig. 2).
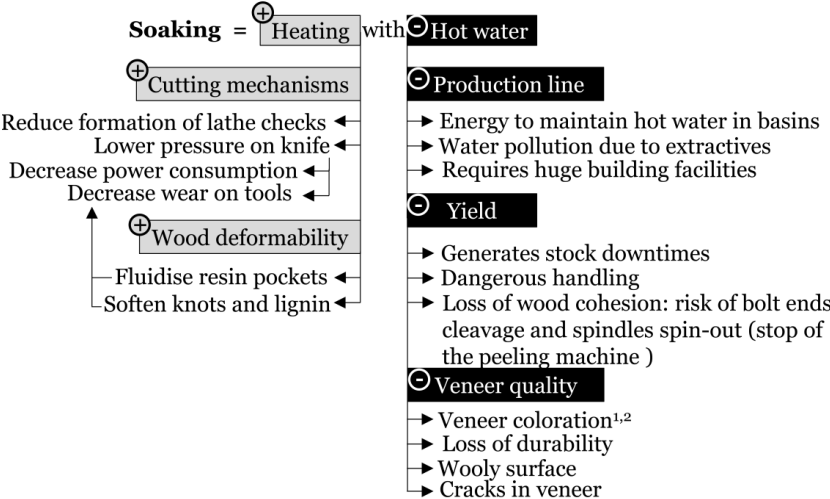
Figure 2 The pros and cons of soaking

The positive and negative effects of soaking detailed below are classified according to their impacts on (1) the production line, (2) yield and (3) veneer quality.

  (1) Soaking increases complexity in the production line for three main reasons. Firstly, soaking is energetically demanding: the energy costs of soaking are high because immersing the whole bolt in hot water for long enough to ensure heat penetration into wood involves significant amounts of water and energy.

  In addition, soaking basins are responsible for considerable energy losses because they are generally located outside and are badly insulated (often with just a tarpaulin to cover them), they can be sources of water leakages

---

[1] Veneer coloration can also be a sought after effect for certain wood species as explained later in this section.

[2] Both heat and the use of hot water are responsible for veneer coloration.

and they are made out of concrete which is a resistant, but poor, insulating material (Fig. 3). Secondly, soaking generates water pollution: during soaking, wood liberates large amounts of phenolic extractives responsible for water pollution. This is particularly true for certain wood species such as oak (Svoradova et al. 2004). In most European countries, ever tighter regulation requires that treatment plants are usually necessary to clean up contaminated water. These expensive water treatment procedures in the post-production phase add extra cost to the soaking process. In Australia, the government, facing severe water supply and water pollution problems, has forbidden the use of water for log soaking, preferring the use of steaming which does not necessitate any post-treatment of water (personal communication). Thirdly, soaking requires substantial building facilities: large-scale soaking basins need a large footprint, which is costly.

Figure 3 Large-scale soaking basins sources of leakage in Bois Déroulés de l'Auxois, France

(2) Soaking impacts negatively on yield for three main reasons. Firstly, soaking generates stock downtimes: being a good insulating material, wood requires a long time (several hours or days) to ensure heat transfer through to the core. This, added to the time necessary for heating-up the soaking water to the required temperature, causes costly stock downtimes and makes the logistics more complex. Consequently, soaking (compared to the high production rates of the peeling machines) is a bottleneck when the producer has to be able to react quickly to respond to specific clients' needs. In order to speed up the soaking process, manufacturers frequently increase the soaking water temperature. However, this practice can lead to the heterogeneous heating of the different parts of wood, creating temperature gradients within the bolt that can, as will be explained below, be detrimental to veneer quality. Secondly, soaking necessitates sophisticated handling: handling the bolts out of the soaking basin to the peeling machine is dangerous for the operators. Thirdly, soaking lowers wood cohesion: with the whole bolt being immersed, the bolt ends are also affected by heat and water. Being 'softened', the bolt ends can cleave on

contact with the spindles of the peeling lathe leading to the fracture of the bolt and finally to the stoppage of the peeling process.

(3) Soaking could impact negatively on veneer quality for three reasons. Firstly, soaking can lead to colour change in the veneer in both a positive way (soaking turns birch veneers lighter and more valuable) as well as in a negative way (soaking results in a non-uniform pink colour in beech veneers whereas its light natural colour is valuable). Secondly, in certain wood species such as oak and chestnut, which have a high extractive content, soaking could lead to a loss in durability. By removing wood extractives, soaking can produce veneers with reduced durability off-setting the efforts of foresters and the forest industry to select, improve and harvest naturally durable species with high amounts of extractives (Svoradova et al. 2004). Thirdly, certain species such as Douglas-fir have rather heterogeneous structures and in these, soaking heats the wood non-uniformly. As a result of differences in density and moisture content (MC) (Mothe et al. 2000), different parts of the log have different thermal properties and as such heat at different rates. In such species, soaking leads to different temperatures in the different parts of the log and it means that the log is peeled at different temperatures - the sapwood is overheated and the heartwood is under-heated in the same peeling log - which causes problems. Overheating the sapwood increases surface roughness, creating a 'woolly' surface, whilst under-heating the heartwood results in the generation of significant lathe checking and tearing of the fibres. This problem of non-uniform heating is emphasised all the more in industrial practices which tend to increase soaking water temperature to speed up the soaking process but which can create temperature gradients within the log. For these species, it is necessary to find techniques to heat the wood more homogeneously. Fourthly, soaking can create cracks in the veneers: by releasing growth strains in wood due to hygrothermal recovery, soaking creates irreversible heart-checks in bolts which are responsible for cracks in the veneer (Thibaut et al. 1995, Gril et al. 1993). Commercially, these cracked veneers are rejected.

1.1. Background

In addition to the numerous disadvantages of soaking, two other reasons have stimulated the search for an alternative solution to heating green wood prior to peeling it. Firstly, in the case of Douglas-fir at least, it is inappropriate to soak it. The MC of green Douglas-fir heartwood is around Fiber Saturation Point (f.s.p) with no free water available to serve as a heat transfer medium and since Douglas-fir is difficult to impregnate, it

necessitates long soaking times (Mothe et al. 2000). Secondly, the contention, supported by many manufacturers, that soaking is a 'cooking' process which requires a long time for the wood to soften (Lutz 1960) has recently been challenged by researchers in the wood micromechanics community with the results from experiments on the electric ohmic heating of wood. In forcing an electric current through the whole bolt which, acting like a resistor heats up (the Joule effect), researchers have demonstrated that the sought 'softening' of green wood does not depend on the heating duration but only on the cell wall temperature (Gaudillière 2003). The understanding that veneer quality might be the same at heating rates significantly higher than those that could be obtained by soaking, pointed towards the feasibility of a more rapid method of log heating which might be directly embedded onto the peeling lathe. Feasibly, this alternative to soaking might be achieved by using radiation instead of conduction to transfer heat within wood. The first trials employed microwave heating which could heat up the whole volume of the log at a heating rate of $2°C.s^{-1}$ and confirmed that the 'softening' effect does not depend on the heating time (Torgovnikov and Vinden 2010, Coste and De Bevy 2005). However, microwave technology necessitating covered waveguides makes it relatively complex to embed within the peeling process. Moreover, in order to speed up heating, another debate began concerning whether it was necessary to bring the whole volume of the bolt to the required heating temperature. Theoretically, a promising solution would be to locally heat the bolt's surface just ahead of the knife and to the depth of the cutting plane - to a depth equal to that of the thickness of the veneer produced (Marchal and Collet 2000). Such surface heating would be beneficial for two main reasons: (1) surface heating avoids the risk of heart-checks which appear in volume heating due to hygrothermal recovery, (2) surface heating can be appropriately dosed and only activated when peeling heartwood: this enables the saving of energy and avoids the unnecessary heating of sapwood (whose MC already confers an acceptable level of deformability) and the core of the wood (which remains unpeeled) and, at the same time, limiting the occurrence of spin-out. An Infrared (IR) heating system may be the most suitable technology in terms of rapid heating rates and such a system might be easy to install on the peeling lathe (Coste and De Bevy 2005). It has been established that IR radiation is characterised by a penetration depth of a few cells rows and, feasibly, is suitable for heating green wood surfaces up to a depth of several millimeters (Gaudillière 2003). From this perspective, the following modification to the plywood manufacturing chain could be considered (Fig. 4b). Embedding a heating system directly onto the peeling lathe would bring 'unity' to the process

(Fig. 4a) and negate the numerous adverse effects of the soaking step in veneer production (Fig. 2). From an economical point of view, it might be expected that simplification of the manufacturing chain resulting from the reduction of two operations - soaking and peeling - to one would lower production costs (by deleting the dangerous, polluting and energetically demanding soaking step) and favour the solution of IR heating.
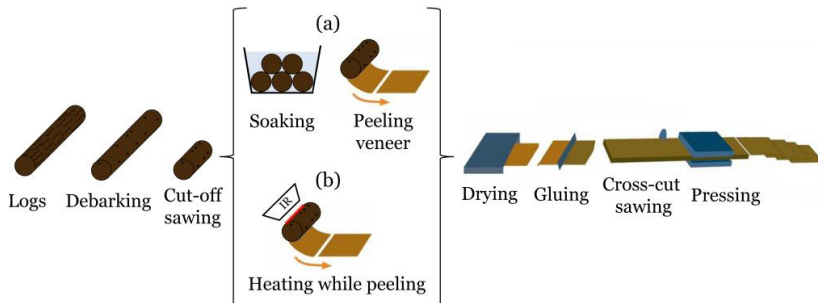
Figure 4 (a) Traditional manufacturing chain of plywood (b) modified by replacing the soaking step by IR heating

1.2. Aims of study

The aim of this study was to investigate the potential of IR radiation to heat a green log rotating on a peeling lathe. Because the study was carried out with the development of veneer production in mind, the parameters studied (heating depth, heating temperature and peeling speed) were chosen accordingly to industrial practices. The heating depths were defined by the cutting plane located from 1 to 3 mm beneath the surface. The heating temperatures were redefined to optimise the effect on cutting effort and veneer quality (Section 4.1). The peeling speed was chosen for the high production capacity of industrial peeling lathes, but was not considered as a limiting factor for the feasibility of IR heating. Indeed, lower peeling speeds could balance the disparities between peeling and drying rates and could benefit the whole veneer production process because : (1) the inability of driers to cater for the high peeling rates demanded generate buffer stocks in the production line so that lower peeling speeds would necessitate a rearrangement of the production into several shifts but would not decrease the veneer production (2) heat storage and loss of MC in veneers during IR heating would reduce drying times.

A series of distinct and practical questions were raised which form the basis of the papers that make up this thesis.

Paper I. What benefits are desired when heating wood prior to peeling it? What are the 'minimum-optimum' heating temperatures required for adequate veneer quality?

Paper II. How does IR radiation interact with green wood?

Paper III. How do MC and anisotropy modify heat transfer in wood?

Papers IV. and V. What heating rates can be achieved in green wood under an external IR heating?

   These are the key-questions that have to be assessed even before considering the economic feasibility and feasibility at pilot scale. Chapter 2 provides an overview of the answers to these key-questions found in the literature. Chapter 3 describes the materials and methods used in the different research works performed in this study. Within Chapter 3, Section 3.2 is particularly helpful in clarifying the research needs and in understanding the research plan executed in order to answer them. Chapter 4 presents the results obtained from each of the research works and discusses them. Points for further work are discussed in the last chapter (Chapter 5).

2. Literature review

2.1. Heating green wood prior to peeling

2.1.1. The benefits of heating wood prior to peeling it

Both mechanical and chemical perspectives are necessary to understand the desired effects of heating green wood prior to peeling it. The basic idea is that by heating wood it 'softens' which facilitates cutting.

From a mechanical point of view, Baldwin (1975) stated that heating logs to increase the mechanical deformability of green wood under the cutting knife is a key stage in industrial veneer production. Using an energy approach to study the properties of wood surfaces and the fracture behaviour of wood, it has been demonstrated that the ratio of fracture energy (to create a new unit surface) to shearing (or compression) energy increases with heating (Thibaut and Beauchêne 2004). A diminution in the energy dissipated in the shearing of wood lowers the pressure applied by the bolt on the cutting knife, thereby decreasing the effort required in debarking - and therefore presumably in peeling (Bédard and Poulain 2000). This consequently results in reduced power consumption and cutting tool wear (Marchal et al. 2004). Secondly, the reduction in the fracture energy required to create a unit area of surface reduces the formation of checks and therefore improves veneer quality (Thibaut and Beauchêne 2004).

From a chemical point of view, the mechanical deformability of wood is increased by softening the lignin moiety (Baldwin 1975, Matsunaga and Minato 1998, Bardet et al. 2003, Yamauchi et al. 2005). For this purpose, the heating temperature should ideally exceed the glass transition temperature, Tg, of lignin at the MC of green wood. This temperature is lower than the Tg of cellulose and hemicelluloses (Engelund et al. 2013) and dominates the behaviour of the wood material. This statement remains true for wood polymeric constituents either isolated or embedded in the native hemicelluloses-lignin matrix (Navi and Sandberg 2012). Reaching

the Tg of lignin would also fluidise resin and soften knots. The softening of knots also contributes to a reduction in cutting tool wear (Marchal et al. 2004).

2.2. Optical properties of green wood under IR radiation

The technical feasibility of IR heating as a means of warming wood prior to peeling necessitates that IR radiation can heat wood rapidly. This depends on the ability to 'deposit' IR energy deep into wood so that heat can transfer within wood more rapidly than by the slow process of conduction. This issue raises the following questions: how deep can IR radiation penetrate wood? What proportion of the incident radiation is absorbed by the wood? Can the physical parameters of wood (such as density, surface roughness and MC) significantly impact on IR absorption to enhance it? The following state of knowledge reviews the latest findings on the interaction between wood material and IR radiation to understand better which of these issues have already been addressed, so as to determine precisely the research needs. However, some basic laws regarding IR radiation are first reviewed in Section 2.2.1.

2.2.1. Basic laws of IR radiation

IR are electromagnetic waves which propagate at wavelengths, L, ranging from 0.78 to 1000 µm (i.e. wavenumbers σ ranging from 12 820 to 10 cm^{-1} with σ = 1/L) in the form of photons. Depending on the wavelength, IR radiation can be classified into 3 or 4 spectral bands: near-infrared (NIR), mid-infrared (MIR), far-infrared (FIR) and even extreme infrared (EIR).
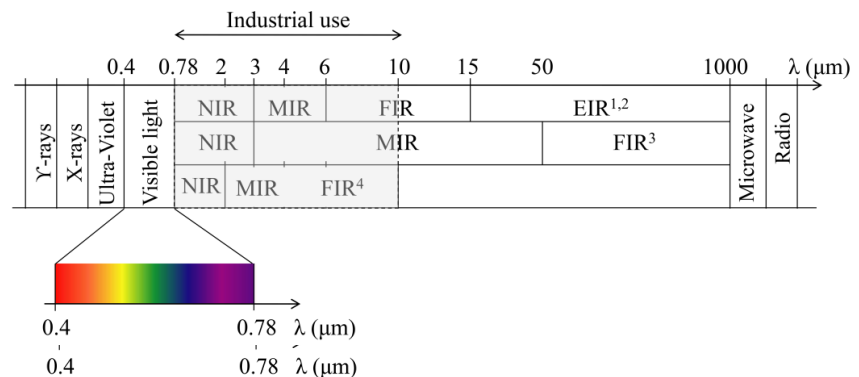
Figure 5 IR classification according to ISO (2007)[1], Flir Systems(2004)[2], Meola and Giovanni (2004)[3], Dory et al. (1999)[4]

9

These subdivisions are arbitrarily chosen by authors, which can be confusing (Fig. 5). However, the classification can be summed up in the following way: NIR features wavelengths and properties close to visible light while MIR and FIR exhibit far different characteristics.

 IR spectroscopy used in wood studies, utilises the interaction between IR radiation and wood's molecular components - which vibrate at specific IR wavelengths - to determine its chemical composition. Usual IR spectroscopy focuses on the region from 2.5 to 25 μm (4000 to 400 cm^{-1}) i.e. in the MIR region where most of the fundamental vibrational modes of molecular chains occur (ASM International Handbook Committee 1986). However, wood components are also excited by IR radiation of shorter wavelengths, that is in the NIR range - from 0.78 to 2.5 μm - but the vibrations are less numerous (Berthold et al. 1998, Kelley et al. 2004). Heating wood with IR consists in exciting wood molecules with IR radiation in order to heat the wood material. In the case of green wood, the aim of IR heating is to directly heat the wood cell wall material and so avoid the unnecessary, and energy consuming, heating of water. For this purpose, it would be necessary to irradiate the wood with IR wavelengths specific to the wood molecular components in order to excite them and not the water molecules present in wood (either free or bound to the cell wall). In particular, since lignin has the lowest Tg at high MC (Section 2.1.1), exciting lignin molecules could be sufficient to soften green wood and its knots (since lignin is a major component of knots) and so aid the peeling process. The first step in the study is therefore to gain an understanding of IR penetration depth and IR absorption by green wood. For this reason, using a broad IR band that encompasses a spectrum of wavelengths larger than the specific wavelengths of lignin is precise enough. In this perspective, the IR band from 550 to 5500 cm^{-1} used by the integrating sphere (Section 3.4) fits the purpose of the study. If the results were to be convincing, further study could try to select specific wavelengths to enhance the heating of green wood cell wall and avoid the heating of water.

2.2.2. IR penetration depth in wood

The notion of penetration of IR radiation into wood appears for the first time in the literature in 1983 when Grimhall and Hoel (1983) mentioned that IR is 'intensively' absorbed by the surface of oak. More recently, Potter and Andresen (2010) reported a similar qualitative observation that living trees are heated via IR radiation. Measuring the temperature profile deep within the wood as an indirect measure of the penetration depth of IR

radiation, Makoviny and Zemiar (2004) suggested that in all probability the penetration depth of IR was less than 0.1 mm in oak at MCs of between 0 and 20%. However, with Makoviny and Zemiar's method it remains difficult to precisely evaluate the penetration depth of IR radiation absorbed by wood because the measurement technique is necessarily biased by heat transfer through conduction (Cserta et al. 2012). More precise estimates of IR penetration into wood have been achieved by recent developments in IR spectroscopy. The penetration depth has been calculated to be from 0.13 to 2.15 μm depending upon the wavelength (Zavarin et al. 1991) with a maximum depth of penetration of 37-138 μm recorded at 2242 cm^{-1} (Zavarin et al. 1990).

2.2.3. Influence of wood physical parameters on IR absorption

All authors agree that any modification of the wood surface quality will influence IR absorption by wood as clearly stated by Jones et al (2008). But there is some controversy about the effect of surface roughness on absorbance. Bennett and Porteus (1961) highlighted that the rougher the wood surface, the greater the reflection and the less absorption. This behaviour was confirmed by De Santo (2007) who noted that surface roughness increases light scattering and is proportional to surface reflectance but this was in contrast to previous studies who found the opposite to be the case (Zavarin et al. 1990, 1991). It has also been reported that the effect of surface roughness on absorbance differs according to wavelength (Tsuchikawa et al. 1996). There are fewer studies concerning the effect of wood density on energy absorption, however, Zavarin et al. (1990) noted that both wood density and fibre orientation are minor factors influencing energy absorption and the penetration depth in wood (Zavarin et al. 1990).

2.2.4. Influence of wood MC on IR absorption

However, all the above mentioned studies were carried out on dry wood or wood below the f.s.p and data on the penetration depth into green wood (wood above the f.s.p which has never been dried) are lacking. The only study on the effect of MC on the optical properties of wood is with regard to its emissivity. The emissivity, ε, of a surface is its ability to absorb (and emit) energy by radiation. The more absorbent a surface is, the higher its emissivity. Kollmann and Côté (1968) reported that wet wood absorbs more IR energy than dry wood and that ε increases with MC up to f.s.p, at which

point the emissivity of wood is the same as that of water (ε = 0.93). Emissivity values provided by the manufacturers of IR thermography cameras (e.g. Flir System 2004) are given for all wavelengths of incident IR radiation, and the wood MC is referred to as either 'dry' or 'damp' which is not precise enough to obtain a clear picture of the dependence of optical properties on MC. Some experimental work has investigated the transmission and absorption of wet Douglas-fir, beech and oak veneers in the near- and mid-IR range using a flux meter located underneath exposed veneer (Marchal et al. 2004). From this work, it was concluded that veneers of between 0.5 and 2 mm absorb around 50% and transmit around 10% of the incident flux. These values were constant irrespective of the source wavelength and transmission was found to increase with increasing MC but decrease with sample thickness. However, it is believed that these results should be considered with care because the flux meter used may have been influenced by extraneous ambient light.

In view of the lack of accurate data concerning the ability of wood to absorb IR energy to a certain depth, the optical properties of green wood were investigated and the findings reported in Sections 3.4 (for the method) and 4.2 (for the results).

2.3. Thermal properties of green wood

Thermal conductivity (λ), heat capacity (C) or specific heat (c), and thermal diffusivity (κ) are the most important properties characterising the thermal behaviour of materials, including wood (Sonderegger et al. 2011, Suleiman et al. 1999). The characteristics of these properties are summarised in Table 1. The present review focuses on: (1) the influence of wood MC on wood thermal properties because the research needs concern the IR heating of wood in the green state, (2) the influence of anatomical orientation (radial or tangential) on wood thermal properties because they are the main directions of heat flow when heating wood in the transverse direction.

2.3.1. Influence of MC on thermal properties

At MCs between 0% and f.s.p, wood is considered to be a good insulating material with low λ, moderate C, and consequently low κ. The porosity of wood explains its low λ, because the λ of air filling the void spaces is lower (λ_{air} = 0.03 W.m^{-1}.K^{-1} at 300 K, Rohsenow et al. 1973) than that of the wood cell wall (λ perpendicular to the grain = 0.42 W.m^{-1}.K^{-1}, Kollmann and Côté

1968). Heat flows preferentially through the wood cell walls, which act like heat bridges, whilst the air present in the lumens below f.s.p forms a barrier to heat flow (Kollmann and Côté 1968). The conductivity of water (λ_{water} = 0.613 W.m^{-1}.K^{-1} at 300K, Rohsenow et al. 1973) is higher than that of air. Accordingly, wood conductivity increases linearly with increasing MC (Sonderegger et al. 2011). Free water conducts more heat than bound water, thus the incremental increase in λ with MC above f.s.p is greater (Siau 1971).

Thermal properties	Unity	Definition
Thermal conductivity, λ	W.m^{-1}.K^{-1}	Rate or power (in W) at which heat is transferred through 1 m thickness of the sample material when subjected to a gradient of 1 K, measures the ability to transfer heat flux.
Heat capacity, C	J.m^{-3}.K^{-1}	Amount of heat (or energy, in J) needed to increase 1 m^3 of material of 1 K, measures the thermal inertia.
Specific heat, c	J.kg^{-1}.K^{-1}	Amount of heat (or energy, in J) needed to increase 1 kg of material of 1 K, defined by $C = \rho \cdot c$ with ρ is material density, measures the thermal inertia.
Thermal diffusivity, κ	m^2.s^{-1}	Speed at which heat transfers within the material, defined by λ/C, measures the transient thermal behaviour.

Table 1 Definitions of thermal conductivity, λ, heat capacity, C, specific heat, c, and thermal diffusivity, κ

The presence of water strongly affects the heat capacity (C) of wood because of the high C of water; the specific heat capacity of water, c_{water}, is 4.18 kJ.kg^{-1}.K^{-1} at 300 K (Rohsenow et al. 1973). As a first approximation, the specific heat, c, of wet wood can be calculated by a simple rule of mixtures by adding the specific heats of water, c_{water}, and of oven-dry wood, c_o, in their relative proportions (equations detailed in Paper III). But considering wet wood to be a mixture of two independent materials may be an oversimplification and some authors have suggested that this relationship only holds true when the MC is greater than 5% (Sonderegger et al. 2011, Jia et al. 2010). Some authors propose an additional coefficient,

Ac (Table 1 in Paper III), to take into account the energy lost during the wetting of the cell wall due to the creation of H-bonds between the hydroxyl groups of cellulose and water (Sonderegger et al. 2011, Simpson and TenWolde 1999). However, Ac values vary among authors and are only valid below f.s.p. Other authors modify the coefficients in the rule of mixtures as a function of MC (Siau 1995, Koumoutsakos et al. 2001). Studies focusing on the heat diffusion, κ, of wet and dry wood are scarce. According to Kollmann and Côté (1968), κ decreases slightly with MC.

2.3.2. Influence of wood anisotropy R-T on thermal properties

The effect of wood anisotropy radial-tangential (R-T) on transverse conductivity is somewhat controversial. Some authors report the same λ values in the radial (λR) and tangential (λT) directions (Siau 1971, Simpson and TenWolde 1999, Suleiman et al. 1999), whereas others claim that transverse conductivity is higher in the R than in the T direction. The ratio of λR and λT is thought to be governed by the volume of ray cells in hardwoods, and the volume of latewood in softwoods (Steinhagen 1977). Similar λR and λT data were obtained for hardwood species with rather uniform wood structure or a low amount of latewood, such as in young softwoods (Suleiman et al. 1999). However, studies on beech and spruce support the concept that λR predominates (Sonderegger et al. 2011). Logically, there is no influence of orientation on specific heat, c, as this property is mainly dependent upon the cell wall material itself. The specific heat of oven-dry wood at 20°C is generally regarded to be constant with not much variation from one specie to another (Jia et al. 2010) and hardly any influence of density (Sonderegger et al. 2011). Since κ is proportional to λ, it is logical that diffusivity is also anisotropic since both ρ and c are isotropic properties (Steinhagen 1977). Therefore, the κR should be higher than κT because of the lower tangential λT (Kollmann and Côté 1968). However, as with λ, some findings do not corroborate the anisotropic nature of κ (Suleiman et al. 1999).

It was decided to clarify the influences of MC and wood anisotropy on thermal properties by the experimental measurements presented in Sections 3.5 (for the methods) and 4.3 (for the results).

2.4. Heating rates of green wood under external IR source

The investigation reported herein question the existence in the past of experimental or simulation trials to heat green wood with IR radiation. Potter and Andresen (2010) have demonstrated, using a finite-difference method, that living trees are heated via IR radiation. However, the promising results on IR induced heating rates of these authors have not been extended to conditions of dynamic rotational movement of the log. From an experimental perspective, the ability of IR radiation to raise both the surface temperature and the temperature below the surface in green wood has been positively confirmed for both the purpose of heating the wood (Bédard and Laganière 2009) and for drying it (Cserta et al. 2012). With heating source flux densities of 126 kW.m^{-2}, it has been shown that it is possible to achieve surface temperatures of 50°C in green logs of beech, Douglas-fir and okoumé rotating at speeds corresponding to peeling speeds of 0.25-0.5 m.s^{-1} with source power densities of 126 kW.m^{-2} (Coste and De Bevy 2005). Similar results have been obtained in spruce logs rotating at 0.1 m.s^{-1} using relatively low IR flux densities of 4-20 kW.m^{-2} for the purpose of thawing logs (Bédard and Poulain 2000). Several studies have been conducted to evaluate the time taken to achieve a peeling temperature of 50°C at different depths (0.5 mm, 1 mm, 2 mm and 5 mm) in samples of beech, Douglas-fir and oak as a function of the input power of the IR source (Gaudillière 2003, Marchal et al. 2004, Chave and Vial 2003, Makoviny and Zemiar 2004). As might be expected, the greater the input power of the IR source, the faster the target temperature of 50°C is achieved at a particular depth. However, for the purpose of heating the wood surface prior to peeling, the input power of the IR source should be adjusted in order to avoid overheating and eventual burning of the surface.

The multiplicity of experimental results generated by the diversity of experimental situations (due to different wood species, wood MCs, IR power densities, etc.) has highlighted the need for building a numerical model which could simulate the heating rates of green wood under IR radiation as a function of the different parameters cited above (Section 3.6 for the methods and Section 4.4 for the results). The accuracy of the model has then been tested by comparison with simplified solutions of analytical equations and with some experimental data (Section 3.7 for the methods and Section 4.4 for the results).

3. Materials and methods

3.1. Wood material

Four wood species were used in this study: two hardwoods - beech (*Fagus sylvatica* (L.)) and birch (*Betula pendula* (Roth)) and two softwoods - Douglas-fir (*Pseudotsuga menziesii* (Mull) Franco) and spruce (*Picea albies* (L.) Karst). This choice was guided by the industrial needs of veneer production in the two countries involved in this co-tutelle PhD - France and Finland. Birch and spruce are the most significant wood species harvested in Finland to produce veneers, whilst beech is the most important species for the production of veneer in France. Douglas-fir was studied as a potential resource for veneer production in order to take advantage of the plantations from the 1950s, which are nowadays reaching harvestable age. These four species were chosen because they all require soaking to ensure successful peeling. Moreover, the application of IR heating would likely be beneficial in the case of Douglas-fir which is not well suited to soaking because of its heterogeneous structure, arising from differences in the densities of earlywood and latewood, the presence of knots and heartwood dryness. The beech and Douglas-fir logs used for this study were obtained from forests near Cluny, France whilst the birch and spruce logs were harvested in Finland.

This wood material was processed into samples different of differing dimensions and form (Fig. 5), to fit the requirements of the various experimental tests carried out, as follows:

- Bolts of 400 mm diameter were cut to a length of 600 mm to fit the dimensions of the industrial peeling lathe available at Arts et Metiers ParisTech Cluny, France and to maximise the number of bolts and tests per log. For each species, all the bolts tested originated from the same log and each bolt was tested at one soaking temperature. The nominal veneer thickness (e_{nom}) was 3 mm; however, this differed from the actual measured thickness due to the wood structure. In order to evaluate only the influence of heating temperatures on the peeling process and veneer surface quality,

the peeling speed, s, and the compression rate of the pressure bar, Bp, were kept constant (s = 1 m.s⁻¹; Bp = 5 %; vertical gap = 1 mm). This low Bp value compared to the 15-20 % pressure bar values usually used in industry was chosen to highlight that the checking phenomenon occurs with the slightest influence of the pressure bar. To assess veneer quality using the 'fuitometer' for an indirect measure of veneer roughness (explained in Section 3.3.1) and the 'SMOF' for lathe checking (described in Section 3.3.2), bands of veneer, 600 mm in length, were peeled from initially green bolts (①️ in Fig. 6);

- Discs, 30 mm diameter (②️ in Fig. 6), were cut with a circular cutter from different thicknesses of the aforementioned green veneer to characterise optical properties using the integrating sphere detailed in Section 3.4;
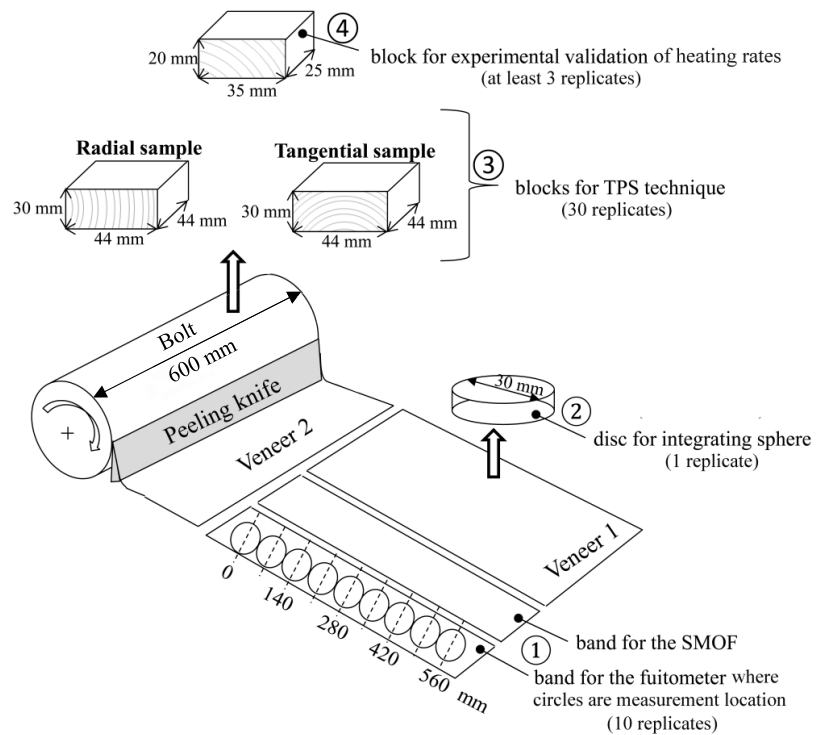
Figure 6. The different samples sizes and forms into which the wood material was processed for the experimental test (with the number of replicates in brackets[3])

---

[3] The measure with the integrating sphere is done on a wide surface so that it is possible to consider that one replicate is already representative of the mean value for the surface being characterised ('representative surface').

- To characterise thermal properties using the TPS technique introduced in Section 3.5, knot free blocks having dimensions of 44×44×30mm³ were sawn from freshly cut trees in the tangential and radial directions with respect to grain orientation (③ in Fig. 6);

-Knot free blocks with dimensions of 44×35×20mm³ were sawn from freshly cut trees (④ in Fig. 6, Section 3.7) and were used to experimentally validate heating rates.

3.2. Research plan

The research plan was organised so as to render possible an estimation of the heating temperatures achievable within a green log rotating under IR radiation (Fig. 7). This estimation was based on a numerical simulation presented in Paper IV and validated by experiments (Paper V). For this purpose, it was necessary to know the 'minimum-optimum' target heating temperatures (Paper I), to feed the model with accurate thermal property data (Paper III) and to know whether the equations predicting the heating of wood layers beneath the surface by an external IR source should take into account the volumetric absorption of IR energy within wood and not only the transfer of the heat absorbed by the surface layers by conduction to the inside layers (Paper II).
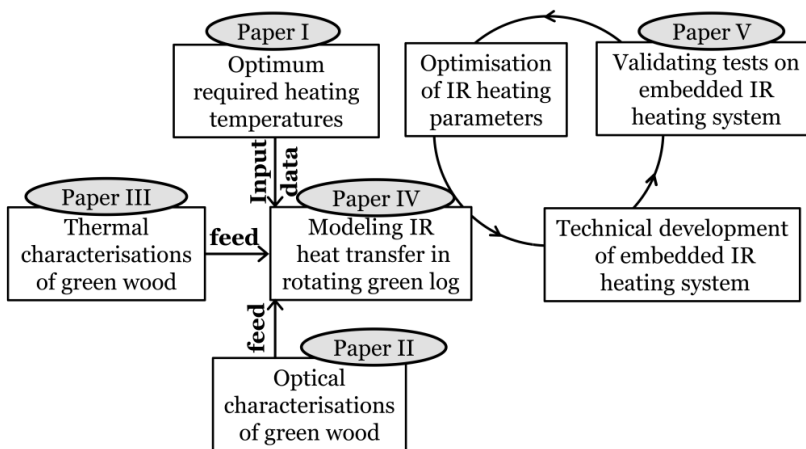
Figure 7. Schematic representation of the research plan carried out

3.3. Assessing veneer quality: the fuitometer and the SMOF (Système de Mesure de l'Ouverture des Fissures)

Veneer quality can be assessed by three factors: (1) veneer surface topography (including roughness and waving), (2) thickness variation and (3) lathe checking. It is well known that heating temperature in particularly influences the latter factor, which can be described by two parameters: checking interval (CIn) and checking depth (CD). This section presents the materials used to evaluate veneer quality as a function of soaking temperature in order to investigate 'minimum-optimum' heating temperatures (by soaking), with a view to assessing the possibility of reducing log heating temperatures compared to the temperatures currently in-use in the industry (research question raised in Paper I). Given the lack of a standard for veneer surface quality evaluation, it was decided to assess it by measuring: (1) air leakage on the veneer surface (as an indirect measure of veneer roughness) using a pneumatic rugosimeter - also referred to as a 'fuitometer', (2) thickness variation and (3) lathe checking with the SMOF (Système de Mesure de l'Ouverture des Fissures) device (Palubicki et al. 2010). Further details on the experimental procedures can be found in Paper I.

3.3.1. Measuring veneer air leakage: the fuitometer

The principle of the fuitometer is simple (Pouzeau and Pradal 1957). It is based on pressure loss when air flows through an annular-shaped pipe impinging on the uneven veneer surface (Fig. 8a). In the case of an uneven surface, air leaks through the pipe: the pressure at the output of the pipe decreases leading to a pressure loss indicated by the water column whose level gets higher. The difference between input and output pressure readings on a water column is a function of veneer air permeability. The fuitometer also gives the Checking Index (CI) which is calculated from the difference in air leakage between the 'tight' and 'loose' sides of the veneer (El Haouzali 2009) (Eq. 1, Fig. 8a).

$$CI (in \ mm \ of \ water) = water \ level_{on \ tight \ side} - water \ level_{on \ loose \ side} \quad (1)$$

CI measures air leakage through the veneer which is influenced by lathe check formation (Palubicki et al. 2010): the more lathe checks there are, the greater the tearing of the fibers and the more uneven the surface. This results in greater air leakage and a higher water level and consequently a lower column reading.
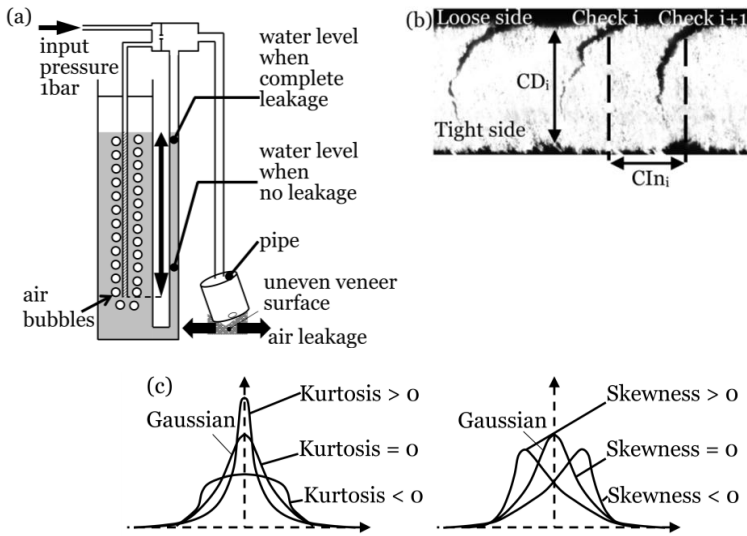
Figure 8. Schematic showing the principle of the fuitometer (a), SMOF output image with checking depth CD_i and checking interval CIn_i (b), definitions of kurtosis and skewness for a distribution of data (c) (Paper I)

3.3.2. Measuring veneer lathe checking : the SMOF

The purpose of the SMOF device is to detect the lathe checks which form on the 'loose' side of the veneer in contact with the knife (Fig. 8b, Palubicki et al. 2010). Lathe checking is brought about by a sudden tearing of wood fibers under the cutting knife due to an increase in the energy dissipated by wood shearing (Thibaut and Beauchêne 2004). The mechanisms behind the formation of lathe checking are influenced by the deformability of the wood and so, in turn, depend upon the peeling temperature. The principle of the SMOF involves bending a band, or ribbon, of veneer over a pulley in such a way as to open-up the checks that are then illuminated by a laser. A camera automatically takes images of the veneer edge that enables a continuous recording of the veneer cross-section to be made. The images obtained from the SMOF (Fig. 8b) enable the interval between two checks (CIn_i) and checking depth (CD_i) for each check to be calculated. For each check, i, the checking ratio, CR_i, is given by Eq. 2.

$$CR_i = \frac{CIn_i}{CD_i} \qquad\qquad (2)$$

The distributions of CIn_i and CD_i are then displayed in the form of histograms (Section 4.1.3): for each log heating temperature, the number of lathe checks (in terms of percentages of total number of lathe checks on the measured veneer) is represented for each range of CIn_i and CD_i displayed

on the X-axis. In some cases the distributions are spread widely so that determining the most frequent values is not a statistically relevant way to characterise the checking distribution along the veneer length. For this reason a statistical analysis was chosen based on an evaluation of the coefficients of skewness and kurtosis illustrated in diagrams presented in Fig. 8c. Skewness is a measure of the asymmetry of the distribution while kurtosis is a measure of its peakedness.

3.4. Characterising green wood optical properties: the integrating sphere

The objective of using the integrating sphere was to determine the optical properties of green wood under IR radiation. The characterisation involved the experimental measurement of diffuse reflectance and transmittance IR spectra and is fully detailed in Paper II. Using this approach, it was possible to estimate the amount of energy absorbed by the wood and the penetration depth of the IR radiation into the wood (addressing the research questions raised in Paper II).

   The integrating sphere device, consisting of a Bruker Vertex 70 spectrometer equipped with a 6 inch integrating sphere (Hoffman SphereOptics) with a diffuse reflective gold coating, provided reflectance (R) and transmittance (Tr) calculated from different spectra (Eqs. 3 and 4). For each wavelength of the incident radiation, R gives the amount of energy which leaves the incident sample surface without being absorbed because of reflectivity at the air-material interface or back-scattering by the wood fibres. For each wavelength of the incident radiation, Tr gives the amount of energy transmitted through the sample. In order to suppress any parasitic contribution appearing in reflectance mode, the reflectance spectra, R, were background corrected with a measure of the ambient spectra (spectra Amb in Fig. 9a). Reference spectra (M) were acquired with a mirror used as a gold diffuse reference (Fig. 9b). Spectra of the flux reflected by the sample surface, E_R, and spectra of the flux transmitted through the sample surface, E_T, were obtained by using the adequate integrating sphere configurations shown in Fig. 9c and Fig. 9d respectively (Labsphere). A simple energy balance shows that the absorptivity, A, the amount of energy absorbed by the material is given by Eq. 5 (Palmer et al. 1995).

(a) Configuration of spectra Amb   (b) Configuration of spectra M

(c) Configuration of spectra E_R (d) Configuration of spectra E_T
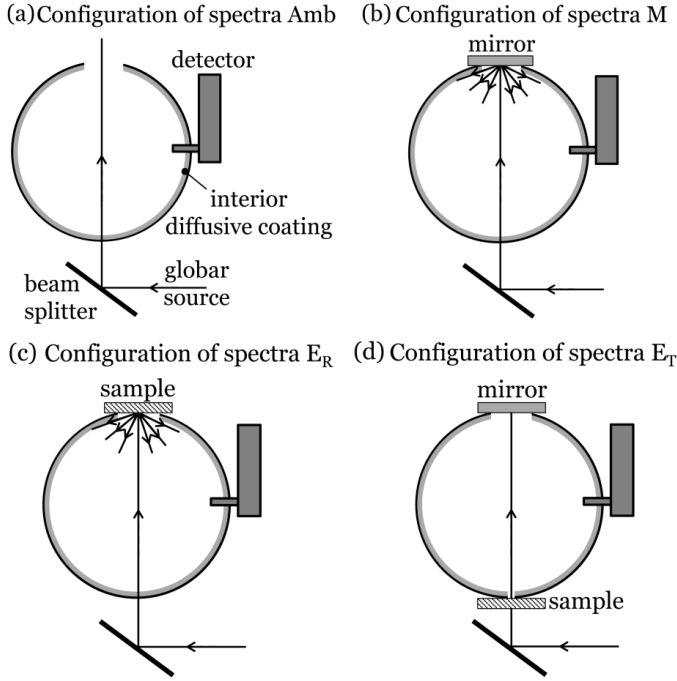
Figure 9. Scheme of the different configurations of the integrating sphere to obtain (a) ambient spectra Amb, (b) reference spectra M, (c) spectra of reflected flux E_R and (d) spectra of transmitted flux E_T (adapted from Paper II)

$$R = \frac{E_R - Amb}{M - Amb} \tag{3}$$

$$Tr = \frac{E_T}{M} \tag{4}$$

$$A = 1 - R - Tr \tag{5}$$

Due to its heterogeneous structure (porosity, fibres, etc.), light scattering is strong inside wood and so the penetration depths of these samples cannot be simply defined by the inverse of the absorption coefficient. Rather, a qualitative penetration depth is estimated by testing samples of decreasing thicknesses. As long as transmission is nearly equal to zero – meaning that all incident radiation is absorbed or reflected by the sample – the penetration depth is known to be less than the sample thickness. Table 2 shows the different thicknesses of all samples: increments of 0.1 mm could not be obtained because of the difficulty of peeling to such tight tolerances. The penetration depth reported in this study (Section 4.2) is thus given by

default by the thinnest veneer section which gives a non-zero value for transmission.

Species	Sample thicknesses (mm)
Beech	0.2; 0.3; 0.5; 1.2; 2.0; 2.2; 3.1; 3.2
Birch	0.6; 0.9; 1.0; 1.1; 2.1; 2.3; 3.0; 3.2
Douglas-fir	0.5; 0.6; 0.7; 1.1; 2.1; 2.3; 3.2
Spruce	0.6; 1.1; 1.2; 2.1; 2.3; 3.2

Table 2 Thicknesses of the samples tested for the integrating sphere

3.5. Characterising green wood thermal properties: the TPS (Transient Plane Source) technique

The lack of data in the literature on the thermal properties of green wood provided the impetus for investigating the transverse (radial and tangential) thermal conductivity (λ), heat capacity (C) and thermal diffusivity (κ) of green wood at MC above f.s.p (Paper III) using the TPS technique. The TPS technique was chosen over the guarded hot plate and transient techniques such as the Transient Hot Wire (THW), the Transient Hot Strip (THS) and the flash method, which are other commonly used methods of thermal characterisation for the reasons summarised in Paper III. The general theory of TPS has been comprehensively described by Gustafsson (1991) and is detailed in Paper III. The TPS technique entails recording the resistance change as a function of time of the heat source, in the form of a disk, which serves as the measuring sensor. The TPS element is sandwiched between two specimens whilst an electrical current is passed through it with sufficient power to slightly increase its temperature (by between 1 and 2 K) (Fig. 10). The TPS technique consists of measuring λ and κ while C is calculated from the relationship $\kappa = \lambda/C$. Fitting the TPS experimental results with the analytical models presented by Gustafsson (1991) leads to values for λ and κ.
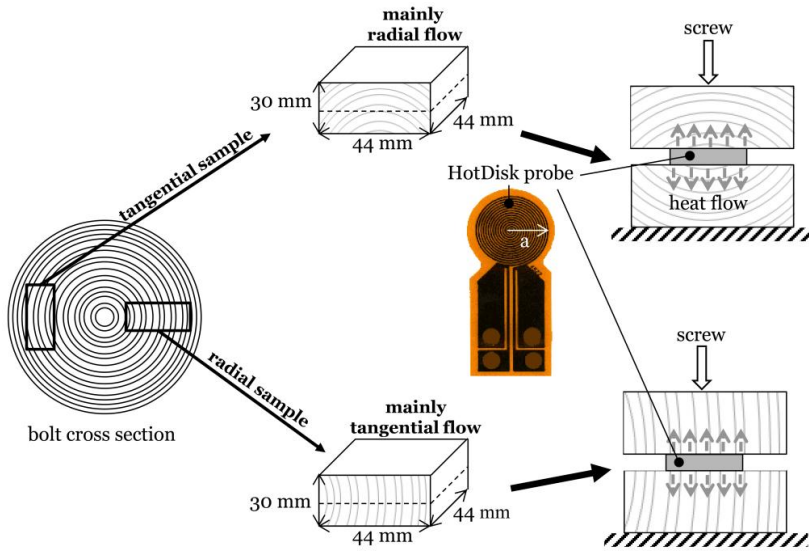
Figure 10. Sampling identical samples and TPS measurement configuration (adapted from Paper III)

3.6. Numerical modelling

The simulation consisted of numerically modelling the heating of green wood logs by an external IR radiation source during peeling in order to estimate the heating kinetics of a green wood cylinder rotating with decreasing radius (more details about the model can be found in Paper IV). Comsol Multiphysics (Comsol Inc., Burlington, MA, USA) software was used to solve the partial differential equations based on the finite element (FE) method with the overall procedure implemented under the flexible MatLab (MathWorks Inc., Natick, MA, USA) environment. The model meshes the log cross-section with 2D finite elements (in the radial and tangential directions) whilst the bolt length (the longitudinal direction) is not considered since heat transfer in the longitudinal direction can be neglected. To predict heat transfer accurately in the vicinity of the bolt surface, the mesh, which consisted of Lagrange-quadratic elements with triangular shapes as the basic functions, was refined close to the bolt surface and the cutting plane (Fig. 11b).

The cross-section of the bolt was divided into subdomains with specific initial settings in terms of physical properties (wood density, ρ) and thermal properties (C, λ). All the parameters needed to describe the bolt structure – such as bolt diameter, annual ring width (earlywood/latewood), heartwood/sapwood width, pith eccentricity – were defined by modifiable

24

input values, since it is likely that structural properties influence heat transfer into wood because of the variations in densities and therefore in thermal characteristics. According to Kollmann and Côté (1968), the effect of MC is greater than the effect of density on the thermal characteristics of wood, both below and above f.s.p. This assumption is supported by the results presented in Fig. 22. Therefore, the variation of wood's thermal characteristics with wood density were not taken into account and only the influence of MC on wood thermal properties (C, λ) was considered in this study. For geometric convenience, the real situation was modelled by supposing an immobile bolt with an IR heat source turning around it; this is a valid simplification since only the movement of the IR source relative to the wood is important. The bolt surface was divided into 20 sections with uniform boundary settings. Only the IR source's external input heat flux q (in W.m^{-2}) was successively activated with a Boolean operator for each section of the bolt arc surface being radiated. The boundary conditions at the bolt surface were defined by Eqs. 6a and 6b with, n, the vector normal to the boundary.

- on the arc surface (radiated) x: $-n.(-\lambda \nabla T) = \varepsilon.Q.H(x)$ (6a)

- on the unradiated rest of the surface: $-n.(-\lambda \nabla T) = h\,(T - T_{ext})$ (6b)

where H is the Heaviside function (Fig. 11), ε the emissivity of the wood surface, T_{ext}, the external temperature (in K), q, the heat flux (in W.m^{-2}) and, h, the heat transfer coefficient fixed at 5 W.m^{-2}.K^{-1} (Quéméner et al. 2003). The mean value ε = 0.85 was chosen because the emissivity of un-planed wood is said to vary from 0.70 to 0.98 for temperatures ranging from 17 to 70°C (Flir Systems 2004). Wood emissivity here is independent of the IR wavelength (total emissivity) because the whole emission spectrum of the IR source (independently of the wavelength) is taken into account.

Eq. 7 is the thermal equation solved by Comsol Multiphysics to predict the heating of wood surface and of the layers beneath the surface by an external IR source. It is derived from Fourier's law and only takes into account the transient transfer of the heat absorbed by the surface layers by conduction to the inside layers without integrating any volumetric absorption of IR into wood. This assumption was confirmed by the results obtained on optical properties of green wood (section 4.2.4).

$$\rho c \frac{\partial T}{\partial t} = \nabla(\lambda \nabla T) \qquad\qquad (7)$$

The continuous removal of the wood surface layer by peeling was modelled by turning the physical properties of each cut segment from that of wood into air. In Fig. 11b segments in blue, having a density of 1.2 kg.m^{-3} represent air, i.e. segments that have been cut from the bolt. In this case, the subdomain settings are functions of time and are automatically modified with Boolean functions. At each angular step, each element of the angular section reaches a new temperature resulting from the input of the external IR source and is calculated with Eqs. 6a and 6b. After each angular step, the IR is moved (by modifying the boundary settings) and the last heated section is removed (by turning its density to that of air). After each turn, the final calculated temperature of each element is used as the initial temperature of the new meshing element at the bolt surface.
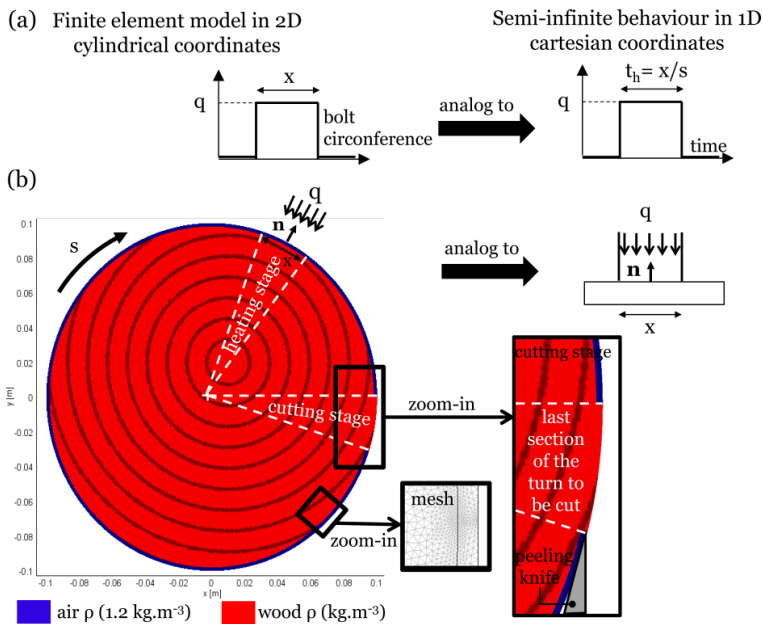
Figure 11. (adapted from Papers IV and V + additional data) (a) Analogy with semi-infinite behaviour in 1D Cartesian coordinates of (b) the modelling in 2D cylindrical coordinates of a bolt meshed with Finite Elements and heated with IR

3.7. Experimental and analytical validations of the numerical simulation of heating rates

In order to check its reliability in predicting the heating of a green log rotating under an IR heating source, this 2D numerical model in cylindrical coordinates was validated by experimental measurements. For this

26

purpose, simplified analytical solutions of thermal transfer in a semi-infinite body in 1D Cartesian coordinates - proven to describe accurately this experimental situation (Section 4.4) - were necessary to estimate the effective flux density, q (Fig. 12), received by the sample by the inverse method of deconvolution proposed by Beck et al. (1985) (Paper V).

3.7.1. Experimental setting

The physical experiments consisted of conveying samples of green wood at a speed, s, of 0.0032 m.s^{-1} under an electric IR lamp composed of a quartz tube delivering a heat flux, q (in W.m^{-2}), onto a surface approximately 0.03 m wide (the gridded surface shown in Fig. 12). The samples were shaped in the form of rectangular prisms because (1) it is easier to record internal temperature rises in a block in motion than in a rotating cylinder, (2) the numerical simulation mentioned below has demonstrated that, with characteristics of the IR source used in the model, blocks behave in a similar manner to cylinders. The increase in surface temperature over time was recorded using a surface thermocouple, tightly stapled to the surface in order to minimize thermal contact resistance. Holes were drilled into the samples to insert the thermocouples which were used to measure the temperatures within the block. The holes were drilled at a depth of 3 mm millimeters beneath the exposed tangential surface (Fig. 12).
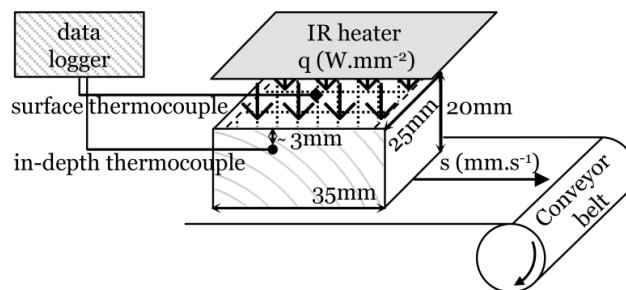
Figure 12. The experimental set-up for measuring the sample surface temperature under IR heating

A tight fit and filling the drilled holes with wood dust after inserting the thermocouples ensured minimal heat losses and thermal contact resistance. The thermocouples were connected to a data acquisition system which recorded the temperature every second. The samples were initially in the

green state and at least 3 replicate tests were carried out on each species (in both sapwood and heartwood).

3.7.2. Simplified analytical solutions

Firstly, given the large dimension of the bolt diameter, D, compared to x, the arc surface of the green log subjected to external IR heating (x = D/20), it is possible to reduce the situation to one dimension in Cartesian coordinates (Fig. 11a). Secondly, in view of the very low thermal diffusivity of green wood of green wood (Paper III), the behaviour can be assumed to be that of a semi-infinite body with a spatially uniform step heat flux diffusing normally to the surface, x, applied during a heating time, t_h, where t_h = x/s and s is the peeling speed (i.e. the constant linear speed at which veneer is generated at the output of the peeling lathe). The problem therefore becomes analogous to a 1D-transient problem where the spatial variable, x, is replaced by the temporal variable t_h. With these assumptions, the evolution of the sample surface temperature, T_{surf}, with the square root of time is linear according to Eq. 8 (Taler and Duda 2006).

$$T_{surf} = \frac{2q}{\sqrt{\pi}\sqrt{\lambda\rho c}}\sqrt{\frac{x}{s}} \qquad \text{or} \qquad T_{surf} = \frac{2q}{\sqrt{\pi}\sqrt{\lambda\rho c}}\sqrt{t} \qquad (8)$$

The exact solution of the temperature, T_d, attained at depth, d, within the sample is then given by Eq. 9 with the diffusivity of wood, $\kappa = \lambda/(\rho c)$ (Taler and Duda 2006).

$$T_d = \frac{2q}{\sqrt{\pi}\sqrt{\lambda\rho c}}e^{-d^2/4\kappa t} - \frac{d}{\lambda}q\,\text{erfc}\frac{d}{2\sqrt{\kappa t}} \qquad (9)$$

where erfc is the complementary error function which tends to 1 when time tends to infinity. Therefore, the long-term behaviour of T_d is given by the asymptotic solution obtained when time tends to infinity (Eq. 10). It can be seen that at extended heating times the temperature at depth, d, also evolves at a rate proportional to the square root of time.

$$T_d = \frac{2q}{\sqrt{\pi}\sqrt{\lambda\rho c}}\sqrt{t} - \frac{d}{\lambda}q \qquad (10)$$

4. Results and discussions

4.1. Optimum heating temperatures

In order to determine 'minimum-optimum' heating temperatures, the experimental plan involved heating bolts, by soaking them in water over a 48 h period at temperatures ranging from 20 to 80°C, then peeling and sampling them (Section 3.1). The soaking period was long enough to ensure that the temperature within the relatively small bolt (400 mm diameter, 600 mm length) was homogeneous, so as to avoid any temperature gradient within the bolt. The conclusions on the influence of heating temperature on veneer thickness variation, air leakage (measured with the fuitometer) and lathe checking (measured with the SMOF) are detailed in Paper I and are summarised below.

4.1.1. Effect of heating temperature on thickness variation

Although the effect of heating on thickness variation differs between softwoods and hardwoods, Fig. 13 shows reasonably small thickness variation (COV) commensurate with the relatively low pressure bar setting used during the experiments (Bp = 5 %, Section 3.1). For softwood species such as spruce, heating reduces variation in veneer thickness, making it more uniform, as can be seen from the decreased thickness variation as heating temperature rises (Fig. 13).

	20°C	30°C	40°C	50°C	60°C	70°C
Beech	83	83	83	85	83	83
Birch	84	84	84	84	84	84
Spruce	91	91	91	91	91	91

Table 3 Number of samples tested to measure thickness variation

For spruce, the inconsistency in the COV at 30 and 70°C might be explained by two factors: (1) experimental error (most probably the predominant factor at 30°C) and (2) the heterogeneous microscopic structure of spruce (likely to be the predominant factor at 70°C) (Navi and Heger 2005). At 70°C, the earlywood fibres of spruce weaken and tear under the cutting knife creating an uneven, 'woolly', surface which explains the increase in thickness variation. The heterogeneous (compared with the rather more homogeneous structures of beech and birch) structure of spruce probably explains why the phenomenon is so visible in this species. The results of CI obtained in spruce at 80°C (see next section) also support this assumption.
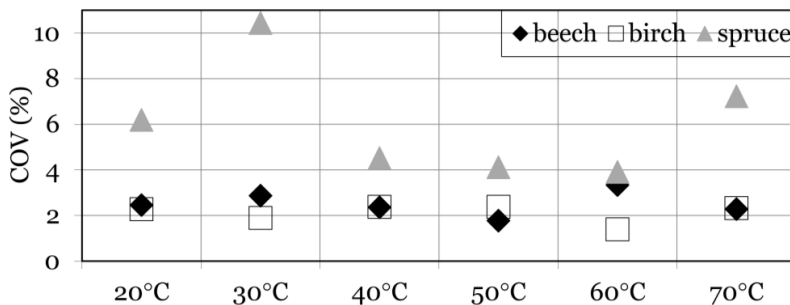
Figure 13 Influence of heating temperatures on thickness variation (COV) – results are not available at 80°C due to experimental error

4.1.2. Effect of heating temperature on veneer checking index

Apart from the inconsistent results for spruce at 80°C, which may be due to experimental error, the CI[4] is always found to be positive denoting that air leakage on the 'loose' side is higher than on tight side (Fig. 14). This observation confirms that the fuitometer may be used to qualitatively evaluate the amount of lathe checking that forms on the 'loose' side of the veneer (El Haouzali 2009). As may be seen from Fig. 14, up to a temperature of 70°C, there is a tendency for the CI to decrease with increasing heating temperature demonstrating the positive influence of heating on reducing veneer lathe checking. Fig. 15 confirms this positive influence by showing a reduction in lathe check depth at 70°C, which is more noticeable in beech and birch.

---

[4] $CI \, (in \, mm \, of \, water) = water \, level_{on \, tight \, side} - water \, level_{on \, loose \, side}$ (4)
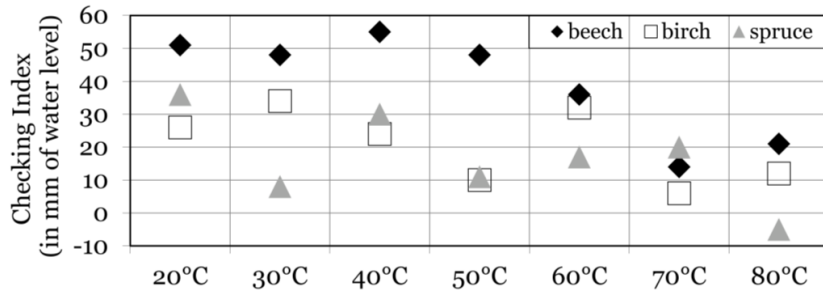
Figure 14 Influence of heating temperature on checking index (CI)

The slight increase in CI at 80°C (Fig. 14) observed in both beech and birch and the negative CI of spruce at the same temperature, may be due to the formation of 'woolly' surfaces and deeper checks. The results shown in Fig. 14 are mean values calculated on the number of specimens presented in Table 4.

	20°	30°C	40°C	50°C	60°C	70°C
Beech	83	83	83	85	83	83
Birch	84	84	84	84	84	84
Douglas-fir	68	73	80	107	82	78
Spruce	91	91	91	91	91	91

Table 4 Number of samples tested to measure CI

4.1.3. Effect of heating temperature on the distribution of checks

All three species exhibited the same behaviour with respect to check depth. As may be seen from Fig. 15, when the most frequent values are considered, check depths were roughly constant up to a temperature of 50°C, before decreasing at 60 and 70°C. This means that high heating temperatures produce veneers with shallower lathe checks. With respect to the interval between two adjacent checks, beech and birch behave alike and in the same manner as check depth, namely that high heating temperatures tend to produce veneers with a greater number of more closely spaced checks (Fig. 16). These results should, in theory, be verified by a constant Checking Ratio, CR (Eq. 2)[5] , which is only confirmed in the case of beech (Fig. 17).

---

[5] $CR = \dfrac{CIn}{CD}$ 　　　　　　　　　　　　　　(2)
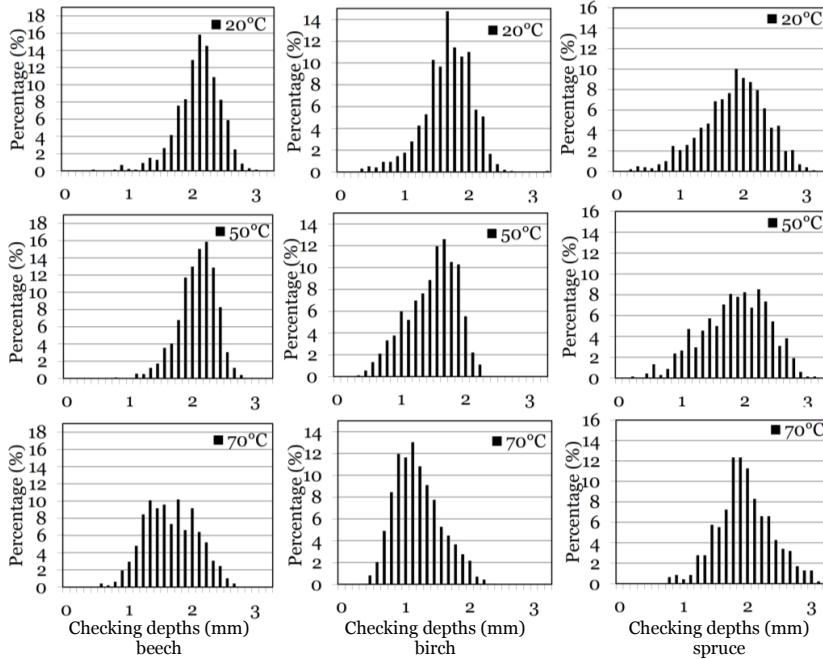
Figure 15 The distribution of check depth as a function of heating temperature[6]
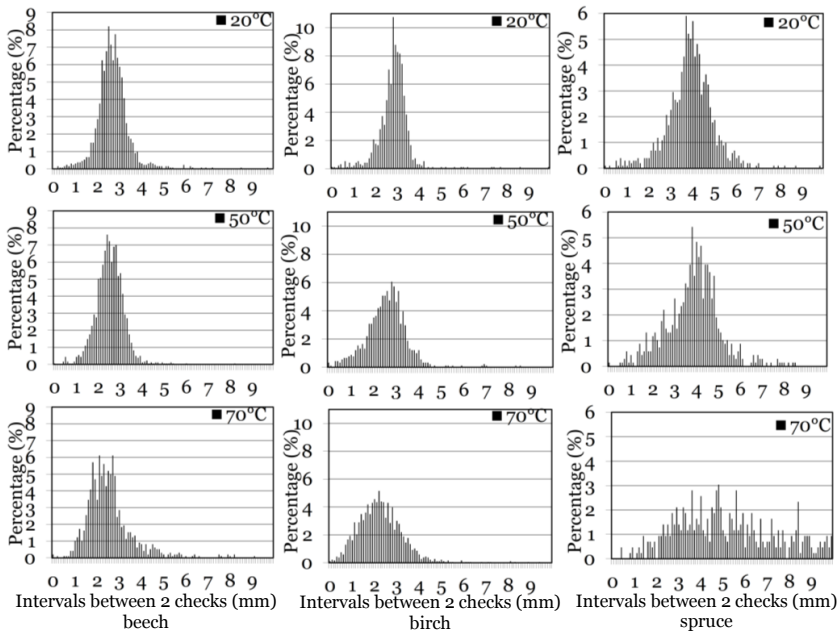
Figure 16 The distribution of the intervals between two checks as a function of heating temperature[6]

---

[6] See Paper I for diagrams at all temperatures (20°C, 30°C, 40°C, 50°C, 60°C, 70°C) for beech, birch and spruce. Diagrams at 60°C and 70°C differ from diagrams from 20°C to 50°C that exhibit roughly the same characteristics
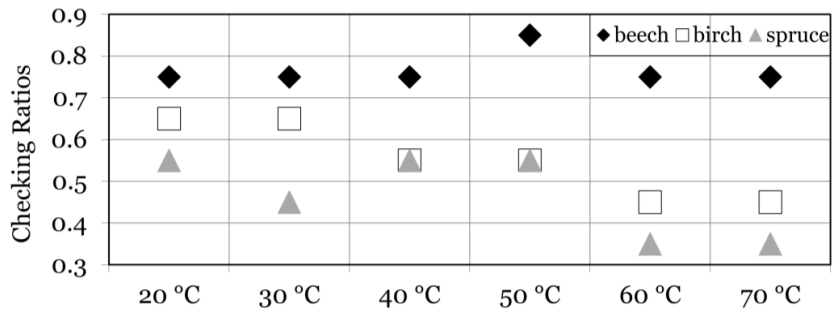
Figure 17 The influence of heating temperature on checking ratio (CR)

Another observation from Figs. 15 and 16 is that both distributions get gradually broader as temperature increases. Spruce, however, exhibits curious behaviour at 70°C: as may be seen from Fig. 16, the distribution of the intervals between two checks becomes so broad that there is no clear maximum frequency value. When the distributions are so broad, determining the most frequent values is not a statistically relevant way of characterising the checking distribution. For this reason a statistical analysis based on evaluating the coefficients of skewness[7] and kurtosis[8] of the distributions (Section 3.3.2) was chosen. For all species, the skewness and kurtosis of the intervals between two checks tends to decrease with increasing heating temperature (Fig. 18). The skewness and kurtosis of spruce are lower than that of beech and birch at all temperatures and skewness drops to 0 and kurtosis becomes negative at high temperatures. The conclusions that can be drawn from this confirm that the checks are deeper and more widely spaced at low temperatures than at high temperatures which produce smaller but more closely packed checks.

The mechanisms of lathe check formation therefore seem to become more unpredictable as the heating temperatures rise. One hypothesis is that this phenomenon is an indication of the growing impact of wood anatomy and the reduction in the stress field as a result of reaching the glass transition temperature, which occurs in the range of 50–100°C for green wood (Olsson and Salmén 1997). This hypothesis is supported in particular in the case of spruce, in which there is a big difference between earlywood and latewood (Raiskila et al. 2006) as well as higher lignin content (Fengel and Wegener 1984). This may explain why the impact of heating temperature is

---

[7] Skewness is a measure of the asymmetry of the distribution

[8] Kurtosis is a measure of the peakedness of the distribution

more visible in spruce than in a more homogeneous species such as beech. Trying to establish a link between this phenomenon and wood anatomy remains awkward and would need further investigation.
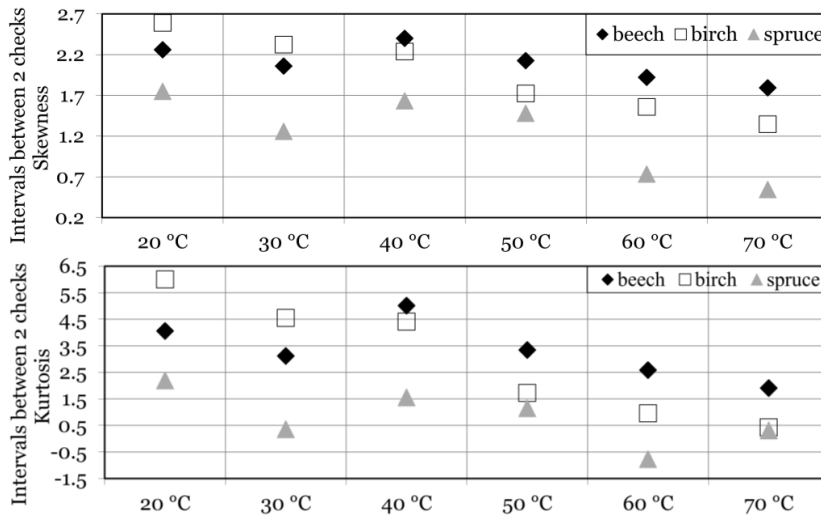
Figure 18 Influence of heating temperatures on skewness and kurtosis for intervals between two checks

4.1.4. Conclusions about optimum heating temperatures

For beech, birch and spruce, it is difficult to define 'minimum-optimum' heating temperatures based on the results that have been obtained. It appears that low temperatures produce veneers with deeper and more widely spaced checks than high temperatures where the checks are shallower and closer. At high temperatures, the check formation mechanism is less periodic and becomes governed by wood anatomy and is therefore less predictable - especially in the case of heterogeneous spruce. Even at 50°C, the positive effect of heating ensures efficient peeling. All the findings presented above indicate that there is no need to heat up the wood to higher temperatures (at least in terms of check formation). This criterion of 50°C increases the chances that an IR heating system embedded on a lathe would be able to heat wood quickly enough to ensure successful peeling. Overall, however, these results demonstrate the efficiency of the SMOF device in quantifying veneer lathe checking (by means of the intervals between two checks and check depths measured on the very long length of veneer ribbon tested) but that its use is restricted to the research

scale given the difficulty in developing the SMOF device into on-line measurement system operating on the edge of the veneers.

4.1.5. Supplementary studies on cutting efforts

The precise measurement of cutting effort as a function of the soaking temperature of the bolts being peeled would be a useful tool that would bring additional data to determine more accurately 'minimum-optimum' heating temperatures. Supplementary tests were carried out using the industrial peeling lathe available at Arts et Metiers ParisTech, Cluny, France that was equipped with in-line Kistler piezo-electric sensors providing data about cutting efforts. The resulting data are the mean and standard deviation of cutting effort (in daN) applied on the cutting knife - Xk and Yk (Fig. 19).
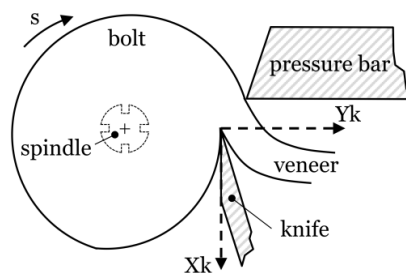
Figure 19 Efforts applied on the cutting knife (Xk is vertical and Yk horizontal)

Looking at the results with the pressure bar, bolts heated to either 30°C or 50°C result in roughly the same amount of efforts on the cutting tools as the unheated control bolt at 20°C (Fig. 20). Up to 50°C, heating temperature influences the cutting efforts in the case of Douglas-fir to a small extent (10% in Xk, 20% in Yk). This finding is at variance to observations in oak and chestnut (Marchal 1989). However, above 50°C, a decrease begins leading to a reduction of 31% in Xk and of 46% in Yk as the temperature rises from 50°C to 80°C (Fig. 20). The difference in cutting efforts measured with or without the pressure bar diminishes as the heating temperature increases, showing that the transfer of effort from the pressure bar to the cutting knife, present when the wood is unheated, disappear when the wood is heated. Nevertheless, coefficients of variation (COV) in cutting efforts (the error bars in Fig. 20) do not, as might be expected, exhibit any regular decrease as heating temperature increases. COV in

35

cutting efforts measure noises due to vibrations caused by the cutting tools encountering knots. Consequently, the heating of bolts aimed at softening knots locally should reduce the impact of intra-ring heterogeneity and limit the efforts on the cutting tools (Marchal et al. 2004). However, at only 2%, the percentage of knots in the Douglas-fir veneers tested was small and might well account for the lack of reduction in coefficients of variation.
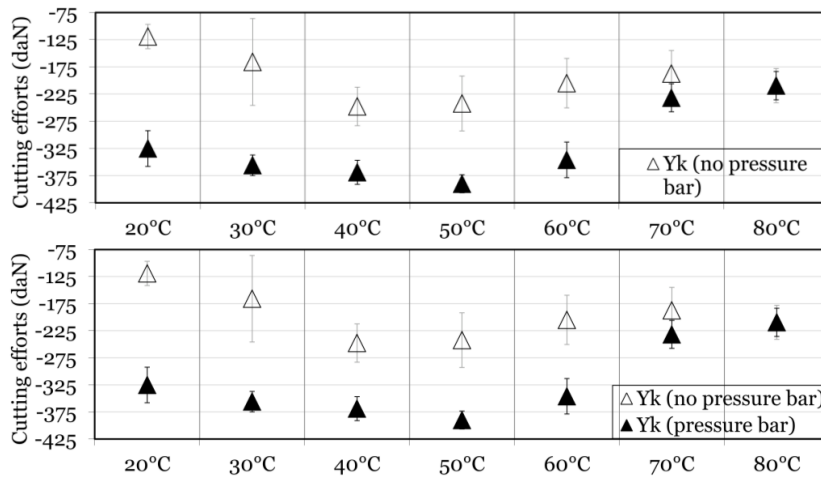
Figure 20 Influence of heating temperatures on cutting efforts of the cutting knife for Douglas-fir (standard deviations detailed) with pressure bar Bp at 5 % and without pressure bar

Unfortunately, due to measurement difficulties, the cutting efforts on the other wood species under investigation could not be studied. It would be of great interest to continue such a study on cutting efforts using the micro-lathe available at Arts et Metiers ParisTech, Cluny, France. This device can peel disks free from defects, providing more accurate results on the one hand but, due to the thickness of the disk, increasing the difficulty of controlling the heating temperature on the other.

4.2. Optical properties of wood

An integrating sphere enabled the experimental measurement of the spectra of normal hemispherical spectral reflectance and transmittance over the wavenumber σ range 550 to 5500 cm^{-1} (i.e. wavelengths L from 1.8 to 18 μm) in green wood samples to be made. From these results it was

possible to estimate the amount of energy absorbed by the wood and the penetration depth of the IR radiation. Such data are necessary to develop accurate numerical models designed to simulate the thermal behaviour of wood being heated by an external IR source (Section 4.4), but which are lacking in the literature – especially in green wood where the MC distribution is complex. If it could be shown that wood can absorb IR energy to a certain depth, then equations predicting the heating of wood layers beneath the surface by an external IR source should take into account the volumetric absorption of IR energy within wood and not only the transfer of the heat absorbed by the surface layers through conduction to the inside layers. This study also investigated the influence of moisture and knots on the optical properties of green wood as well as the effect of remoistening wood which is not detailed here, but can be found in Paper II.

4.2.1. Amount of energy absorbed and penetration depth

Fig. 21 shows that both transmission and reflection increase with higher frequencies, i.e. at shorter wavelengths. The amount of energy effectively absorbed by the wood is more significant at longer wavelengths than in the near-IR range next to the visible range, below 2500 cm^{-1}. Up to 4000 cm^{-1}, the 0.5 mm sample absorbs nearly all incident energy (absorption is close to 0.95) and no energy is transmitted through the samples. In contrast, the 0.2 and 0.3 mm thickness samples were found to transmit energy. In the 1800-3000 cm^{-1} range, transmission was found to be around 0.3 for the 0.2 mm thick samples and around 0.1 for the 0.3 mm thick samples. This indicates that between 550 and 4000 cm^{-1} around 70% of the incident radiation is absorbed by the first 0.2 mm of wood and around 90% of the incident IR radiation in the first 0.3 mm of wood. The thinner the sample, the more radiation transmitted through it and the thicker the sample, the greater the amount of reflected and absorbed radiation. The relatively low penetration depth of 0.3 mm might be explained by the heterogeneous structure of wood which can be modelled as a network of cellulose microfibrils embedded in a matrix of hemicelluloses and lignin, interspersed with water and void spaces. In the case of homogeneous materials, radiation propagates linearly with progressive exponential absorption following Beer-Lambert's law. However, the different refractive indices in heterogeneous materials backscatter the penetrating radiation preventing linear propagation, so that the strength of the radiation becomes smaller as it penetrates deeper.

Figure 21 Reflection, transmission and absorption spectra for 0.2mm, 0.3mm and 0.5mm thick green beech samples (at 53.1%, 50.0% and 52.3% respective MC)

4.2.2. Effect of moisture on the optical properties of wood

Fig. 22 shows the reflection, transmission and absorption spectra at different MC for a 1.6 mm thick beech sample. All samples with thicknesses greater than 0.5 mm, and all species tested, exhibited similar behaviour. Reflection varied between 10 and 30% with the most significant amount of reflected radiation occurring on drier wood. Transmission could be neglected because it remains constantly weak (less than 5%) without being influenced by the amount of water in wood. Therefore, Tr is negligible and the complement to 1 of reflectivity gives absorptivity A[9] (Eq. 5). Absorption varied from 70 to 90% with the most significant amount of absorbed radiation occurring in wetter wood. The presence of water in wood is thus beneficial in terms of IR penetration because it increases the amount of absorbed energy. However, if this substantial increase serves to heat the water present in wood, it is of no interest for the purpose being investigated herein, namely to heat the wood cell walls with IR radiation.

---

[9] $A = 1 - R - Tr$ (5)
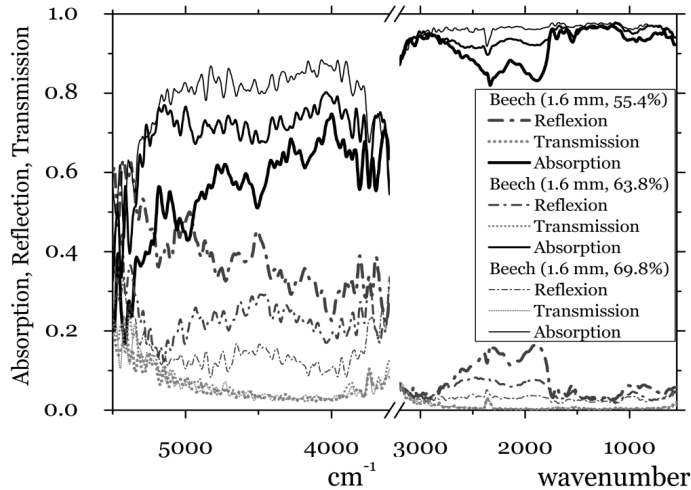
Figure 22 Reflection, transmission and absorption spectra for 1.6mm thick green beech sample at 55.4%, 63.8% and 69.38% MC

4.2.3. Effect of knots on the optical properties of wood

This investigation is of interest since the characteristics of knots – for instance high density and variable grain direction (Kollmann and Côté, 1968) are known to be detrimental to cutting tools. If knots were to absorb more energy than the surrounding wood, IR could be used, for example, to preferentially heat the knots thereby softening them and making them easier to be cut across the grain during veneer peeling. Experimental results have shown that the presence of knots may be seen to increase penetration depth by several tenths of millimeters (Fig. 23). Fig. 23a (resp. Fig. 23b) shows that samples of 0.9 mm (resp. 0.5 mm) of birch (resp. Douglas-fir) feature absorption curves that are less close to 1 than the ones at 1.1 and 0.7 mm respectively – which means that they enable some IR radiation to transmit. A possible explanation for this is that the denser wood in knots contains a relatively greater number of molecules able to absorb energy. Moreover, the different orientation of the fibres around the knots may also affect energy absorption. Both wood density and fibre orientation have been noted by Zavarin et al. (1990) to be factors influencing energy absorption in wood.

(a)

Birch (0.9 mm, 44.6%)
without knots
– – Reflection
· · · Transmission
—— Absorption
Birch (1.1 mm, 44.8%)
with knots
– – Reflection
· · · Transmission
—— Absorption

(b)

Douglas-fir (0.5 mm, 19.0%)
without knots
– – Reflection
· · · Transmission
—— Absorption
Douglas-fir (0.7 mm, 20.1%)
with knots
– – Reflection
· · · Transmission
—— Absorption
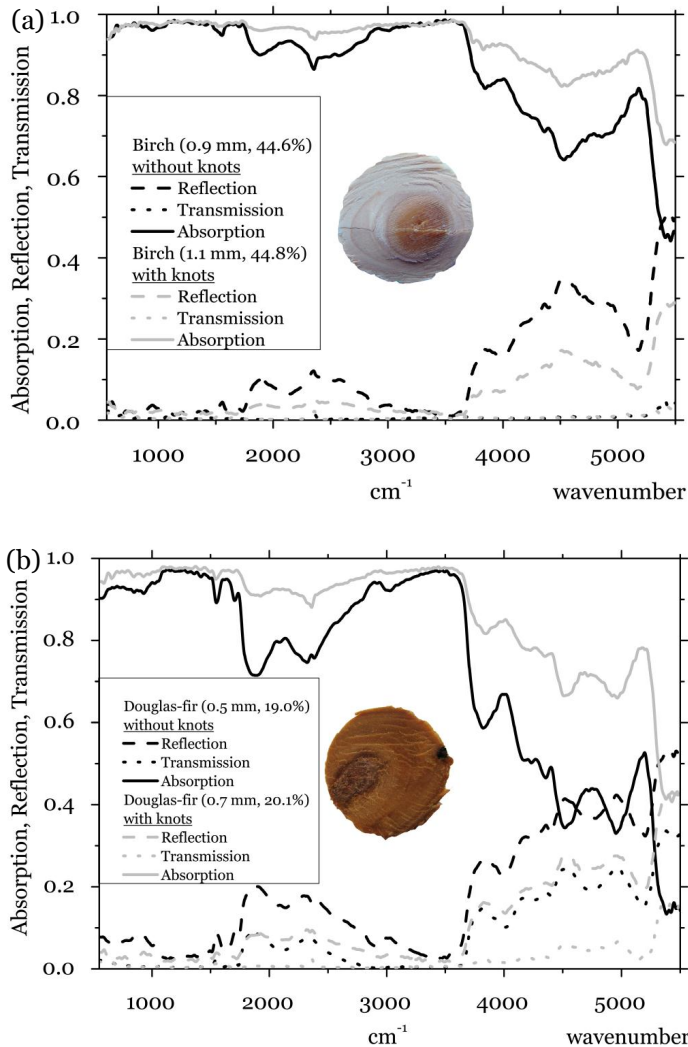
Figure 23 Reflection, transmission and absorption spectra of samples with and without knots for (a) birch and (b) Douglas-fir (thickness sample and sample MC in brackets)

4.2.4. General conclusions on optical properties of wood

For clear wood, it is not possible to deliver energy deeper than up to 0.3 mm below the wood surface because 70 to 90% of all incident IR radiation on the wood surface is absorbed in this layer. In the case of knots, however, it is possible to deliver the energy several tenths of millimeters deeper. These results illustrate that IR radiation can heat the surface layers, but then penetration deeper into the wood is by conduction. Some wood features, such as the presence of knots and of free water in wood (the latter two having a more significant effect), increase the amount of energy

40

absorbed. These findings do not necessarily suggest that the IR heating of green wood is impracticable, but they highlight the fact that IR radiation is mainly absorbed near the surface without penetrating deeply into the wood. Equations predicting the heating of wood layers beneath the surface by an external IR source should only take into account the transfer of the heat absorbed by the surface layers by conduction to the inside layers. Consequently, the equations governing the numerical modelling should not integrate any volumetric absorption of IR into wood but are governed by Eq. 7[10] - the transient heat transfer equation for conduction derived from Fourier's law.

4.3. Thermal properties of green wood

The TPS technique was used to characterise the thermal behaviour of green wood, providing empirical equations to predict the values of thermal conductivity, λ, heat capacity, C, and thermal diffusivity, κ, at the macroscopic level on the one hand and wood MC on the other. The target of this work was to feed the numerical models with these inputs. For this purpose, the natural features of wood such as its anisotropy and knots were also studied because of the possible influence on the thermal behaviour of green wood.

With the TPS technique, the temperature measurement is localised at the heating element. As explained earlier (Section 3.5), the probe size is limited by the characteristic time and by the size of the sample to avoid edge effects: the probe cannot encompass the whole sample. The influence of heterogeneities cannot be completely eliminated if the probe location is changed: the pattern of annual rings varies and the heat flows through the different densities of earlywood and latewood at different rates. However, the repeatability of the experiments was demonstrated by moderate standard deviations. The coefficients of determination, R^2, relative to the equations presented in Figs. 24 , 25 and 26 and in Table 6 are based on calculations made on the number of tests presented in Table 5.

---

[10] $\rho c \dfrac{\partial T}{\partial t} = \nabla(\lambda \nabla T)$ (7)

	With knots	Without knots	
		radial	tangential
Beech	11	49	63
Birch	8	47	86
Douglas	8	64	82
Spruce	20	70	78

Table 5 Number of tests to measure the thermal properties

4.3.1. Relationship between thermal conductivity, λ, and MC

Fig. 24 compares the λ values obtained experimentally with the HotDisk®
with those obtained by the steady-state guarded hot plate method
(Sonderegger et al. 2011). Apart from beech, the experimental values for λ
consistently match the results from the literature (Sonderegger et al. 2011).

The reason for this difference might arise from the different experimental
methods used between the literature and the experiments performed here.
There is no significant difference in λ between the radial and tangential
directions for wood in the green state – apart from spruce. It seems that the
presence of free water in the cell overrides any effects arising from the
anisotropy of the wood. The exception in the case of spruce might be
explained by the presence of ray cells that promote heat transfer in the
radial direction ($\lambda R > \lambda T$).

4.3.2. Relationship between heat capacity, C, and MC

Fig. 25 compares the C values obtained in this work with those of
Sonderegger et al. (2011) and oven-dry values at 20°C found in the
literature (Jia et al. 2010, Kollmann and Côté 1968, Steinhagen 1977). The
gradients of the linear relationships between C and MC above f.s.p are
steeper than below the f.s.p (results from literature), most probably arising
from the dominating effect of the free water. The scattered results for
Douglas-fir and spruce can be interpreted to mean that C in the green state
is not unique for all wood species. There are probably two different ranges
of C values depending on whether the material is a hardwood or softwood:
the former in the green state would need more energy for heating than
softwoods. This behaviour is different from that described in the literature
below the f.s.p. Fig. 25 also confirms the assumption made in Section 3.6
that the effect of MC on C is more significant than the effect of density
because from 0 to 30% MC, at constant density, C retains the same value
but increases highly with MC above f.s.p.
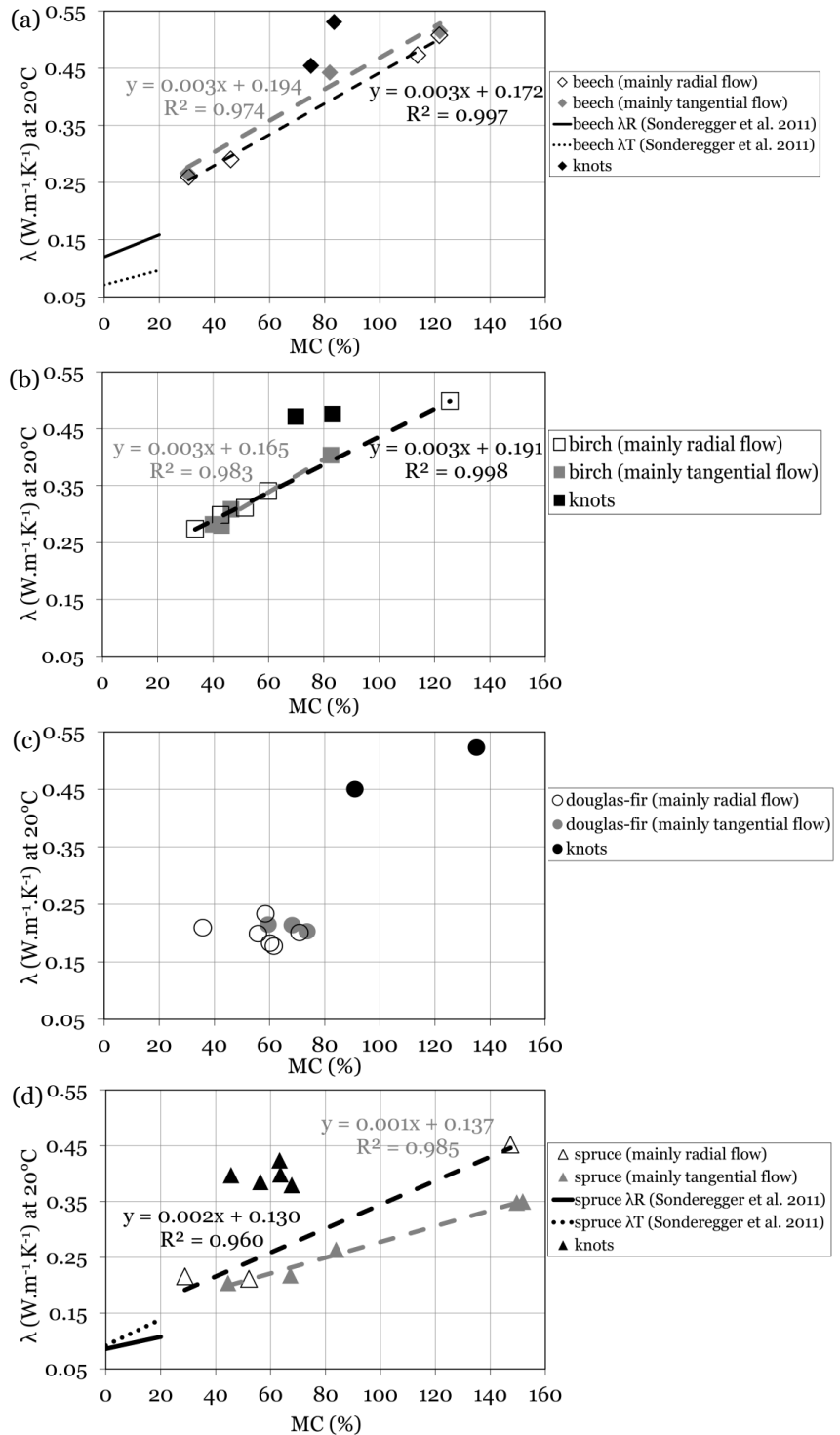
Figure 24 Thermal conductivity λ (in W.m⁻¹.K⁻¹) of (a) beech, (b) birch, (c) Douglas-fir and (d) spruce in the green state with and without knots obtained using the HotDisk® (dotted lines are linear regressions on experimental data)
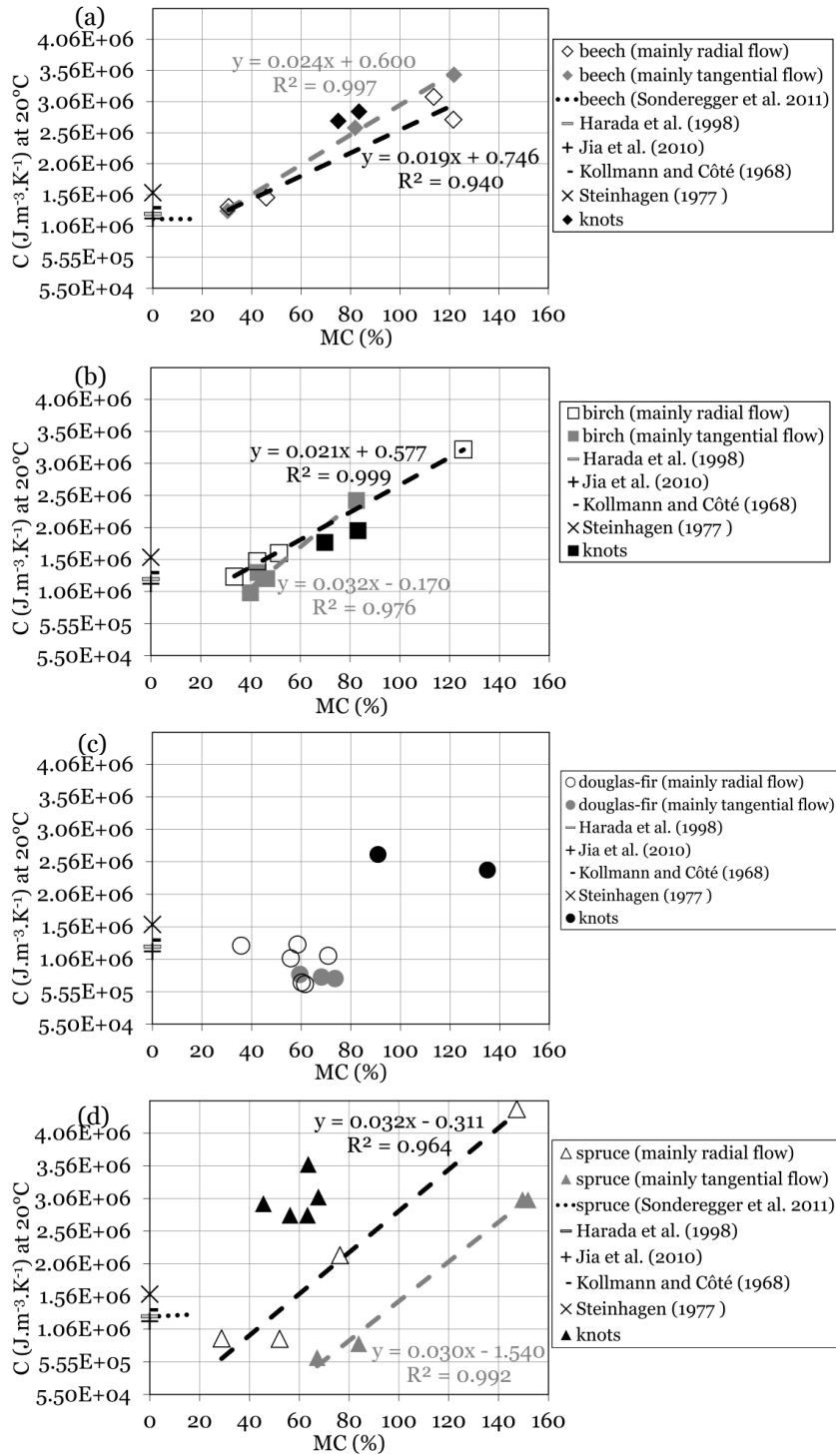
Figure 25 Heat capacity C (in J.m^{-3}.K^{-1}) of (a) beech, (b) birch, (c) Douglas-fir and (d) spruce, with and without knots, in the green state measured using the HotDisk® (dotted lines are linear regressions on experimental data)

4.3.3. The relationship between thermal diffusivity, κ, and MC

Fig. 26 shows κ values obtained experimentally. The comparison is available only in the radial direction because samples for the flash method were obtained from veneers peeled tangentially (Beluche 2011). The results obtained with both methods are close to each other while the flash method differs from the HotDisk®: the flash method consists of (nearly) instantaneously radiating a sample on its front face and then recording, as a function of time, the temperature increase on its rear face (Parker et al. 1961). The percentage differences between both methods are low (4% difference for Douglas-fir at 56% MC and 7% difference for beech at 46% MC). The similarity of the data in Fig. 26 is an indication of its reliability.

4.3.4. Thermal characteristics of knots

In Figs. 24, 25 and 26, the black points represent the thermal characteristics of knots measured with the HotDisk® method compared to the values of clear wood (mainly tangential flow in grey, mainly radial flow in white, Fig. 10). For all species, λ is higher for knots than for clear wood. Apart from spruce, C is also higher for knots than for clear wood. This is quite logical as the density of knots is higher, therefore representing more material to heat and requiring more energy. The different results for spruce might be explained by the resin content of the softwood or might be due to some experimental difficulty in covering the knots with a HotDisk® probe of correct radius (see the pictures of some tested knots in Fig. 23). In any case, such a study on knots would necessitate further experimental tests to confirm the results found here namely that knots require more energy to heat but diffuse heat more rapidly to the inside of the wood.
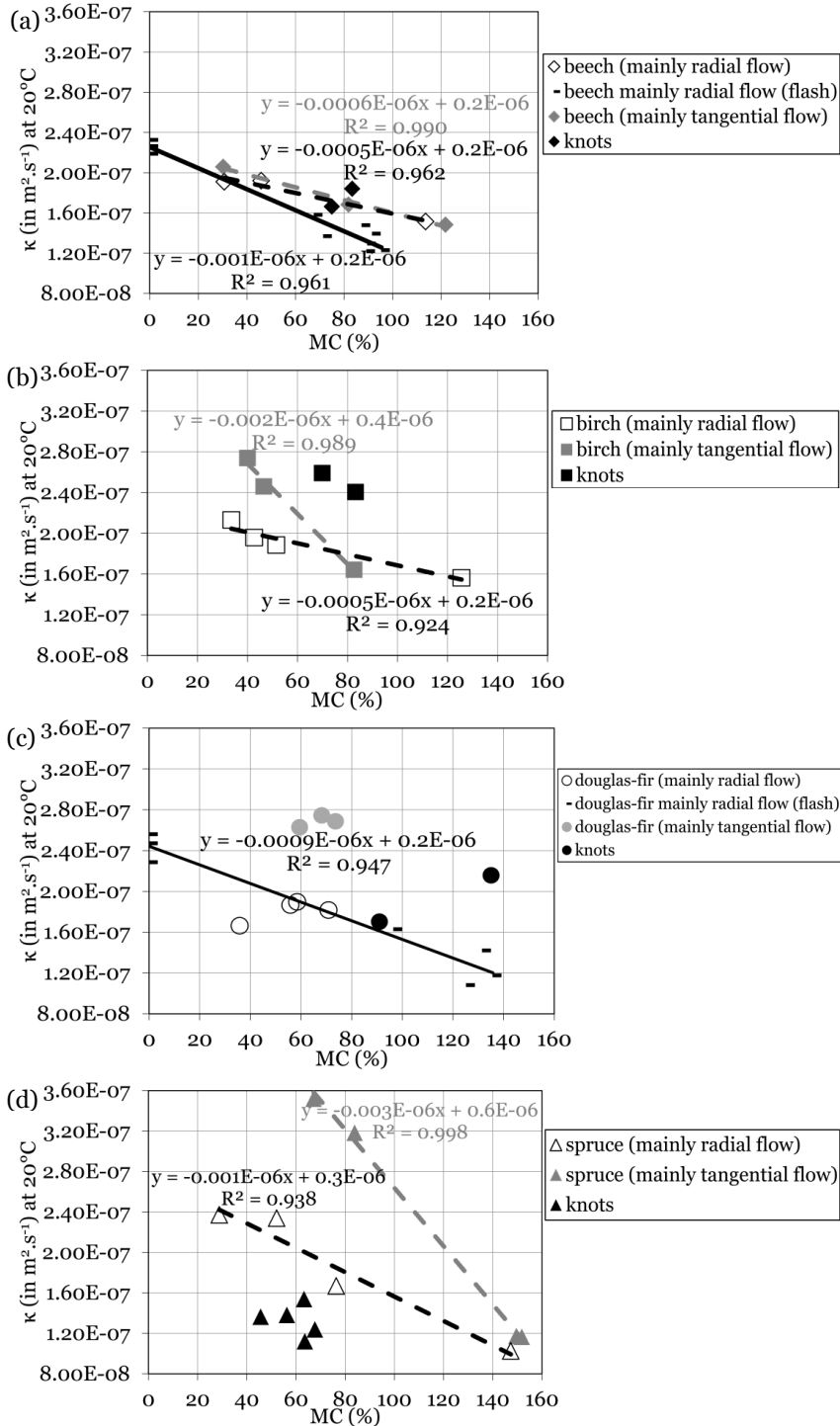
Figure 26 Thermal diffusivity κ (in m².s⁻¹), measured in the green state with the HotDisk® method, of (a) beech, (b) birch, (c) Douglas-fir and (d) spruce, with and without knots (dotted lines are linear regressions of experimental data with the HotDisk®, straight lines are linear regressions of experimental data with the flash method, Beluche 2011)

46

4.3.5. Conclusions on wood thermal properties

Table 6 presents the predictive equations for λ, C, and κ obtained by the HotDisk®. As is clearly visible, the relationship with MC above the f.s.p is good, as expressed by the high coefficients of determination, R^2. From these results, it can be concluded that:

(1) the thermal behaviour of water, which is more conductive and which has a higher heat capacity than wood, overrides that of wood, thus at higher MC the thermal behaviour of green wood tend towards that of water. However, the insulating properties of wood material limit the thermal behaviour of green wood which never reaches that of water at any MC, even above 100%.

(2) in clear wood above the f.s.p, there is still a linear relationship between the thermal properties λ, C and κ on the one hand, and MC on the other. Wood C and λ increase with MC but wood κ decreases with MC. Therefore wet wood requires more input energy in heating than dry wood but it takes more time for heat to transfer within wet wood and the temperature reached at a given depth in a given amount of time is higher in the case of wet wood.

(3) in the green state, the influence of anisotropy R-T is negligible in these species, with λ being the same in the radial and tangential directions, whilst C would differs between hardwoods and softwoods, being higher in hardwoods.

Table 6 and conclusions (1) and (2) are significant: by knowing the wood MC, it is now possible to deduce the thermal properties (λ, C) that would be necessary to calculate the heating rates (Section 4.4). Conclusion (3) strengthens the knowledge of the thermal behaviour of green wood but is of less interest for the purpose of the study.

Predictive equations for thermal conductivity (λ), thermal diffusivity (κ), and heat capacity (C)	
Equations in radial direction	**Equations in tangential direction**
HotDisk®	
Beech	$\lambda R = 0.003\ MC + 0.172\ (R^2\ 0.997)$	$\lambda T = 0.003\ MC + 0.194\ (R^2\ 0.974)$
Birch	$\lambda R = 0.003\ MC + 0.191\ (R^2\ 0.998)$	$\lambda T = 0.003\ MC + 0.165\ (R^2\ 0.983)$
Spruce	$\lambda R = 0.002\ MC + 0.130\ (R^2\ 0.960)$	$\lambda T = 0.001\ MC + 0.137\ (R^2\ 0.985)$
Beech	$CR = 0.019\ MC + 0.746\ (R^2\ 0.940)$	$CT = 0.024\ MC + 0.600\ (R^2\ 0.997)$
Birch	$CR = 0.021\ MC + 0.577\ (R^2\ 0.999)$	$CT = 0.032\ MC - 0.170\ (R^2\ 0.976)$
Spruce	$CR = 0.032\ MC - 0.311\ (R^2\ 0.964)$	$CT = 0.030\ MC - 1.540\ (R^2\ 0.992)$
Beech	$\kappa R = -0.0005\ MC + 0.2\ (R^2\ 0.962)$	$\kappa T = -0.0006\ MC + 0.2\ (R^2\ 0.990)$
Birch	$\kappa R = -0.0005\ MC + 0.2\ (R^2\ 0.924)$	$\kappa T = -0.002\ MC + 0.4\ (R^2\ 0.989)$
Spruce	$\kappa R = -0.001\ MC + 0.3\ (R^2\ 0.938)$	$\kappa T = -0.003\ MC + 0.6\ (R^2\ 0.998)$
Flash	
Beech	$\kappa R = -0.001\ MC + 0.2\ (R^2\ 0.961)$	
Douglas-fir	$\kappa R = -0.0009\ MC + 0.2\ (R^2\ 0.947)$	

Table 6 Equations and coefficients of determination of linear regressions plotted for λ, C and κ in the radial and tangential directions (adapted from Paper III)

4.4. Results and comparison of heating rates simulated numerically, calculated analytically and measured experimentally

With all the results obtained by this stage, it is possible to:

- simulate numerically the heating rates of a rotating green bolt by implementing in the model the equations which govern the heat transfer in the green bolt i.e. the equations of conduction with no volumetric absorption of IR radiation;

- check the reliability of this simulation by comparison with experimental results – using the MC of real case samples to characterise them thermally and simulate their behaviour under IR heating in the model;

- verify the feasibility of an IR heating system – by considering that achieving a temperature of 50°C in the time-frame allowed by the peeling process would be a criterion for success.

4.4.1. Validating the hypothesis of semi-infinite behavior in 1D Cartesian coordinates

In comparing experimental data to numerical results, the difficulty of assessing the effective real flux density received by the sample, which is necessary input data for the numerical simulation, was faced. Since it was not possible to reliably measure the absolute value of the flux density experimentally, the following alternative approach was adopted. If the experimental situation could be reduced to semi-infinite behaviour in 1D Cartesian coordinates described by simple analytical considerations, the surface temperatures could be used to derive the flux density received by the sample. This hypothesis would be validated if the surface temperatures plotted as a function of the square root of time $T_{surf} = f(\sqrt{t})$ showed the same linear behaviour as predicted by the simplified analytical equation, Eq. 8[11]. In view of the variability of the experimental measurements of $T_{surf} = f(t)$ on the different replicate samples (due to the natural heterogeneity of wood) it is more reliable to check this hypothesis on the results of $T_{surf} = f(\sqrt{t})$ obtained by numerical simulation. Fig. 27 shows the results for beech in the early stages of heating (up to $3\sqrt{s}$). The table inserted in Fig. 27 summarises the corresponding results obtained in the cases of birch, Douglas-fir and spruce. From the results presented in Fig. 27, two conclusions can be drawn. Firstly, the linearity of the relationship $T_{surf} = f(\sqrt{t})$, confirmed by the high coefficients of determination R^2, validates the assumption that the log can be treated as a semi-infinite body with a step increase in surface temperature of a half-space. Secondly, for the four species, the near equivalence of α_{surf}^{simul} (calculated by linear regression analysis of numerical simulation curves) and $\alpha_{surf}^{anal} = \dfrac{2\,q}{\sqrt{\pi}\sqrt{\lambda\rho c}}$ (calculated with the simulation parameters) confirms the suitability of a 1D analytical equation in Cartesian coordinates (Eq. 8[11]) to be used to evaluate the surface temperature increase of a green log rotating under external IR heating. The slight difference between α_{surf}^{simul} and α_{surf}^{anal} in the case of spruce and Douglas-fir can be explained by the lack of linearity at the beginning of the curve (which is also visible in the other species) due to a perturbation at the early stages attributable to the numerical simulation.

---

[11] $T_{surf} = \dfrac{2q}{\sqrt{\pi}\sqrt{\lambda\rho c}}\sqrt{t}$ $\qquad\qquad\qquad\qquad$ (8)
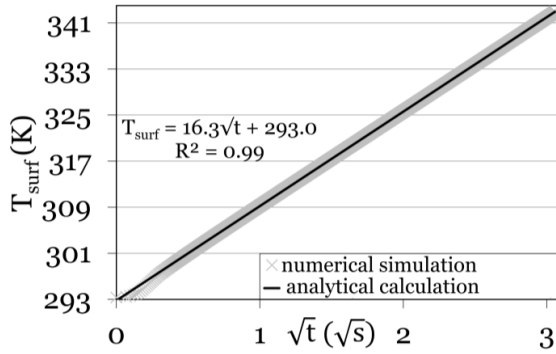
49

	$R^2(*)$	α_{surf}^{simul}	α_{surf}^{anal}
Beech	0.99	16.3	16.3
Birch	1	15.4	15.4
Douglas-fir	1	24.4	24.3
Spruce	0.99	19.6	19.5

(*) calculated on 80 values

Figure 27 Comparison of Finite Element simulated surface temperatures of rotating log and analytically calculated surface temperature response of half space. The temperatures are represented as a function of the square root of time for beech. Table: Comparison of numerical and analytical values of the slopes α_{surf}^{simul} and α_{surf}^{anal} of $T_{surf} = f(\sqrt{t})$ with their corresponding coefficients of determination, R^2, in the case of beech, birch, Douglas-fir and spruce

By deconvoluting the recorded surface temperature data, T_{surf}, using the inverse method proposed by Beck et al. (1985), it is possible to recover the signal q as it existed before becoming convoluted by the impulse response of the half-space. The result of this procedure gives the maximum value (found to be around 10 000 W.m^{-2}) of the estimated heat flux density, q_{est}, and the spatial profile of the effective real flux density received by the sample which is necessary data for input into the model in order to compare the simulation to the experimental results (Fig. 28). Fig. 28 compares for one sample the normalised values of the estimated heat flux density, q_{est}, with the measured IR sensor signal, q_{mes} - which corresponds directly to the electric signal produced by an IR sensitive sensor placed on the sample surface. The reliability of the deconvoluting procedure is assessed in Fig. 28 by the good fitting of the two curves. This provides further confirmation (with the results presented above) of the ability of analytical equations to describe the temperature increase in a rotating green log under external IR heating.
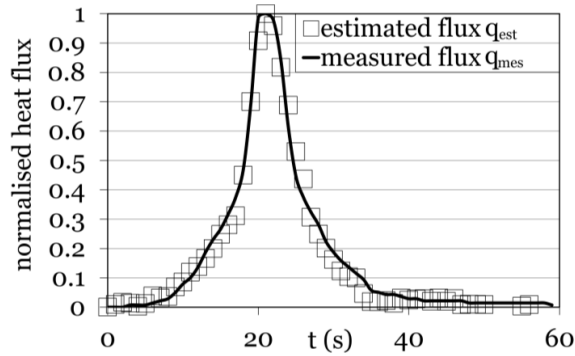
Figure 28 Comparison of estimated heat flux density and the measured IR sensor signal on the sample surface (normalised values are represented)

4.4.2. Heating rates of surface temperatures

In Figs.29, 30 and 31, the residuals are calculated with the difference between experimental and modelled results and are plotted below each graph. Fig. 29a compares the surface temperatures $T_{surf} = f(t)$ of beech at 43% MC, obtained experimentally from surface thermocouples (Section 3.7) with the numerical simulation results modelled using similar parameters. Similar results were also obtained for birch at 85% MC (Fig. 29b), Douglas-fir at 115% MC (Fig. 29c) and spruce at 55% MC (Fig. 29d). In the 20 first seconds, the increasing slopes of the experimental curves are steeper than simulated (the residuals drop consequently below 0). This difference might be explained by some eventual moisture gradient within wood created when drying, being responsible for heterogeneity in the thermal properties of wood which are impossible to evaluate accurately and to implement in the model. Moreover variations in the surface emissivities of different wood samples can lead to some errors in the heat flux received by the samples. However, apart from this difference, these results show reliable agreement between the numerical estimation and measurement (as can be seen by residuals which balance around 0).
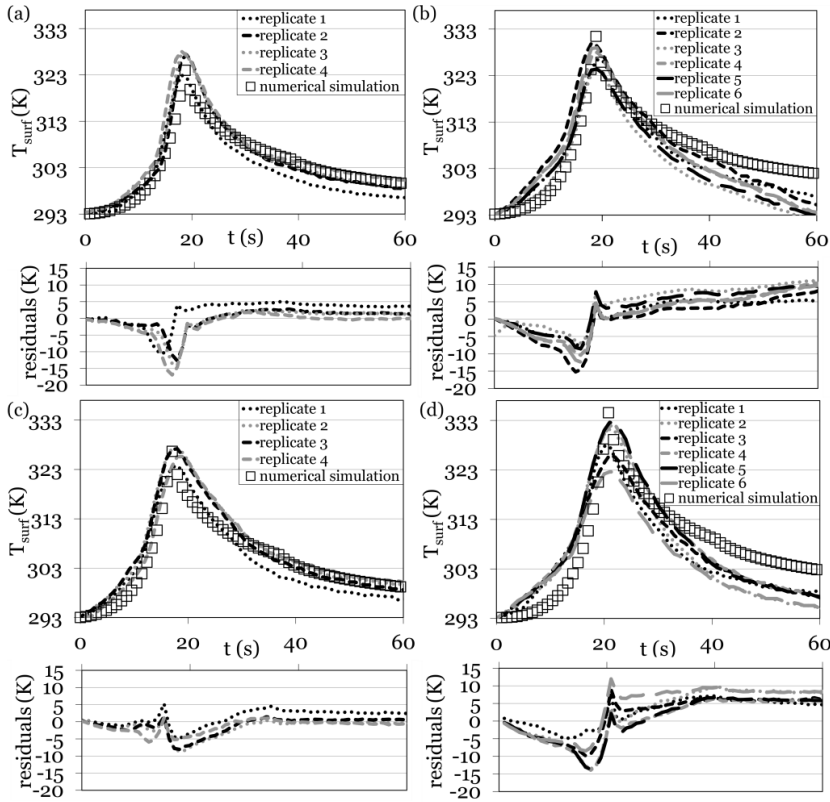
Figure 29 Comparison of numerical simulation curves of surface temperatures T_{surf} = f(t) to experimental results obtained on different replicates of (a) beech at 43% MC, (b) birch at 85% MC, (c) Douglas-fir at 115% MC and (d) spruce at 55% MC (residuals are plotted below each graph)

4.4.3. Heating rates within wood

For several replicates of birch at 85% MC and Douglas-fir at 115% MC, Figs. 30a and 30b compare the temperatures T_{3mm} = f(t) obtained experimentally from the thermocouples embedded 3 mm below the wood surface, with numerical simulation results modelled using similar parameters. These results show good agreement between numerical estimation and measurement with low residuals relatively close to 0.
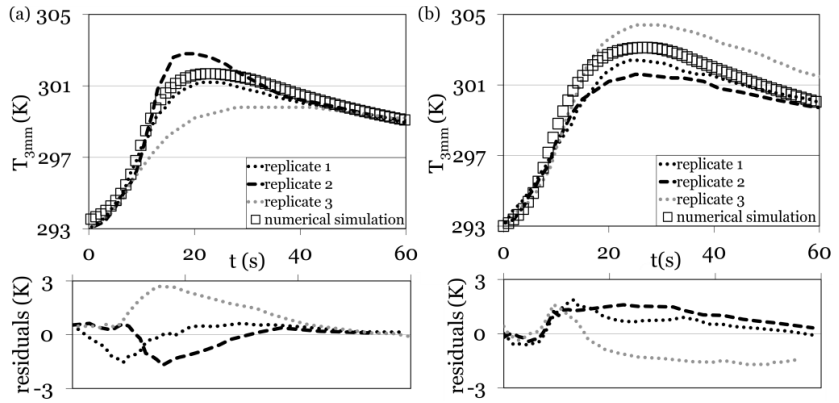
Figure 30 Comparison of numerical simulation curves of temperatures measured at 3 mm depth T_{3mm} = f(t) to experimental results obtained on different replicates of (a) birch at 85% MC, (b) Douglas-fir at 115% MC (residuals are plotted below each graph)

However, around the maximum temperature, the residuals increase. Difficulty in fitting the numerical simulation to the experimental data may arise from three factors: (1) the imprecise insertion depth of the thermocouples; the margin of error in the insertion depth of the thermocouples was estimated to be ±0.5 mm, which clearly might have had an effect, (2) the effect of drying during heating; the difference in the block MC before and after heating, ΔMCs, remained low (never exceeding 5%), however, even though it could not be reliably measured, this change was attributed to water evaporating from the surface layers of the samples, (3) the influence of sawing; the differences in densities (and thus in thermal properties) between earlywood and latewood may have a greater influence in quarter sawn samples where annual rings are parallel to the IR flux (Fig. 6). In order to take the effect of drying on thermal properties of wood into account, it is possible to estimate to 50% the margin of error in the MC. Assuming both effects (1) and (2), Fig. 31 plots the envelope curves (in dotted lines) of temperatures below the wood surface, T_{3mm} = f(t), simulated numerically in the most favourable case, where both insertion depth and MC are underestimated (Fig. 31a plots $T_{2.5mm}$ = f(t) at 21% MC and $T_{3.5mm}$ = f(t) at 65% MC for birch) and in the least favourable case when insertion depth and MC are overestimated (Fig. 31b plots $T_{2.5mm}$ = f(t) at 27% MC and $T_{3.5mm}$ = f(t) at 83% MC for spruce). When plotting these envelope curves, the effect of drying (2) predominates over the effect of the imprecise insertion of the thermocouples (1). The envelope curves surround all the experimental curves, which demonstrate that taking into account these two effects is more representative of the reality of the experiments.
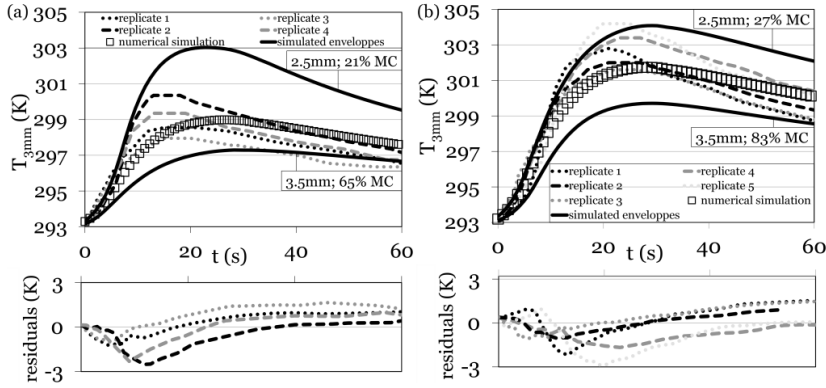
Figure 31 Comparison of experimental results measured at a depth of 3 mm with numerical simulation curves of temperatures $T_{3mm} = f(t)$ and their envelopes $T_{3\pm0.5mm} = f(t)$ (dotted lines) obtained on different replicates of (a) beech at 43±22% MC, (b) spruce at 55±28% MC (residuals are plotted below each graph)

4.4.4. Conclusions on heating rates

By comparing experimental to numerical simulation results, the ability of the numerical model using finite elements to simulate, in 2D, heat transfer within a log and to output the temporal evolution of surface and below surface temperatures, has been validated. During this validation process, it has been demonstrated that simple analytical equations, that assume the behaviour to be that of a semi-infinite body in 1D Cartesian coordinates, can estimate the heating rates and the maximum temperatures achievable at the surface and below the surface (Eqs. 8 and 10). With both methods, the inputs are the thermal and physical properties of green wood and the heat flux density of the IR source. With these analytical equations (Eqs. 8 and 10), it is possible to rapidly calculate the temperature at a certain depth below the surface and the maximum surface temperature reached by a green log which is be particularly useful in setting up the parameters for an IR heating system. None of the simulation presented could achieve temperatures around the required temperature of 50°C established beforehand. Increasing the IR heat power enables the heating of the wood surface but the temperature at the cutting plane, located at several millimeters beneath the surface, remains low and the time needed for the heating of wood by conduction is too long compared to the time available at existing industrial peeling speeds.

5. Conclusions and perspectives

The results of this study demonstrate that, at peeling speeds currently used in the plywood and LVL industry, it is not possible to heat green wood with on-line IR radiation and achieve a temperature of 50-60°C at the cutting plane. With regard to this problem, however, an experimentally validated numerical mode has been developed, which can for a given peeling speed, s, determine the heating flux density, q, required to reach a given heating temperature several millimeters beneath the wood surface. Conversely, for a given heat flux density, q, the temperature at a given depth can be used to determine the appropriate peeling speed. Additionally, it has been demonstrated that the situation of a log rotating under external IR heating could be described by simplified 1D analytical equations of a half space, which would be useful for rapid calculations.

When talking about the future of IR as means of warming logs prior to peeling, one opportunity would be to use IR as additional heating on the lathe to maintain the hot log at the required temperature while turning on the lathe. The means of preheating could be microwave, given its efficiency at heating logs rapidly (Coste and De Bevy 2005). In this regard, the results of an going investigation (not reported herein) being carried out at Aalto University to assess the influence of the heating method (soaking or IR) on the surface properties (colour and wettability at 12% MC) of green wood would be particularly important in order to understand whether IR can degrade the surface of veneer.

However, in achieving the main targets of this study, deeper knowledge has been gathered about green wood and some significant new findings have been obtained especially concerning (1) green wood interaction with IR radiation and (2) green wood thermal characteristics.

(1) clear wood absorbs 70 to 90% of all incident IR radiation in the first 0.2 to 0.3 mm surface layers;

(2) above the f.s.p, clear wood requires more input energy in heating than dry wood (higher C for wet wood); it takes more time for heat to transfer within wet wood and the temperature reached at a given depth in a given amount of time is higher in the case of wet wood (lower κ for wet wood). Above the f.s.p, there is still a linear relationship between the thermal properties λ, C and κ on the one hand, and MC on the other but, in the species tested, the influence of anisotropy on thermal properties in the transverse directions is negligible.

Below are listed some conclusions that have arisen through using the different techniques applied to this research:

- Concerning the fuitometer

The fuitometer – whose primary aim is to measure surface quality – has proven his ability to be used as an indirect measure of lathe checks formed on veneer 'loose' side and degrading veneer surface quality. The results are less valuable and not as precise as the results from the SMOF in terms of different CD_i and CIn_i because it gives a mean value of the measured surface quality. However, the fuitometer is a reliable alternative to the SMOF for stiff veneers which cannot bend over the pulley.

- Concerning the SMOF

This study supports the view that the SMOF could form the basis of an important, non-destructive, testing method to monitor the quality of veneer produced at the research level. However, further studies should establish the link between lathe checking and gluing with respect to the mechanical properties of plywood since recent studies on the influence of check depth on bond quality in plywood have demonstrated that this has a significant impact (Rohumaa et al. 2013). Heating temperatures would then be determined according to the check distribution required as a function of the end-uses of the veneers. Future work could describe lathe checking with checking frequency CF by taking into account peeling speed, s (Eq. 11). The interest in using CF over checking intervals CIn_i would be to correlate with the frequencies of acoustic signals emitted by the cutting knife during peeling (Denaud et al. 2012). Using CF would also enable the development of an on-line monitoring system for lathe checking, which is not possible with the SMOF due to the long time required for screening the veneers compared to the industrial rate of peeling.

$$CF\,(\text{in Hz}) = \frac{1}{x_{i+1} - x_i} \cdot s \qquad\qquad (11)$$

where x_i is the position of the lathe check along the veneer length

- Concerning the TPS

The comparisons with proven older techniques such as the steady-state and flash methods have demonstrated similar results, establishing that the TPS technique offers new opportunities for characterising the thermal properties of wood especially in the green state. The difficulty encountered in this work concerned water transport which could have affected the results because one part of the absorbed heat may have contributed to water transfer instead of an increase in temperature, thereby leading to erroneously higher measured λ values. However, the small input power of the HotDisk® leads to a maximum temperature increase of 1 to 2 K, which is insufficient to bring about water mass transfer by evaporation. Moreover, if during the present experiments, it was not possible to take into account eventual water transfer by capillarity within the sample, the MC was nearly constant with very limited changes during the short measurement time.

- Concerning the integrating sphere

Future work studying temperature rise within the absorption area would contribute to a deeper understanding of the interaction between IR radiation and wood. Precise characterisation of the values used for the emissivity of green wood would contribute to a more accurate model from the physical point of view, but would not significantly influence the resulting temperatures. When thinking about some of the limits encountered during this study, consideration should be given to the difficulty in maintaining the MC wood samples above f.s.p. In addition to which, the notion of there being an 'minimum-optimum' heating temperature at the cutting plane is open to conjecture in light of the knowledge already acquired by Marchal et al. (1993) concerning the exact microscopic scale location at which the maximum efforts occur. The idea is that if the maximum efforts would effectively occur slightly above the cutting plane, it would not be necessary to heat the wood so deeply. This would promote the idea of heating green wood by a radiant energy penetrating into the wood but not validate the feasibility of IR heating, the penetration of which into green wood remains limited.

References

ASM International Handbook Committee (1986). ASM Handbook, Vol. 10 - Materials Characterization. ASM International. Online version available at: http//www.knovel.com/web/portal/browse/display?_EXT_KNOVEL_DIS PLAY_bookid=3114&VerticalID=0.

Baldwin R.F. (1975) Plywood Manufacturing Practices. Miller Freeman Publications Inc., San Fransisco, California, USA, 62-78.

Bardet S., Beauchêne J., Thibaut B. (2003) Influence of basic density and temperature on mechanical properties perpendicular to grain of ten wood tropical species. *Ann For Sci **60***, 49-59.

Beck J.V., St Clair C.R., Blackwell B. (1985) Inverse heat conduction. John Wiley and Sons Inc., New York, USA.

Bédard N., Poulain A. (2000) Application de l'infrarouge au réchauffage de billes pour produits forestiers Donohue-essais de laboratoires (Application of infrared heating to bolts for forest products Donohue-experimental tests). Technical report, HydroQuébec (in French).

Bédard N., Laganière B. (2009) Debarking enhancement of frozen logs. Part II: infrared system for heating logs prior to debarking. Forest Prod J 59, 25-30.

Beluche G. (2011) Modélisation numérique et développement d'un système expérimental de la diffusivité et de la transmission infrarouge (Numerical modeling and development of an experimental system for diffusivity and IR transmission). Arts et Metiers ParisTech (in French).

Bennett H.E.J., Porteus J.O. (1961) Relation between surface roughness and specular reflection at normal incidence. *J Opt Soc Am **51(123)***.

Berthold J., Olsson R.J.O., Salmén L. (1998) Water sorption to hydroxyl and carboxylic acid groups in carboxymethylcellulose (cmc) studied with nir-spectroscopy. *Cellulose **5(4)***, 281-298.

Chave T., Vial F. (2003) Caractérisation du chauffage par infrarouge de bois déroulé (Characterisation of IR heating for peeled wood). Technical report, CETIAT (in French).

Coste N., De Bevy T. (2005) Interest of radiant energy for wood peeling and slicing process. Master's thesis, Arts et Metiers ParisTech.

Cserta E., Hegedus G., Nemeth R. (2012) Evolution of temperature and moisture profiles of wood exposed to infrared radiation. *Bioresources 7(4)*, 5304-5311.

Denaud L., Bléron L., Eyma F., Marchal R. (2012) Wood peeling process monitoring: a comparison of signal processing methods to estimate veneer average lathe check frequency. *Eur J Wood Prod 70*, 253-161.

De Santo J.A. (2007) Overview of rough surface scattering. Light Scattering and Nanoscale Surface Roughness. Springer, 211-235.

Dory J.P., Evin F., Piro M. (1999) Infrared heating - chauffage par rayonnement infrarouge. In Techniques de l'ingénieur - Génie électrique.

El Haouzali H. (2009) Déroulage du peuplier: effets cultivars et stations sur la qualité des produits dérivés (Peeling of poplar: effects of cultivars and stations on the quality of derived products). PhD thesis, Arts et Metiers ParisTech (in French).

Engelund E.T., Thygesen L.G., Svensson S., Hill C. (2013) A critical discussion of the physics of wood-water interactions. *Wood Sci Technol 47*, 141-161.

Fengel D., Wegener G. (1984) Wood: chemistry, ultrastructure, reactions. Walter de Gruyter.

Flir Systems ThermaCAM User's Manual (2004).

Gaudillière, C. (2003) Contribution au développement d'une chauffe électrique rapide de bois vert de Douglas en vue de son déroulage (Contribution to the development of rapid electric heating of green Douglas-fir prior to peeling). Master's thesis, Arts et Metiers ParisTech (in French).

Gril J., Berrada E., Thibaut B. (1993) Recouvrance hygrothermique du bois vert. II. Variations dans le plan transverse chez le châtaignier et l'épicéa et modélisation de la fissuration à coeur provoquée par l'étuvage (Hygrothermal revovery of green wood. II. Transverse variations in

chestnut and spruce and modelling of the steaming-induced heart checking). *Ann For Sci* **50(5)**, 487-508 (in French).

Grimhall C.G., Hoel O. (1983) Method of slicing veneer US Patent 4,516,614.

Gustafsson S.E. (1991) Transient plane source techniques for thermal conductivity and thermal diffusivity measurements of solid materials. *Rev Sci Instru* **62(3)**, 797-804.

ISO 20473 (2007) Optics and photonics - spectral bands. International Standard Organisation.

Jia D., Afzal M.T., Gongc M., Bedane A.H. (2010) Modeling of moisture diffusion and heat transfer during softening in wood densification. *Int J Eng* **4**, 191-200.

Jones P.D., Schimleck L.R., Daniels R.F., Clark A., Purnell R.C. (2008) Comparison of Pinus taeda L. whole-tree wood property calibrations using diffuse reflectance near infrared spectra obtained using a variety of sampling options. *Wood Sci Technol* **42(5)**, 358-400.

Kelley S. S., Rials T.G., Snell R., Groom L.H., Sluiter A. (2004) Use of near infrared spectroscopy to measure the chemical and mechanical properties of solid wood. *Wood Sci Technol* **38(4)**, 257-276.

Kollmann F.F.P., Côté W.A. (1968) Principles of wood science. I-Solid wood. Springer-Verlag.

Koumoutsakos A., Avramidis S., Hatzikiriakos S.G. (2001) Radio frequency vacuum drying of wood. I. Mathematical model. *Dry Technol* **19**, 65-84.

Labsphere Technical Guide: Integrating sphere theory and applications, Labsphere Inc.

Lutz, J.F. (1960) Heating veneer bolts to improve quality of Douglas-fir plywood. Technical report USDA Forest Service General FPL-2182. Forest Products Laboratory, Madison, WI, USA.

Makoviny I., Zemiar J. (2004) Heating of wood surface layers by infrared and microwave radiation. *Wood research* **49(4)**, 33-40.

Marchal R. (1989) Valorisation par tranchage et déroulage des bois de chênes méditerranéens (Valorisation of mediterranean oaks by peeling and slicing). PhD thesis, Institut Polytechnique de Lorraine (in French).

Marchal R., Jullien D., Mothe F., Thibaut B. (1993) Mechanical aspects of heating wood in rotary veneer cutting. *11th International Wood Machining Seminar*, 257-278.

Marchal R., Collet R. (2000) Contribution au développement d'une chauffe électrique rapide de bois vert de Douglas en vue de son déroulage (Contribution to the development of rapid electric heating of green Douglas-fir prior to peeling). Technical report, Arts et Metiers ParisTech (in French).

Marchal R., Gaudillière C., Collet R. (2004) Technical feasibility of an embedded wood heating device on the slicer or the peeling lathe. *1st International Symposium Veneer Processing and Products Proceedings*, 29-44.

Matsunaga M., Minato K. (1998) Physical and mechanical properties required for violin bow materials II: Comparison of the processing properties and durability between pernambuco and substitutable wood species. *J Wood Sci* **44**, 142-146.

Meola C., Giovanni C. (2004) Recent advances in the use of infrared thermography. *Meas Sci and Technol* **15**, 27-58.

Mothe F., Marchal R., Tatischeff W.T. (2000) Sécheresse à cœur du Douglas et aptitude au déroulage: recherche de procédés alternatifs d'étuvage. I. Répartition de l'eau dans le bois vert et réhumidification sous autoclave (Heart dryness of Douglas-fir and ability to rotary cutting: Research of alternative boiling processes. I. Moisture content distribution inside green wood and water impregnation with an autoclave.) *Ann For Sci* **57(3)**, 219-228 (in French).

Navi P., Heger F. (2005) Comportement thermo-hydromécanique du bois (Thermo-hydro-mechanical behaviour of wood). PPUR, Lausanne, Switzerland (in French).

Navi P., Sandberg D. (2012) Thermo-hydro-mechanical processing of wood. EPFL Press, Lausanne, Switzerland, 159-191.

Olsson A.M., Salmén L. (1997) The effect of lignin composition on the viscoelastic properties of wood. *Nord Pulp Pap Res* **12(31)**, 140-144.

Palmer J.M., Bass M., Van Stryland E.W., Williams D.R., Wolfe W.L. (1995) Handbook of Optics: Devices, Measurements, and Properties, Vol. II, Second Edition, 25.1-25.25. McGraw-Hill, New York, NY, USA.

Palubicki B., Marchal R., Butaud J.C., Denaud L., Bléron L., Collet R., Kowaluk G. (2010) A method of lathe checks measurement: SMOF device and its software. *Eur J Wood Prod* **68(2)**, 151-159.

Parker W.J., Jenkins R.J., Butler C.P., Abbott G.L. (1961) Flash method of determining thermal diffusivity, heat capacity, and thermal conductivity. *J Appl Phys* **32(9)**, 1679-1684.

Potter B.E., Andresen J.A. (2010) A finite-difference model of temperatures and heat flow within a tree stem. *Revue Canadienne de Recherche Forestière* **32**, 548-555.

Pouzeau P., Pradal H. (1957) Aspects nouveaux dans la technique de déroulage de l'Okoumé (New look in Okoumé peeling method). *Bois et Forêts des Tropiques* **54**, 41-50.

Quéméner O., Battaglia J.L., Neveu A., (2003) Résolution d'un problème inverse par utilisation d'un modèle réduit modal. Application au frottement d'un pion sur un disque en rotation (Solving an inverse problem by using a modal reduced model. Application to the friction of a pin on a rotating disk). *Int J Therm Sci* **42(4)**, 361-378 (in French).

Raiskila S., Saranpaa P., Fagerstedt K., Laakso T., Loija M., Mahlberg R., Paajanen L., Ritschkoff A. (2006) Growth rate and wood properties of Norway spruce cutting clones on different sites. *Silva Fenn* **40(2)**, 247-256.

Rohsenow W., Hartnett J., Ganic E. (1973) Handbook of Heat Transfer Fundamentals. McGraw-Hill Book Company, New York, NY.

Rohumaa A., Hunt C.G., Hughes M., Frihart C.R., Logren J. (2013) The influence of lathe check depth and orientation on the bond quality of phenol-formaldehyde-bonded birch plywood. *Holzforschung* DOI 10.1515/hf-2012-0161.

Siau J.F. (1971) Flow in Wood. Syracuse University Press, Syracuse, NY, USA.

Siau J.F. (1995) Wood: Influence of Moisture on Physical Properties. Virginia Polytechnic Institute and State University, Blacksburg, VA, USA.

Simpson W., TenWolde A. (1999) Physical properties and moisture relations of wood. In: Wood Handbook – Wood as an Engineering Material, Chapter 3. Forest Products Laboratory, Madison, WI, USA.

Sonderegger W., Hering S., Niemz P. (2011) Thermal behaviour of Norway spruce and European beech in and between the principal anatomical directions. *Holzforschung* **65**, 369-375.

Steinhagen H.P. (1977) Thermal conductive properties of wood, green or dry, from -40 to + 100°C: a literature review. Forest Products Laboratory, Madison, WI, USA.

Suleiman B.M., Larfeldt J., Leckner B., Gustavsson M. (1999) Thermal conductivity and diffusivity of wood. *Wood Sci Technol* **33**, 465-473.

Svoradova M., Charrier F., Marchal R., Bléron L., Charrier B., Butaud J-C. (2004) Influence of conditioning and the peeling process on the natural durability of European oak veneers. *2nd International Symposium on Wood Machining*, 405-414.

Taler J., Duda P. (2006) Solving direct and inverse heat conduction problems. Springer, Berlin.

Thibaut B., Fournier M., Jullien D. (1995) Contraintes de croissance, recouvrance différée à l'étuvage et fissuration des grumes: cas du châtaignier (Growth-related stresses, differed size recovery during heating and splitting in timber: the case of sweet chestnut). *Forêt Méditerranéenne* **16(1)**, 85-91 (in French).

Thibaut B., Beauchêne J. (2004) Links between wood machining phenomena and wood mechanical properties: the case of 0/90° orthogonal cutting of green wood. *2nd International Symposium on Wood Machining*, 149-160.

Torgovnikov G., Vinden, P. (2010) Microwave wood modification technology and its applications. *Forest Prod J* **60(2)**, 173-182.

Tsuchikawa S., Hayashi K., Tsutsumi S. (1996) Nondestructive measurement of the subsurface structure of biological material having cellular structure by using near-infrared spectroscopy. *Appl Spectrosc* **50(9)**, 1117-1124.

Yamauchi S., Iijima Y., Doi S. (2005) Spectrochemical characterization by FT-Raman spectroscopy of wood heat-treated at low temperatures: Japanese larch and beech. *J Wood Sci* **51**, 498-506.

Zavarin E., Jones S.G., Cool L.G. (1990) Analysis of solid wood surfaces by Diffuse Reflectance Infrared Fourier-Transform (DRIFT) spectroscopy. *J Wood Chem Technol* **10(4)**, 495-513.

Zavarin E., Cool L.G., Jones S.G. (1991). Analysis of solid wood surfaces by internal-reflection fourier-transform infrared-spectroscopy (FTIR-IRS). *J Wood Chem Technol* **11(1)**, 41-56.

Errata

I

The effect of log heating temperature on the peeling process and veneer quality: beech, birch, and spruce case studies

**Anna Dupleix · Louis-Etienne Denaud ·
Laurent Bleron · Rémy Marchal · Mark Hughes**

Abstract Heating green-wood prior to peeling is necessary to improve both peeling process and quality of veneer. This study investigates optimum heating temperatures by soaking of beech, birch and spruce. Experiments have studied the influence of heating temperatures from 20 to 80 °C on thickness deviations and veneer lathe checking using a pneumatic rugosimeter and image analysis of opening checks with the SMOF device (Système de Mesure de l'Ouverture des Fissures). Conclusions account for reduced heating temperatures compared to the temperatures currently in-use in the industry. Already at 50 °C, positive effects of heating ensure efficient peeling process. Low temperatures produce veneers with deeper and more spaced checks than high temperatures when checks are closer and less deep, becoming even unpredictable especially in case of spruce. These results establish the SMOF as an essential non-destructive control device to control the quality of the veneer produced at research level.

Einfluss der Aufheiztemperatur des Rundholzes auf den Schälprozess und die Furnierqualität am Beispiel von Buche, Birke und Fichte

Zusammenfassung Um den Schälprozess und die Qualität von Furnier zu verbessern, muss das Rundholz vor dem Schälen aufgeheizt werden. Dieser Artikel beschäftigt sich mit der Untersuchung der optimalen Aufheiztemperatur bei der Wässerung von Buche, Birke und Fichte. Unter Verwendung eines druckluftbetätigten Rugosimeters und digitaler Bildanalyse mittels SMOF-Apparat wurde der Einfluss einer Temperatur zwischen 20 und 80 °C auf die Dickenschwankungen und Risse der Furniere untersucht. Die Ergebnisse zeigen, dass die aktuell in der Industrie verwendeten Temperaturen reduziert werden könnten. Schon bei 50 °C kann ein effizienter Schälprozess erreicht werden. Bei niedrigeren Temperaturen treten tiefere Risse in größerem Abstand auf. Im Vergleich dazu sind bei höheren Temperaturen der Abstand und die Tiefe der Risse geringer, beim Schälen von Fichte sogar kaum meßbar. Die Ergebnisse zeigen, dass der SMOF-Apparat zur zerstörungsfreien Qualitätsprüfung von Furnieren im Rahmen von Forschungsarbeiten geeignet ist.

A. Dupleix (✉) · L.-E. Denaud · L. Bleron · R. Marchal
Arts et Metiers ParisTech LaBoMaP, Rue Porte de Paris,
71250 Cluny, France
e-mail: anna.dupleix@ensam.eu

A. Dupleix · M. Hughes
Department of Forest Products Technology,
School of Chemical Technology, Aalto University,
00076 Aalto, Finland

1 Introduction

For almost all hardwood and softwood species, the heating of green wood prior to peeling is necessary in order to successfully produce veneer. Industrially, this is generally accomplished by soaking—immersing the whole logs in hot water basins—or by steaming them in vats. These traditional methods mainly use water as the medium to transfer heat into the bulk wood (Daoui et al. 2007). Heating is a key stage in the processing of wood prior to peeling since it influences material properties and consequently modifies cutting mechanisms. An energy approach has shown that the ratio of fracture to shearing energies increases with heating (Thibaut and Beauchene 2004). This has a positive effect on (1) the peeling process and (2) veneer quality. Firstly, a diminution in the energy dissipated in the shearing of wood lowers the pressure applied

by the bolt on the cutting knife, thereby decreasing the effort required in peeling (Bédard and Poulain 2000) and consequently diminishing power consumption and cutting tools wear (Marchal et al. 2004). Secondly, the reduction in the fracture energy required to create a unit area of surface, reduces the formation of checks and therefore improves veneer quality (Thibaut and Beauchene 2004).

In practice, the effects of peeling temperature on cutting effort and veneer quality are species dependent. The results from various experimental factors are then interpreted to reach a compromise leading to threshold temperatures defined as the optimum heating temperatures. Determining the optimal conditions for each species necessitates dedicated experimental campaigns. On the one hand, measuring cutting forces requires peeling lathes equipped with automated sensors that are both costly and difficult to install in an industrial environment. On the other hand, veneer "quality" (encompassing thickness variation, veneer roughness and lathe checking) necessitates only basic instrumentation and can be evaluated by hand or by manual image analysis, but is time-consuming and, as yet, cannot be done online. This is the reason why current experimental results tend to be qualitative and provide only limited statistical accuracy. This lack of a rigorous analysis procedure has led to the introduction of empirical approaches by industrial operators who use temperature as a guide to obtaining satisfactory veneer quality. Consequently, soaking temperatures are not even consistent from one company to another for the same species. Soaking temperatures are often raised to increase thermal transfer and reduce soaking duration. It is all the more problematic as the consequences of overheating are known to be detrimental to veneer quality as it leads to the formation of 'wooly' surfaces and can cause block spin-outs due to a reduction in the shear strength of wood. Overheating at reduced soaking times also affects the temperature homogeneity within the bolt; the outer sapwood is overheated whilst the temperature of the heartwood is not high enough. Recent research has, however, combined the results of quantitative factors to evaluate veneer quality and veneer processing as a function of soaking temperature and could eventually lead to changes in the way industry controls its processes (Dai and Troughton 2011).

This present paper contributes to advances in the evaluation of veneer quality and veneer processing as a function of soaking temperature. The method employs a purpose designed instrument—SMOF (Systeme de Mesure d'Ouverture des Fissures)—for the quantitative measurement of lathe checking (Palubicki et al. 2010)—and the fuitometer—a pneumatic rugosimeter (see Sect. 2)—to assess veneer surface quality. This study was conducted on two hardwood species: beech (*Fagus sylvatica*) and birch (*Betula pendula*)—and one softwood species; spruce (*Picea albies*). These species are amongst the most commonly used

in northern countries to industrially produce wood-based panels and plywood. The aim of this article is to measure the effect of log heating temperatures on the veneer quality of beech, birch and spruce.

2 Materials and methods

Bolts of 400 mm diameter were cut to 600 mm length to fit the dimensions of the peeling lathe. For each species, all tested bolts originate from the same log and each bolt was tested at one soaking temperature. Bolts were heated by soaking in water over a 48 h period at temperatures ranging from 20 to 80 °C. The difference between the actual temperature of the soaking water and the target temperature is represented in Fig. 1. These differences are not significant so that in the following of the article, temperatures refer to target temperatures for more clarity. The importance of knots was evaluated by taking pictures of the veneers and measuring the ratio of knots to the veneer surface with image analysis. However, the percentage of knots was always inferior to 2 % in the tested veneers. Density of bolts before and after soaking varied between 725 and 1,290 kg/m³ (Fig. 2). Mean ring width is presented in Table 1.

3 Peeling process parameters

Bolts were peeled with the industrial peeling lathe available at Arts et Metiers ParisTech Cluny, France. Pressure
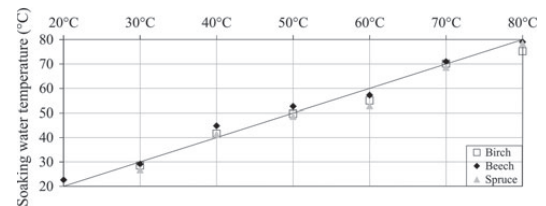

Fig. 1 Effective soaking water temperature as compared to target temperature
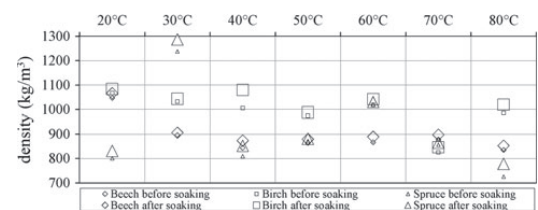**Abb. 1** Vorhandene Wassertemperatur im Vergleich zum Sollwert

Fig. 2 Density of the bolts before and after soaking
Abb. 2 Dichte der Stammabschnitte vor und nach der Wässerung

Table 1 Mean rating width of each tested bolt (in mm)
Tab. 1 Mittlere Jahrringbreite der untersuchten Stammabschnitte (in mm)

	20 °C	30 °C	40 °C	50 °C	60 °C	70 °C	80 °C
Beech	2.7	2.3	2.1	2.4	1.9	2.4	2.7
Birch	N/A	2.5	4.4	N/A	3.3	N/A	2.6
Spruce	2.4	2.2	1.2	1.7	2.3	2.3	2.4

bar and peeling speed influence veneer quality (Mothe 1988). The nominal veneer thickness e_{nom}—or input thickness on the peeling machine different to the actual measured thickness of the veneer due to wood structure—was 3 mm. In order to evaluate only the influence of heating temperatures on the peeling process and veneer surface quality, peeling speed, f, and compression rate of the pressure bar, Bp, were kept constant (f = 1 m/s; Bp = 5 %; vertical gap = 1 mm). This low Bp value compared to the 15–20 % pressure bar values usually used in industry was chosen to highlight the checking phenomenon with the slightest influence of the pressure bar. In order to verify this influence, the first peeling turns on each bolt were carried out without the pressure bar.

4 Heating temperatures

Special attention was paid to the difficulty in measuring the surface temperature of the bolt during peeling. Two methods of measurement were used as means of cross-checking to ensure that bolts remained heated to the target temperature of the core during the whole peeling process. First, the heating water temperature was given by sensors from the soaking basins—the reference temperature. Secondly, a Fluke TiR3 infrared thermal camera whose specifications are detailed in Table 2 was used to continuously monitor in-line bolt surface temperature during peeling. In order to minimize the effects of any disturbing factors (distance object-camera, background temperature and relative humidity), the experiments were carried out in a large hall so that background temperature and relative humidity

Table 2 Infrared thermal camera specifications
Tab. 2 Technische Daten der Infrarot-Wärmebildkamera

Specifications	Analogical fluke TiR3
Detector	Vanadium oxide FPA microbolometer
Image resolution	320 × 240 pixels
Thermal sensitivity	≤0.070 °C at 30 °C
Scan speed	7.5 Hz
Spectral band	8–14 μm
Temperature range	−20 to 100 °C

did not change during experiments as recommended by Flir Systems ThermaCAM User's Manual. Moreover, the change in the distance between the camera and the bolt surface caused by the forward displacement of the knife (around 20 cm) is negligible compared to the several meters separating the bolt surface from the camera (Fig. 3a). To control bolt surface temperatures, the advantage of Infrared Thermography (IRT) over other contact methods lies in its convenience in measuring the surface temperature of objects in motion. In the past, contact methods such as thermocouples to measure bolt surface temperature while rotating have proven to be difficult to implement (Bédard and Poulain 2000).

5 Veneer surface quality

Surface quality was assessed on wet veneers to prevent any effects of drying (Perre 2007). For each temperature, 6 m of veneer band were tested: 10 replicates corresponding to 10 randomly chosen lathe turns, each of 600 mm length (Fig. 3b).

5.1 Thickness variation

Thickness deviation from the nominal thickness, e_{nom}, is a control of veneer surface unevenness. Thickness variation was measured every 70 mm along the veneer length with a digital micrometer (Fig. 3b). The principle relies on a weighed pipe which pins at same pressure the veneer against a marble surface to ensure 10 μm thickness precision.

5.2 Veneer air leakage

Given the lack of standard for veneer surface quality evaluation, it was decided to assess it by measuring air leakage on veneer surface with a pneumatic rugosimeter—also referred to as a fuitometer. The fuitometer offers many advantages amongst which are rapidity—a few seconds per veneer ribbon, ease of handling, low price, the possibility to measure wet surfaces, robustness. This method has proven its ability in the assessment of paper surface quality as well as in particle board and panel manufacturing (Coelho 2005). In case of veneer, roughness, due either to intrinsic defects of the wood structure (tracheids in softwood, annual growth rings in hardwood veneers) or to defects generated by the knife action or the pressure bar during the peeling process, can be assessed by haptic—tactile feeling with fingers, optical or contact methods (Mothe 1985). However, none of these methods are adapted to the assessment of veneer quality in the green state. The haptic procedure—still in use in the industry by
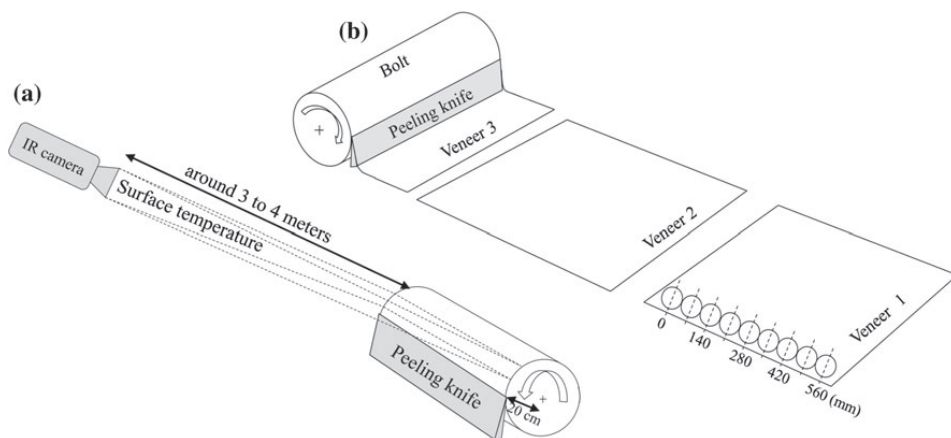
Fig. 3 Thermal imaging location (**a**), sampling details (**b**)
Abb. 3 Anordnung der Wärmebildkamera (**a**), Probenentnahme (**b**)

experienced operators at the end of veneer production lines—uses touch which gives only qualitative results impossible to correlate with quantitative measures of roughness commonly used in surface metrology. Optical rugosimeters—such as laser methods—are also not adapted to evaluate the surface quality of wet veneers: the results are dispersive due to the presence of interacting water. The precision of contact rugosimeters at the micrometer scale compared to the heterogeneity of veneers surface at millimeter scale, limits the measurements that can be conducted in an affordable time to small-size samples which weakens the representativeness of the measurements (Tanritanir et al. 2006).

The principle of the fuitometer is simple (Pouzeau and Pradal 1957). It is based on pressure loss when air flows through an annular-shaped pipe impinging on the uneven veneer surface (Fig. 4a). In the case of an uneven surface, air leaks through the pipe: the pressure at the output of the pipe decreases leading to a pressure loss indicated by the water column whose level gets higher. The difference between input and output pressure readings on a water column is a function of veneer air permeability. The fuitometer gives the Checking Index (CI) calculated from the difference of air leakage between the tight and loose sides of the veneer (El Haouzali 2009) (Eq. 1, Fig. 4a). CI measures air leakage through veneer which is influenced by lathe check formation (Palubicki et al. 2010): the more lathe checks, the more tearing of fibers, the more uneven surface, the more air leakage, and the higher water level and thus the lower column reading. Measurements were taken every 70 mm along the veneer length (Fig. 3b).

$$
\begin{aligned}
\text{CI (in mm of water)} = &\ \text{water level}_{\text{on tight side}} \\
&- \text{water level}_{\text{on loose side}}.
\end{aligned} \tag{1}
$$

Veneer quality was measured in terms of lathe checking and thickness variation continuously along the length of the 10 replicates of veneer bands with the SMOF device (Fig. 3b).

5.3 Lathe checking

Lathe checking is brought about by a sudden tearing of wood fibers under the cutting knife due to an increase in the energy dissipated by wood shearing (Thibaut and Beauchene 2004). The mechanisms behind the formation of lathe checking are influenced by the deformability of the wood and so, in turn, depend upon the peeling temperature. Checks form on loose side in contact with the knife while tight side is in contact with the pressure bar (Fig. 4b). Lathe checking on the loose side was detected with the SMOF device (Palubicki et al. 2010). The principle consists in bending veneer over a pulley to visualize checks exposed to a laser. A camera automatically takes pictures of the veneer thickness enabling a continuous recording of the veneer cross-section. The resulting information given is the interval between two checks CIni (Eq. 2) and checking depths CDi for each check i (Eq. 3). The advantage of the SMOF is that it provides CDi calculated as a percentage of the actual veneer thickness e_i at the position of the check x_i while manual methods refer to nominal veneer thickness e_{nom} (Fig. 4b).
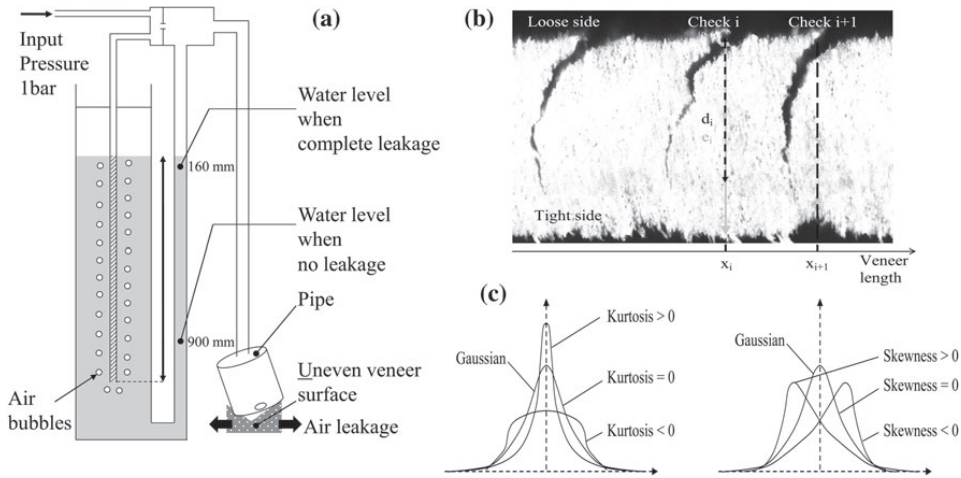
Fig. 4 Scheme of the fuitometer principle (**a**), SMOF output image (**b**), definitions of kurtosis and skewness for a distribution of data (**c**)
Abb. 4 Funktionsprinzip des Fuitometers (**a**), mit SMOF erzeugtes Bild (**b**), Wölbung und Schiefe einer Dichteverteilung (**c**)

$$CIn_i \text{ (in mm)} = x_{i+1} - x_i \qquad (2)$$

$$CD_i \text{ (in \%)} = \frac{d_i}{e_i} \times 100 \qquad (3)$$

For each check i, the Checking Ratio CR_i is given by Eq. (4):

$$CR_i = \frac{CIn_i}{CD_i} \qquad (4)$$

The advantage of SMOF is the automated numerical imaging of the horizontal and vertical positions of lathe checks within the loose face of veneer (Palubicki et al. 2010). It therefore provides an automatic way of assessing the depth and intervals of checking in the large-scale production of veneers. However, the reliability of SMOF needs to be proven in a vast series of experimental tests.

5.4 Thickness variation

This information was provided by a LVDT sensor located on the SMOF device.

6 Results and discussion

In the present experiments, IRT detected small variations in surface temperature during peeling. This may be due to the presence of a residual temperature gradient within the bolt or to the variation of emissivity with modification of surface quality which arise during peeling process (Meola et al. 2004).

6.1 Thickness variation

For beech and birch the standard deviations are low (around 2–3 % of veneer thickness) and are constant with the heating temperature (Fig. 5). These results indicate that the cutting process is already stable at low temperatures with no plunging knife cycles. The standard deviations, at around 4–6 %, are higher in spruce than in either beech or birch. Thickness variation decreased as the heating temperature rose, demonstrating the positive effects of heating on veneer thickness consistency (Fig. 5). However, these conclusions should be treated with a little caution due to some inconsistency in the results obtained at 30 and 70 °C. These inconsistencies results might be explained by the heterogeneous structure of spruce softwood at the microscopic levels compared with the homogeneous structures of beech and birch hardwoods (Navi and Heger 2005).
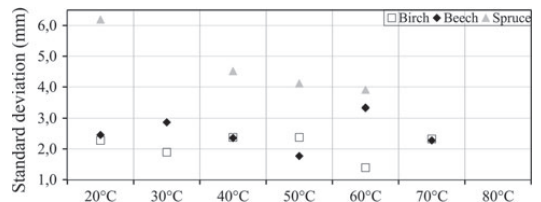
Fig. 5 Influence of heating temperature on thickness variation (COV)
Abb. 5 Einfluss der Aufheiztemperatur auf die Dickenschwankung (COV)

6.2 Veneer air leakage

Apart from the inconsistent results for spruce at 80 °C which may be due to experimental mistake, CI is found to
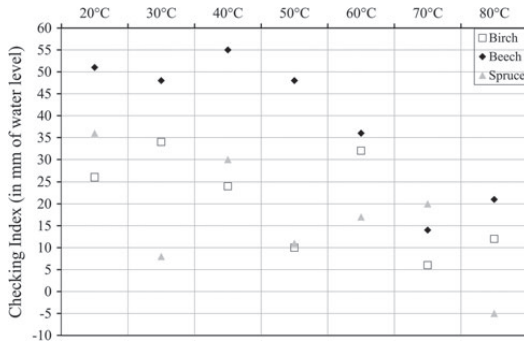
Fig. 6 Influence of heating temperature on checking index (CI)
Abb. 6 Einfluss der Aufheiztemperatur auf den Rissindex (CI)

be always positive denoting that air leakage on loose side is higher than on tight side (Fig. 6). This observation indicates that fuitometer may be used to qualitatively evaluate the amount of lathe checking that forms on veneer loose side (Eq. 1, Fig. 4a). Up to 70 °C, CI decreases with heating temperatures indicating a reduction in lathe check depth and demonstrating the positive influence of heating on reducing veneer lathe checking. The slight subsequent increase noticeable for beech and birch from 80 °C may be due to the commencement of the formation of wooly surfaces and deeper checks (Fig. 6). The fuitometer gives a mean value of the measured surface quality: the results are not as precise results as the SMOF in terms of different CD_i and CIn_i, however. The resulting information is less valuable and offers only a general overview of the influence of soaking temperature on lathe checking. However, the fuitometer is a reliable alternative to the SMOF for stiff species which cannot bend over the pulley.
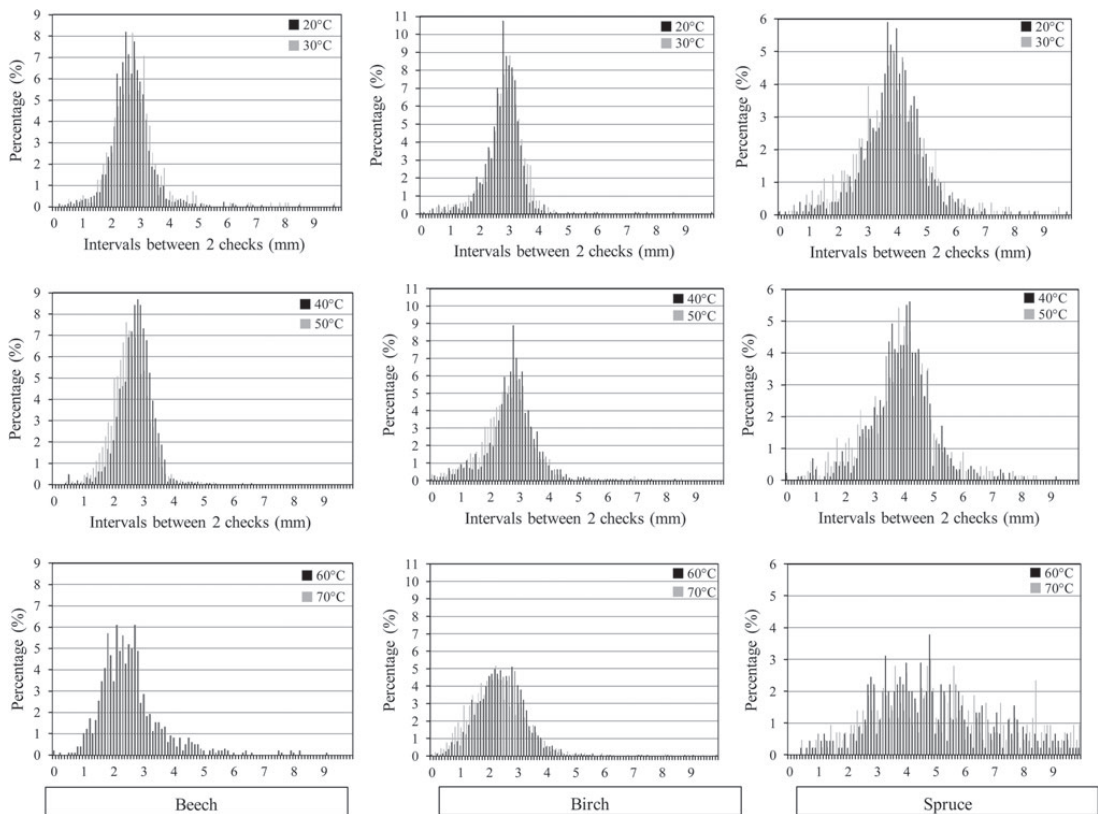
Fig. 7 Diagrams of the distribution of intervals between two checks function of heating temperatures
Abb. 7 Verteilung der Rissabstände in Abhängigkeit der Aufheiztemperatur
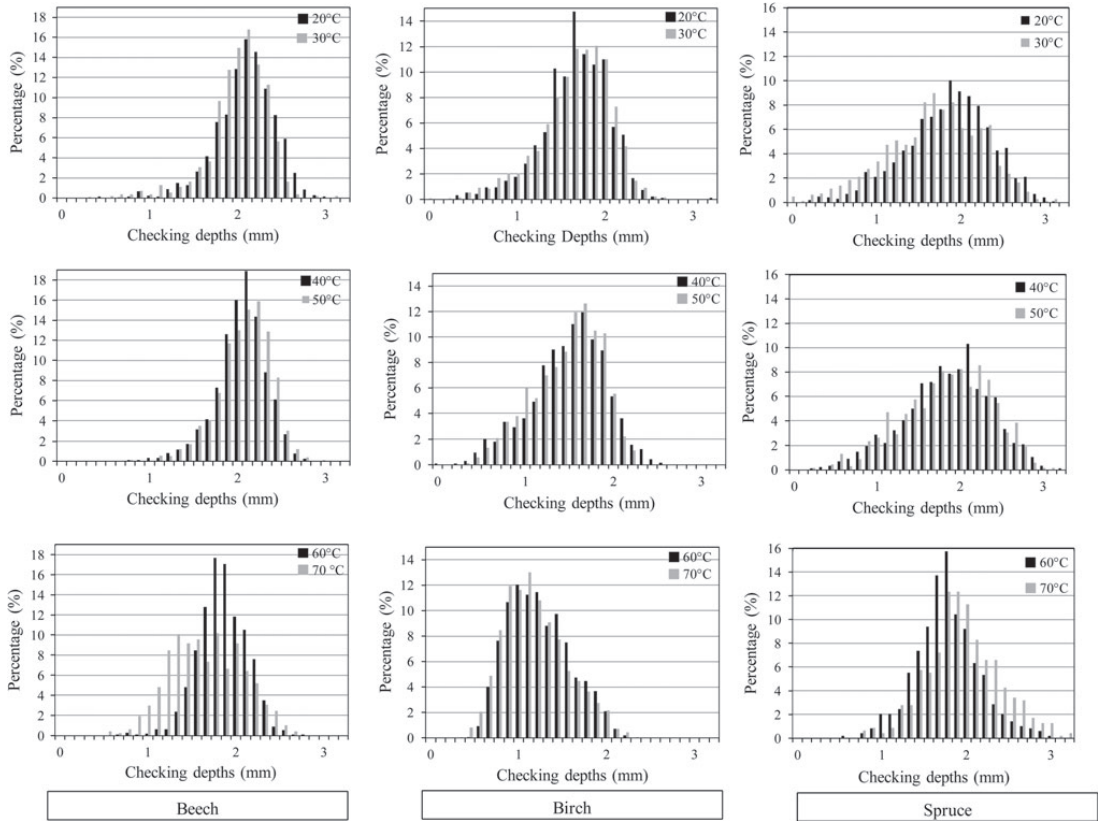
Fig. 8 Diagrams of the distribution of checking depths function of heating temperatures
Abb. 8 Verteilung der Risstiefe in Abhängigkeit der Aufheiztemperatur
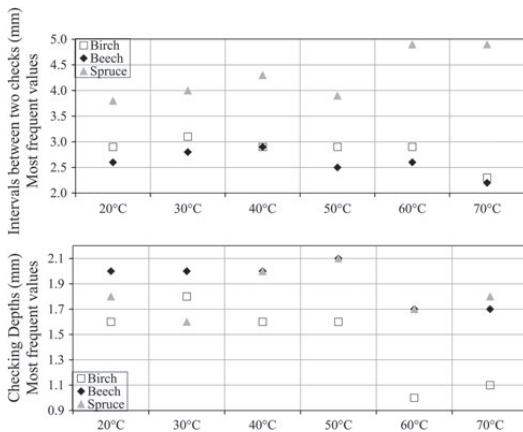
Fig. 9 Influence of heating temperatures on the most frequent values for intervals between two checks and checking depths
Abb. 9 Häufigste Werte der Rissabstände und der Risstiefe in Abhängigkeit der Aufheiztemperatur

6.3 Lathe checking

The SMOF provides statistical data about the intervals between two checks CIn_i (Eq. 2) and check depths CD_i (Eq. 3), giving precise distributions of these two values along all of the 6 meters of tested veneer. The distributions are displayed in the form of histograms (Fig. 7 for the intervals between two checks and Fig. 8 for check depths). For each heating temperature, they represent the number of lathe checks (in terms of percentages of total number of lathe checks on the measured veneer) for each range of CIn_i and CD_i displayed in the X-axis. For each heating temperature, the highest percentage represents therefore the most frequent values of CIn_i and CD_i. The most frequent values offer the advantage over the less representative mean values to bring all information concerning checking distribution along the veneer length (Fig. 9).

All three species feature the same behaviour for check depths: check depths are roughly constant at temperatures
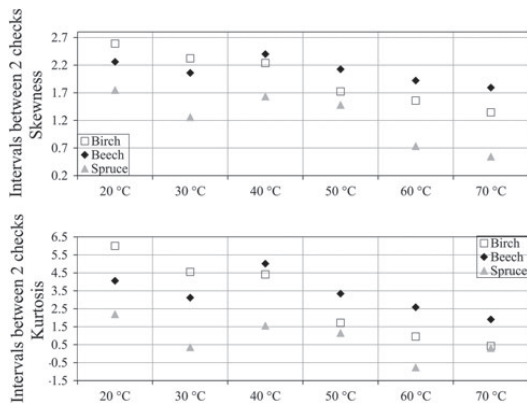
Fig. 10 Influence of heating temperatures on skewness and kurtosis for intervals between two checks
Abb. 10 Schiefe und Wölbung der Verteilung der Abstände zwischen zwei Rissen in Abhängigkeit der Aufheiztemperatur

Fig. 11 Influence of heating temperatures on checking ratios
Abb. 11 Einfluss der Heiztemperatur auf die Rissigkeit

up to 60 °C, before starting to decrease from this point on. This means that high heating temperatures produce veneers with smaller lathe check depth. With respect to the interval between two checks, beech and birch behave alike and in the same manner as for check depths, namely that high heating temperatures tend to produce veneers with a greater number of more closely spaced checks. Spruce, however, does not exhibit the same behaviour at temperatures of 60 and 70 °C. In these two cases, diagrams spread wide so that there is no significant surpassing value and most frequent values are not statistically relevant (Fig. 7). For this reason a statistical analysis is chosen to evaluate the coefficients of skewness and kurtosis for the diagrams (Fig. 4c). Skewness is a measure of the asymmetry of the distribution while kurtosis is a measure of its peakedness. For all species, the kurtosis and skewness of the intervals between two checks tend to decrease with heating temperatures (Fig. 10). Spruce kurtosis and skewness are lower than for beech and birch at all temperatures and skewness drops to 0 and kurtosis becomes negative at high temperatures.

The conclusions that can be drawn are that the checks are deeper and more widely spaced at low temperatures than at high temperatures which produce smaller but more closely packed checks. These results should, in theory, be verified by a constant Checking Ratio (Thibaut 1988) as confirmed in Fig. 11.

This implies that the mechanisms of lathe check formation becomes unpredictable as the heating temperatures rises. This phenomenon could be interpreted as the growing impact of wood anatomy together with a reduction of the stress field—due to reaching the glass transition temperature T_g. The softening of wood is dictated by the glass transition temperature T_g of cell wall lignin which occurs
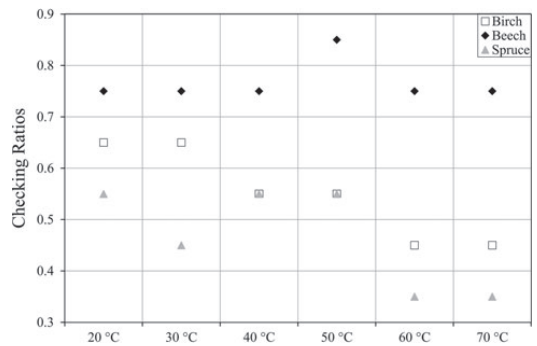
in the range of 50–100 °C for green wood (Olsson and Salmen 1997). These interpretations are confirmed in the case of spruce. Spruce features a strong heterogeneity between early and late wood (Raiskila et al. 2006) and a higher lignin content (Fengel and Wegener 1984), which may explain the more significant impact of heating temperature than on either homogeneous species such as beech or birch.

7 Conclusion

For beech, birch and spruce, it is difficult to define optimum heating temperatures based on the results that have been obtained. However, compared to previous results (Dai and Troughton 2011), the breakthrough in this study is to rely on check distribution as a function of heating temperature. Heating of beech, birch and spruce produces veneers with closer lathe checks of smaller depth than low temperatures which produce veneers with deeper and more widely spaced checks. At high temperatures, the check formation mechanism is less periodic and becomes governed by wood anatomy and is therefore less predictable—especially in the case of heterogeneous spruce. Such results are useful in providing to industrial operators the decision-making values to design optimum heating temperatures with regard to lathe checking tolerance as a function of veneer end uses. In that sense, this study highlights the role played by lowered temperatures in veneer quality. Such lowered temperatures point the way towards the development of an alternative to soaking that would use infrared heating for example (Dupleix et al. 2012). Moreover, this study demonstrates the efficiency of the SMOF device to quantify veneer lathe checking (by means of the intervals between two checks and checking depths) at industrial scale (high number of tested veneer meters). These results establish the SMOF as an essential non-destructive control

tool for plywood manufacturers to control the quality of the veneer produced. This justification of the SMOF creates a potential for industrials to develop the SMOF as in-line measurement system on the edge of the veneers—on the supposition that edge effects do not introduce inaccuracy in the results. Further studies should establish the link between lathe checking and gluing with respect to the mechanical properties of plywood. Heating temperatures would then be determined according to the check distribution required as a function of the end-uses of the veneers.

Future work could describe lathe checking with checking frequency CF by taking into account peeling speed, s (Eq. 5, Fig. 4b). The interest in using CF over checking intervals CIn_i is to draw a comparison with frequencies of acoustic signals emitted by the cutting knife during peeling (Denaud et al. 2012).

$$CF \ (\text{in Hz}) = \frac{1}{x_{i+1} - x_i} \times s \qquad (5)$$

References

Bédard N, Poulain A (2000) Application de l'infrarouge au réchauffage de billes pour produits forestiers Donohue—essais de laboratoires (Application of infrared heating to bolts for forest products Donohue—experimental tests). Technical report, Hydro Québec

Coelho CMP (2005) Influence de l'usinage du bois sur les caractéristiques objectives et sur la perception subjective de l'aspect d'une finition (Influence of wood machining on objective characteristics and subjective perception of the aspect of finishing). PhD thesis, Faculdade de Engenharia da Universidade do Porto

Dai C, Troughton GE (2011) Effect of log conditioning temperature on veneer quality. Technical report, FP Innovations

Daoui A, Douzet J, Marchal R, Zerizer A et al (2007) Valorisation du bois de pin d'alep par déroulage: optimisation de l'étuvage (Valorisation of Aleppo pine for peeling: optimisation of soaking). Bois et Forêts des Tropiques 294(4):51–64

Denaud LE, Bleron L, Eyma F, Marchal R (2012) Wood peeling process monitoring: a comparison of signal processing methods to estimate veneer average lathe check frequency. Eur J Wood Prod 70:253–261

Dupleix A, Ould Ahmedou SA, Bleron L, Rossi F, Hughes M (2012) Rational production of veneer by IR-heating of green wood during peeling: modeling experiments. Holzforschung (accepted)

El Haouzali H (2009) Déroulage du peuplier: effets cultivars et stations sur la qualité des produits dérivés (Peeling of poplar: effects of cultivars and stations on the quality of derived products) PhD thesis, Arts et Métiers ParisTech

Fengel D, Wegener G (1984) Wood: chemistry, ultrastructure, reactions. Walter de Gruyter

Marchal R, Gaudilliere C, Collet R (2004) Technical feasibility of an embedded wood heating device on the slicer or the peeling lathe. 1st International Symposium Veneer Processing and Products Proceedings, pp 29–44

Meola C, Carlomagno GM, Giorlea L (2004) The use of infrared thermography for materials characterization. J Mater Process Technol 155:1132–1137

Mothe F (1985) Essai et comparaison de trois méthodes de classement de surface de bois massif pour leur rugosité: méthodes pneumatique et sensorielles (Test and comparison of three methods for grading the surface of solid wood for roughness: pneumatic and sensorial methods). Annales des Sciences Forestières 42(4):435–452

Mothe F (1988) Aptitude au déroulage du bois de Douglas. Conséquences de l'hétérogénéité du bois sur la qualité des placages. PhD thesis, Institut Polytechnique de Lorraine

Navi P, Heger F (2005) Comportement thermo-hydromécanique du bois: applications technologiques et dans les structures (Thermo-hydro-mechanical behaviour of wood: technological and structural applications). PPUR Presses Polytechniques

Olsson AM, Salmen L (1997) The effect of lignin composition on the viscoelastic properties of wood. Nord Pulp Pap Res 12(31):140–144

Palubicki B, Marchal R, Butaud JC, Denaud LE, Bleron L, Collet R, Kowaluk G (2010) A method of lathe checks measurement: SMOF device and its software. Eur J Wood Prod 68(2):151–159

Perre P (2007) Fundamentals of wood drying. A.R.BO.LOR

Pouzeau P, Pradal H (1957) Aspects nouveaux dans la technique de déroulage de l'Okoumé (New look in Okoumé peeling method). Bois et Forêts des Tropiques 54:41–50

Raiskila S, Saranpaa P, Fagerstedt K, Laakso T, Loija M, Mahlberg R, Paajanen L, Ritschkoff A (2006) Growth rate and wood properties of Norway spruce cutting clones on different sites. Silva Fenn 40(2):247–256

Tanritanir E, Hiziroglu S, As N (2006) Effect of steaming time on surface roughness of beech veneer. Build Environ 41(11):1494–1497

Thibaut B (1988) Le processus de coupe du bois par déroulage, PhD thesis, Institut Polytechnique de Lorraine

Thibaut B, Beauchene J (2004) Links between wood machining phenomena and wood mechanical properties: the case of 0°/90° orthogonal cutting of green wood, 2nd International Symposium on Wood Machining, pp 149–160
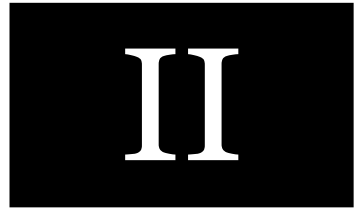
II

Mid-infrared absorption properties of green wood

Anna Dupleix · Domingos De Sousa Meneses ·
Mark Hughes · Rémy Marchal

Abstract   There is a lack of quantitative data on the penetration depth and the amount of energy absorbed by green wood under infrared (IR) radiation. This lack of knowledge is a potential barrier to the development of IR heating as an alternative to soaking as a means of warming logs prior to peeling in the manufacture of plywood. Experimental measurements of normal hemispherical spectral reflectance and transmittance over the range 550–5,500 cm^{-1} wavenumbers on four wood species, beech, birch, Douglas-fir and spruce have brought new knowledge on mid-infrared absorption properties of green wood and removed some uncertainties. For instance, it is not possible to deliver energy deeper than up to 0.3 mm below the wood surface because 70–90 % of all incident IR radiation on the wood surface is absorbed in this layer. Some wood features, such as surface quality, the presence of knots and of free water in wood (the latter two having a more significant effect) influence the amount of energy absorbed. These results illustrate that IR radiation can heat the surface layers, but then heat penetrates deeper into the inside layers of wood by conduction.

Introduction

The objective of the study reported herein was to determine the optical properties of green wood and wood at moisture contents below this level under infrared (IR)

A. Dupleix (✉) · R. Marchal
Arts et Metiers ParisTech LaBoMaP, Rue Porte de Paris, 71250 Cluny, France
e-mail: anna.dupleix@ensam.eu

A. Dupleix · M. Hughes
Department of Forest Products Technology, School of Chemical Technology, Aalto University, 00076 Aalto, Finland

D. De Sousa Meneses
Conditions Extrêmes et Matériaux: Haute Température et Irradiation (CEMHTI), UPR 3079, 1D Avenue de la Recherche Scientifique, 45071 Orleans Cedex 2, France

radiation. Characterisation involved the experimental measurement of diffuse reflectance and transmittance IR spectra. From these results, it was possible to estimate the amount of energy absorbed by the wood and the penetration depth of the IR radiation. This work provides a better understanding of the interaction between wood and IR radiation and gives insight into the technical feasibility of heating green wood using IR radiation. Furthermore, the new knowledge acquired here could be used to improve the accuracy of numerical models designed to simulate the thermal behaviour of wood whilst being heated by an external IR source (Dupleix et al. 2013a). This work is part of a wider project investigating the ability to heat green wood with IR radiation as an alternative technology to soaking prior to peeling.

The heating of logs prior to peeling to increase the deformability of green wood under the cutting knife is a key stage in the manufacture of veneer. This 'softening' of the wood has traditionally been carried out on an industrial scale by soaking the logs in hot water. This softening of the wood benefits the peeling process by lowering the cutting forces (Marchal et al. 2004) and improving veneer quality by reducing the risk of checking (Dupleix et al. 2013b). Ideally, the heating temperature should exceed the glass transition temperature, T_g, of the native hemicelluloses–lignin matrix, which in turn is dominated by the T_g of lignin at the moisture content of green wood (Engelund et al. 2013) and differs from the T_g of the isolated wood polymeric constituents (Navi and Sandberg 2012).

The long soaking times (from 24 to 48 h) needed to soften the log throughout points towards the need for a more rapid method of log heating. Feasibly, this might be achieved by embedding a heating system directly onto the peeling lathe to heat the bolt whilst peeling it. For this, it would be necessary to have a system that heats green wood very rapidly in order to cope with the high peeling rates demanded by industry (from 1 to 10 m/s). The thermal conductivity of wood remains low even at green wood moisture contents (Dupleix et al. 2013c) suggesting that the feasibility of IR heating of green wood whilst peeling depends upon the ability of green wood to absorb radiation from IR exposure and on the efficacy of heat transfer into green wood by radiation rather than by conduction.

Early work on oak reported that IR radiation is 'intensively' absorbed by the surface (Grimhall and Hoel 1983). The rate of IR absorption was determined from the temperature profile within the wood: the increase in temperature deep in the wood was assumed to be an indirect measure of the penetration depth of the IR radiation. Similar measurements applied to oak at moisture contents of between 0 and 20 % suggested that in all probability, the penetration depth of IR was less than 0.1 mm (Makoviny and Zemiar 2004). However, with this method, it remains difficult to precisely evaluate heat absorption into wood by radiation because the measurement techniques are necessarily biased by heat transfer through conduction (Cserta et al. 2012). Recent developments in IR spectroscopy have yielded more precise estimates of IR penetration into wood. The penetration depth has been calculated to range from 0.13 to 2.15 µm depending upon the wavelength (Zavarin et al. 1991) with a maximum depth of penetration of 37–138 µm recorded at 2,242 cm^{-1}, decreasing with wood density (Zavarin et al. 1990). From the forgoing studies by Zavarin et al. (1990, 1991), there is some controversy about the effect of

surface roughness on absorbance and it has also been reported to differ according to wavelength (Tsuchikawa et al. 1996). However, all these results originated from dry wood, and data on the penetration depth into green wood are lacking. The only study on the effect of moisture content on the optical properties of wood refers to emissivity. Kollmann and Côté (1968) reported that wet wood absorbs more IR energy than dry wood and that wood emissivity increases with MC up to fibre saturation point (fsp), at which point the emissivity of wood is the same as that of water ($\varepsilon = 0.93$). Emissivity values provided by the manufacturers of IR thermography cameras (e.g. FLIR System 2004) are given for all wavelengths of incident IR radiation, and the wood moisture content (MC) is referred to as either 'dry' or 'damp' which is not precise enough to obtain a clear picture of the dependence of optical properties on moisture content. Some experimental work has investigated the transmission and absorption of wet Douglas-fir, beech and oak veneers in the near- and mid-infrared range using a flux meter located underneath the exposed veneer (Marchal et al. 2004). From this work, it was concluded that veneers of between 0.5 and 2 mm absorb around 50 % and transmit around 10 % of the incident flux. These values were constant irrespective of the source wavelength, and transmission was found to increase with increasing MC but decrease with sample thickness. However, it is believed that these results should be considered with care because the flux meter may have been influenced by extraneous ambient light.

This paper reports the spectra of normal hemispherical spectral reflectance and transmittance over the wavenumber range 550–5,500 cm^{-1}, i.e., from 18 to 1.8 μm wavelengths, in four wood species: beech (*Fagus sylvatica*), birch (*Betula pendula*), Douglas-fir (*Pseudotsuga menziesii*) and spruce (*Picea abies*) and from ambient MC (around 12 %) to the saturated state. Conclusions about the absorption of IR radiation by wood at various moisture contents are drawn.

Materials and methods

Samples

Locally sourced bolts of beech, birch, Douglas-fir and spruce were peeled on a lathe at 1.5 m/s without prior soaking. Samples were cut from the veneers in the form of 30-mm diameter discs using a circular cutter. Sample thicknesses varied from 0.2 to 3.1 mm (0.2, 0.3, 0.5, 0.7, 0.9, 1.1, 1.2, 1.6, 2.0, 2.1, 2.2, 2.3, 3.0 and 3.1 mm). Green samples that had never been dried were kept wrapped in plastic bags just after peeling to prevent moisture loss. Other samples of veneer, air-dried at ambient temperature, were soaked in cold water to moisten them. The aim of using both green veneer and moistened veneer was to investigate possible differences in the optical properties arising from structural difference in the veneer caused by initial drying, since it is known that hornification takes place on initial drying. MC was determined gravimetrically where the initial weight was the weight measured just after the experiments (Eq. 1). The oven-dry weight was obtained after the samples had been dried in an oven maintained at a temperature

of 103 °C for around 24 h and until the mass loss during a 3-h interval was less than 0.02 g (ASTM 2002).

$$MC\,(\%) = \frac{\text{initial weight (g)} - \text{ovendry weight (g)}}{\text{ovendry weight (g)}} \tag{1}$$

Limiting the time of measurement to a couple of seconds minimised the risk of drying during the experiments. Moreover, as a precaution, the samples were carefully enfolded in plastic bags between each measurement in order to avoid any moisture loss, and the sample MC was determined before and after each measurement to ensure that no moisture loss had occurred. Negligible MC differences, never exceeding 1 %, were recorded in this process.

Integrating sphere device

Optical properties were measured with an integrating sphere device providing reflectance and transmittance spectra. This device consists of a Bruker Vertex 70 spectrometer equipped with a 6-inch integrating sphere (Hoffman SphereOptics) with a diffuse reflective gold coating. Single channel signals were acquired with a resolution of 4 cm^{-1} using an instrumental configuration composed of a globar source, a Ge/KBr beamsplitter and a nitrogen liquid cooled MCT (Mercury Cadmium Telluride HgCdTe) photoconductive infrared detector. Normal hemispherical reflectance R and transmittance T were calculated from different spectra (Eqs. 2 and 3). In order to suppress any parasitic contribution appearing in reflectance mode, the reflectance spectra R were background corrected with a measure of the ambient spectra (spectra A in Fig. 1a). Reference spectra M were acquired with a mirror used as a gold diffuse reference (Fig. 1b). Spectra E_R and E_T were obtained by using the adequate integrating sphere configurations described in Fig. 1c, d, respectively.

$$R = \frac{E_R - A}{M - A} \tag{2}$$

$$T = \frac{E_T}{M} \tag{3}$$

Method

Normal hemispherical reflectance spectra give, for each wavelength of the incident radiation, the amount of energy which leaves the incident sample surface without being absorbed because of reflectivity at the air–material interface or backward scattering by the wood fibres. Normal hemispherical transmittance spectra give, for each wavelength of the incident radiation, the amount of energy transmitted through the sample.

A simple energy balance shows that the amount of energy A absorbed by the material is given by Eq. 4.

(a) Configuration of spectra A

detector

Interior
diffusive coating

Beam
splitter

Globar
source

(b) Configuration of spectra M

mirror

(c) Configuration of spectra E_R

sample

(d) Configuration of spectra E_T

mirror

sample
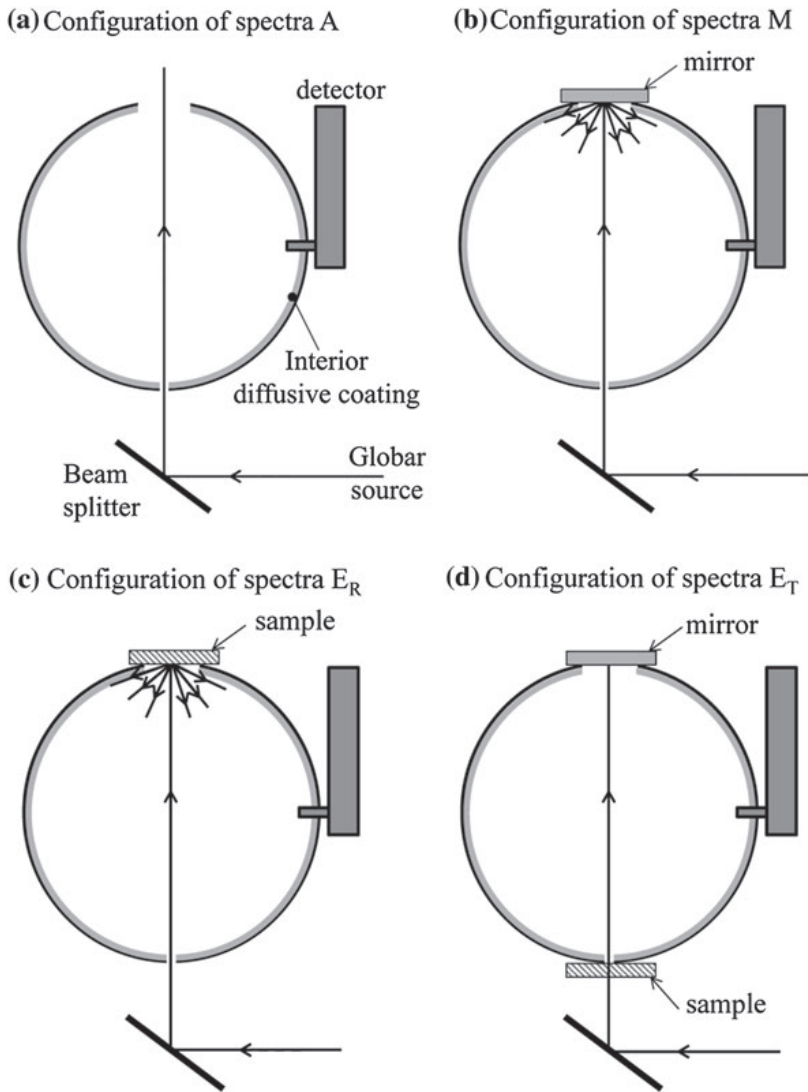
Fig. 1 Scheme of the different configurations of the integrating sphere to obtain **a** spectra A, **b** spectra M, **c** spectra E_R and **d** spectra E_T

$$A = 1 - R - T \tag{4}$$

where $A =$ absorptivity, $R =$ reflectivity, $T =$ transmissivity.

Due to their heterogeneous structures (porosity, fibres, etc.), light scattering is strong inside wood. So the penetration depths of these samples cannot be simply defined by the inverse of the absorption coefficient. Rather, a qualitative penetration depth is estimated by testing samples of decreasing thicknesses. As long as transmission is nearly equal to zero—meaning that all incident radiation is absorbed or reflected by the sample—the penetration depth is known to be less than the sample thickness. In other words, the penetration depth reported in this paper is given by the thinnest veneer section which gives a non-zero value for transmission.

Results and discussion

In Figs. 2, 3, 4, 5, 6, the small peak at around 2,400 cm^{-1} (marked with an arrow) is attributed to the absorption bands of CO_2 present in the surrounding atmosphere. Figure 4 shows a significant peak at 3,500 cm^{-1}, attributed to the surrounding H_2O, which was deleted in the representation of the spectra for improved reading. Above 3,000 cm^{-1}, the low intensity of the measured signals leads to a bad signal-to-noise ratio. The spectra are nevertheless reported up to 5,500 cm^{-1} since they give an indication of the trend of the optical properties in this spectral range. The interpretation of the transmission spectra gives information on the penetration depth, i.e., how deep the IR radiation penetrated into the wood. For thick enough samples, the reflection spectra provide information about the amount of energy accumulated within wood: it is a measure of the efficiency of the energy transfer between the IR source and the tested material.

Both transmission and reflection increase with higher frequencies, i.e., at shorter wavelengths (Figs. 2, 3, 4, 5, 6). The amount of energy effectively absorbed by the wood is more significant at higher wavelengths than in the near-IR range next to the visible range, below 2,500 cm^{-1}. Figure 2 shows the evolution of reflection, transmission and absorption spectra as a function of wavenumber, $1/\lambda$, (in cm^{-1}) for 1.2 and 3.1 mm thick green beech samples (at MCs of 60.7 and 63.6 %, respectively). This figure is representative of the spectra of the four species which exhibit the same behaviour for all thicknesses over 0.5 mm. Reflection varied between 0.02 and 0.3 (i.e. between 2 and 30 %). Transmission remained weak and could be neglected. The complement to 1 of the reflection spectra gives the absorption spectra (T can be omitted in Eq. 3). Absorption varied from 70 to 98 % implying that as soon as the sample thickness exceeds 0.5 mm, there is no radiation
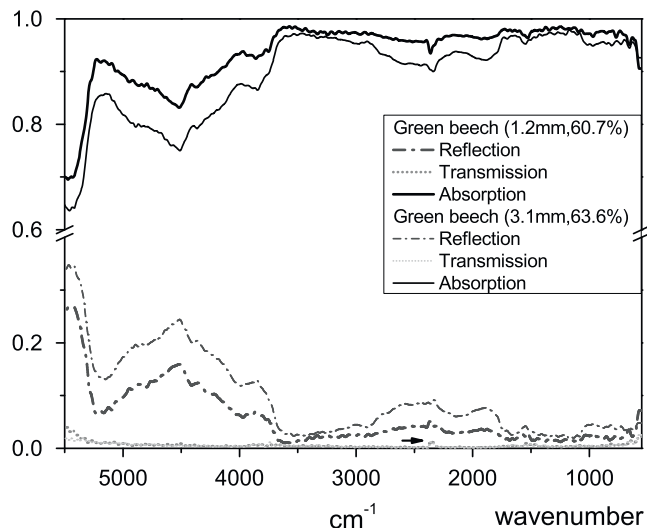
Fig. 2 Reflection, transmission and absorption spectra for 1.2 and 3.1 mm thick green beech samples (at 60.7 and 63.6 % MC)
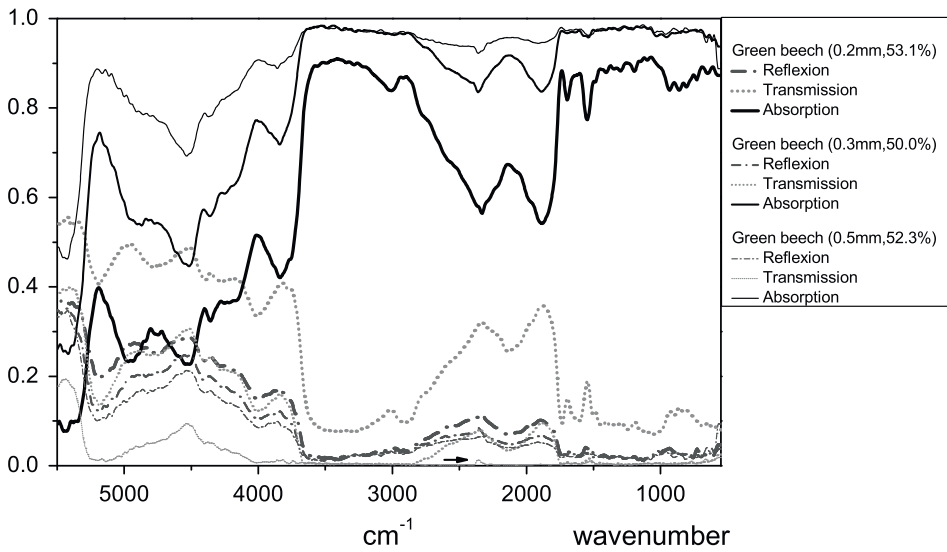
Fig. 3 Reflection, transmission and absorption spectra for 0.2, 0.3 and 0.5 mm thick green beech samples (at 53.1, 50.0 and 52.3 % MC)
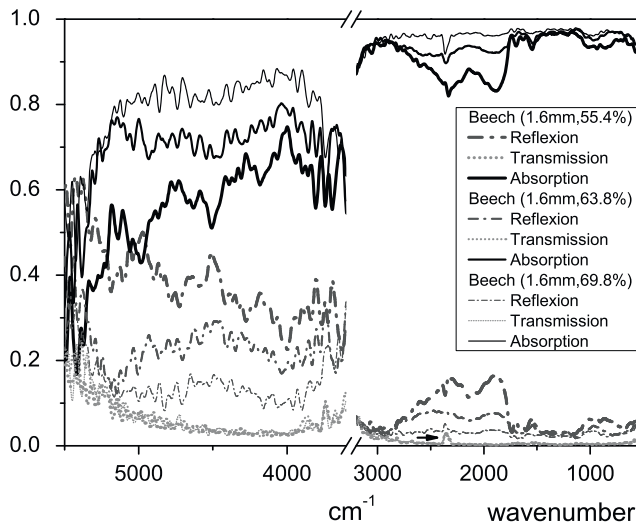
Fig. 4 Reflection, transmission and absorption spectra for 1.6 mm thick beech sample at 53.1, 50.0 and 52.3 % MC

transmitted through the sample and 70–98 % of all incident IR radiation is absorbed by the surface of the samples with no deep penetration of IR radiation within wood.

Thin (between 0.2 and 0.5 mm) beech samples provided precise information about the penetration depths. Figure 3 shows the reflection, transmission and absorption spectra for green beech samples of 0.2, 0.3 and 0.5 mm thicknesses (at MCs of 53.1, 50.0 and 52.3 %, respectively). Up to 4,000 cm^{-1}, the 0.5 mm sample absorbs nearly all incident energy (absorption is close to 0.95) and no energy is
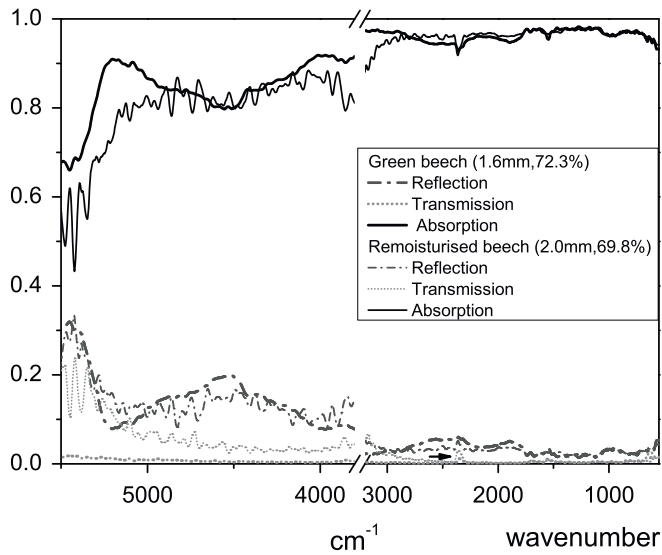
Fig. 5 Reflection, transmission and absorption spectra of green beech (1.6 mm, 72.3 %) and moistened beech (2.0 mm, 69.8 %)
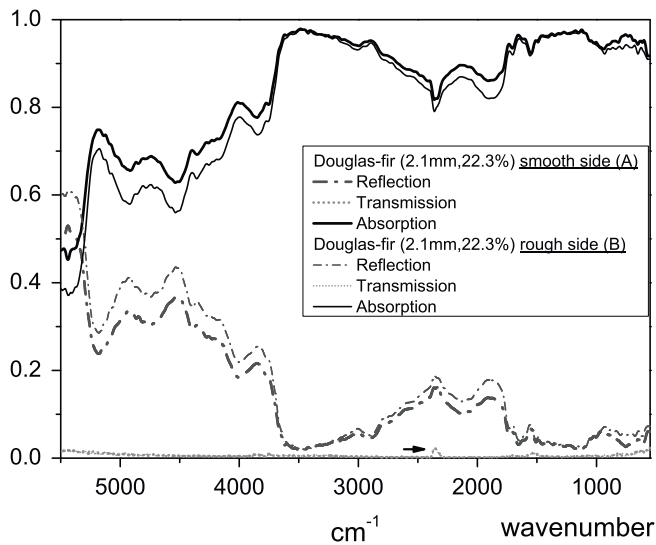
Fig. 6 Influence of the roughness on reflection, transmission and absorption spectra for a 2.1 mm thick green Douglas-fir sample at 22.3 % MC (side *B* is rougher than side *A*)

transmitted through the samples. In contrast, the 0.2 and 0.3 mm thick samples were found to transmit energy. In the 1,800–3,000 cm^{-1} range, transmission was found to be around 0.3 for the 0.2 mm thick samples and around 0.1 for the 0.3 mm thick samples. This indicates that between 550 and 4,000 cm^{-1}, around 70 % of the incident radiation is absorbed by the first 0.2 mm of wood and around 90 % of the incident IR radiation in the first 0.3 mm of wood. The thinner the sample, the more

radiation transmitted through it, and the thicker the sample, the greater the amount of reflected and absorbed radiation. The relatively low penetration depth of 0.3 mm might be explained by the heterogeneous structure of wood which can be modelled as a network of cellulose microfibrils embedded in a matrix of hemicelluloses and lignin, interspersed with water and void spaces. In the case of homogeneous materials, radiation propagates linearly with progressive exponential absorption following Beer–Lambert's law. However, the different refractive indices in heterogeneous materials backscatter the penetrating radiation preventing linear propagation, so that the strength of the radiation becomes smaller as it penetrates deeper.

Figure 4 shows the reflection, transmission and absorption spectra at different MC for 1.6 mm thick beech sample. All samples with thicknesses greater than 0.5 mm and all species tested exhibited similar behaviour. Reflection varied between 10 and 30 % with the most significant amount of reflected radiation occurring on drier wood. Transmission could be neglected because it remains constantly weak (less than 5 %) without being influenced by the amount of water in wood. Therefore, T is negligible in Eq. 3, and the complement to 1 of reflectivity gives absorptivity. Absorption varied from 70 to 90 % with the most significant amount of absorbed radiation occurring in wetter wood. The presence of water in wood is thus beneficial in terms of IR penetration because it increases the amount of absorbed energy. However, if this substantial increase serves to heat the water present in wood, it is of no interest for the purpose being investigated herein, namely to heat the wood material with IR radiation.

A further investigation was carried out on the effect of knots in wood. This issue is of concern since the characteristics of knots—for instance high density and variable grain direction (Kollmann and Côté 1968)—are known to be detrimental to veneer cutting. If knots were to absorb more energy than the surrounding wood, IR could be used, for example, to preferentially heat the knots, thereby softening them and making them easier to cut during veneer peeling. The presence of knots may be seen to increase absorption. A possible explanation for this is that the denser wood in the knots contains a relatively greater number of molecules able to absorb energy. Moreover, the different orientation of the fibres in knots may also affect energy absorption. Both wood density and fibre orientation have been noted by Zavarin et al. (1990) as factors influencing energy absorption in wood.

Figure 5 shows the spectra from the same species of wood (beech) that has either been maintained in the green state (MC of 72.3 %) or has been dried and thereafter moistened to approximately the same MC (69.8 %). As may be seen, there is no significant difference in the y-axis values between the spectra of green and moistened beech. These results are interesting in that whilst green and moistened wood are chemically the same, they are structurally slightly different materials due to the irreversible loss of hydroxyl groups during hornification: in other words, moistening wood does not liberate all hydroxyl groups 'lost' during initial drying from the green state (Suchy et al. 2009). The materials, however, interact in the same way with IR radiation. The absence of spectral differences between moistened and green wood could be explained by the state of water molecules which remains unaffected by drying and rewetting (Hoffmeyer et al. 2011). Figure 6 illustrates the

influence of surface quality on wood absorption for a 2.1 mm thick green Douglas-fir sample at 22.3 % MC. This sample possessed different surface physical characteristics on the two sides. Side A is the tight side of the veneer and side B the loose side. Lathe checking that forms on the loose side increases veneer roughness (Dupleix et al. 2013b). From comparison of sides A and B, it may be concluded that the rougher the surface (the loose side, side B), the greater the reflection and the less absorption. This behaviour was already highlighted by Bennett and Porteus (1961) and De Santo (2007) who found that surface roughness increases light scattering and is proportional to surface reflectance. Clearly, by modifying the veneer surface quality, the peeling process influences wood absorption as also stated by Jones et al. (2008).

Conclusion

These results provided new insights into the interaction between wet wood (either green or moistened from dry) and IR radiation over the wavenumbers range from 550 to 5,500 cm^{-1}, i.e., over wavelengths ranging from 1.8 to 18 μm. In general, reflection varies between 10 and 30 %, and the penetration depth of the radiation is close to 0.3 mm. This means that the wood surface absorbs 70–90 % of all incident IR radiation in the first 0.3 mm of wood, and it is not possible for energy to penetrate deeper than about 0.3 mm. Whether penetration to this depth is sufficient to positively affect the veneer cutting stage by softening wood in the shear plane remains open for further investigation. It was also found that wood absorbs more energy at longer wavelengths, that knots increase energy absorption and that never dried green wood behaves like moistened wood. Furthermore, the roughness of the surface also influences absorption. The influence of water in wood is beneficial to IR penetration because it increases the amount of absorbed energy, but this positive effect remains limited since the energy is partly absorbed by the free water.

These findings do not necessarily suggest that the IR heating of green wood is impracticable, but they highlight the fact that IR radiation is mainly absorbed near the surface without penetrating deeply into the wood. Equations predicting the heating of wood layers beneath the surface by an external IR source should only take into account the transfer of the heat absorbed by the surface layers by conduction to the inside layers (Dupleix et al. 2013a). Future work studying temperature rise within the absorption area would contribute to a deeper understanding of the interaction between wood and IR radiation.

References

American Society for Testing and Materials (ASTM) (2002) Standard test methods for direct moisture content measurement of wood and wood-base materials. ASTM D 4442-92. In: ASTM annual book of standards. ASTM. West Conshohocken, PA

Bennett HEJ, Porteus JO (1961) Relation between surface roughness and specular reflection at normal incidence. J Opt Soc Am 51(2):123–129

Cserta E, Hegedus G, Nemeth R (2012) Evolution of temperature and moisture profiles of wood exposed to infrared radiation. Bioresources 7(4):5304–5311

De Santo JA (2007) Overview of rough surface scattering. Light scattering and nanoscale surface roughness. Springer, Berlin, pp 211–235

Dupleix A, Ould Ahmedou SA, Bleron L, Rossi F, Hughes M (2013a) Rational production of veneer by IR-heating of green wood during peeling: modeling experiments. Holzforschung 67(1):53–58

Dupleix A, Denaud LE, Bleron L, Marchal R, Hughes M (2013b) The effect of log heating temperature on the peeling process and veneer quality: beech, birch, and spruce case studies. Eur J Wood Prod 71:163–171

Dupleix A, Kusiak A, Rossi F, Hughes M (2013c) Measuring the thermal properties of green wood by the transient plane source (TPS) technique. Holzforschung 67(4):437–445

Engelund ET, Thygesen LG, Svensson S, Hill C (2013) A critical discussion of the physics of wood-water interactions. Wood Sci Technol 47:141–161

Flir Systems ThermaCAM User's Manual (2004)

Grimhall CG, Hoel O (1983) Method of slicing veneer US Patent 4,516,614

Hoffmeyer P, Engelund ET, Thygesen LG (2011) Equilibrium moisture content (EMC) in Norway spruce during the first and second desorptions. Holzforschung 65:875–882

Jones PD, Schimleck LR, Daniels RF, Clark A, Purnell RC (2008) Comparison of *Pinus taeda* L. whole-tree wood property calibrations using diffuse reflectance near infrared spectra obtained using a variety of sampling options. Wood Sci Technol 42(5):358–400

Kollmann FFP, Côté WA (1968) Principles of wood science. I-Solid wood. Springer, Berlin

Makoviny I, Zemiar J (2004) Heating of wood surface layers by infrared and microwave radiation. Wood Res 49(4):33–40

Marchal R, Gaudilliere C, Collet R (2004) Technical feasibility of an embedded wood heating device on the slicer or the peeling lathe. In: International symposium veneer processing and products proceedings, pp 29–44

Navi P, Sandberg D (2012) Thermo-hydro-mechanical processing of wood. EPFL Press, Lausanne, pp 159–191

Suchy M, Virtanen J, Kontturi E, Vuorinen T (2009) Impact of drying on wood ultrastructure observed by deuterium exchange and photoacoustic FT-IR spectroscopy. Biomacromolecules 11(2):515–520

Tsuchikawa S, Hayashi K, Tsutsumi S (1996) Nondestructive measurement of the subsurface structure of biological material having cellular structure by using near-infrared spectroscopy. Appl Spectrosc 50(9):1117–1124

Zavarin E, Jones SG, Cool LG (1990) Analysis of solid wood surfaces by diffuse reflectance infrared fourier-transform (DRIFT) spectroscopy. J Wood Chem Technol 10(4):495–513

Zavarin E, Cool LG, Jones SG (1991) Analysis of solid wood surfaces by internal-reflection fourier-transform infrared-spectroscopy (FTIR-IRS). J Wood Chem Technol 11(1):41–56

III

Anna Dupleix*, Andrzej Kusiak, Mark Hughes and Fréderic Rossi

Measuring the thermal properties of green wood by the transient plane source (TPS) technique

Abstract: The thermal properties of wood in the green state have been determined by the transient plane source (TPS) technique. Data are presented on thermal conductivity (λ), heat capacity (C), and thermal diffusivity (κ) at moisture contents (MCs) above the fiber saturation point, which are based on measurements using the HotDisk® apparatus. Four wood species (Douglas fir, beech, birch, and spruce) were tested, and the results are compared with literature data and those obtained by the flash method. A linear relationship was found between the thermal properties λ, C, and κ on the one hand and MC on the other. Equations predicting the thermal values as a function of MC and wood anisotropy are presented. Wood C and λ increase with MC, but wet wood diffuses heat more rapidly than dry wood.

Keywords: green wood, heat capacity, HotDisk®, thermal conductivity, thermal diffusivity, transient plane source (TPS)

*Corresponding author: Anna Dupleix, Arts et Metiers ParisTech LaBoMaP, Rue Porte de Paris, F-71250 Cluny, France,
Phone: +33 3 85 59 53 27, Fax: +33 3 85 59 53 85,
e-mail: anna.dupleix@ensam.eu
Anna Dupleix and Mark Hughes: Department of Forest Products Technology, School of Chemical Technology, Aalto University, FI-00076 Aalto, Finland
Andrzej Kusiak: Université Bordeaux 1, I2M, Esplanade des Arts et Métiers, F-33405 Talence Cedex, France
Fréderic Rossi: Arts et Metiers ParisTech LaBoMaP, Rue Porte de Paris, F-71250 Cluny, France

Introduction

Thermal conductivity (λ), heat capacity (C), and thermal diffusivity (κ) are the most important properties that characterize the thermal behavior of a material and also that of wood (Suleiman et al. 1999; Olek et al. 2003; Sonderegger et al. 2011). At moisture contents (MCs) between 0% and fiber saturation point (FSP), wood is considered to be a good insulating material with low λ, moderate C, and consequently low κ. The porosity of wood has a low λ because the λ of air filling the void spaces is lower (λ_{air}=0.0261

W m^{-1} K^{-1} at 300 K) than that of the cell wall (Rohsenow et al. 1973). Heat flows preferentially through the wood cell walls, which act like heat bridges, whereas the air present in the lumens below the FSP forms a barrier to heat flow (Kollmann and Côté 1968).

The thermal properties of wood are affected by a range of factors including the extractive content, grain direction, knots, checks, microfibril angle, growth rings, ray cells, anisotropy, wood species, and porosity. The MC and temperature are also influential with this regard (Suleiman et al. 1999). Both λ and C increase linearly with temperature, but the λ increment is smaller than that of C (Harada et al. 1998; Simpson and TenWolde 1999). The present study is focused on the effect of anatomical orientation (radial or tangential) and MC on wood's thermal properties.

Influence of anisotropy

The influence of wood anisotropy on transverse conductivity is controversial. Some authors (Siau 1971; Simpson and TenWolde 1999; Suleiman et al. 1999) report the same λ values in the radial (λR) and tangential (λT) directions, whereas other authors claim that transverse conductivity is higher in the R than in the T direction (see Table 1). The ratio of λR and λT is thought to be governed by the volume of ray cells in hardwoods and the volume of latewood in softwoods (Steinhagen 1977). Similar λR and λT data were obtained for hardwood species with a rather uniform wood structure or a low amount of latewood, such as in young softwoods (Suleiman et al. 1999). However, studies on beech and spruce support the concept that λR predominates (Sonderegger et al. 2011). Logically, there is no influence of orientation on specific heat, as this property is mainly dependent upon the cell wall material itself. Consequently, there is hardly any influence of density on c (Sonderegger et al. 2011); neither is there much variation from one species to another (Jia et al. 2010). As κ is proportional to λ, it is logical that diffusivity is also anisotropic because ρ and c are both isotropic properties (Steinhagen 1977). Therefore, the κR should be higher than κT because of the lower tangential λT (Kollmann and Côté 1968). However, as with λ, some findings do not corroborate the anisotropic nature of κ (Suleiman et al. 1999).

Influence of MC

The conductivity of water (λ_{water}=0.613 W m^{-1} K^{-1} at 300 K (Rohsenow et al. 1973) is higher than that of air. Accordingly, wood conductivity increases with higher MC, as there is a linear relationship between these parameters (Table 1). For beech and spruce, the R^2 of this relationship is ~0.95–0.99 (Sonderegger et al. 2011). Free water conducts more heat than bound water; thus, the λ increment is steeper above FSP (Siau 1971). The presence of water strongly affects the heat capacity of wood because of the high of water c_{water}=4.18 kJ kg^{-1} K^{-1} at 300 K (Rohsenow et al. 1973). As a first approximation, the specific heat c of wet wood can be calculated using a simple rule of mixtures by adding the specific heat c_{water} and c_0 (for oven-dried wood) in their relative proportions:

$$c=wc_{water}+(1-w)c_0 \qquad (1)$$

where w is the weight fraction of water in wood based on the mass of wet wood. Expressing w as a function of m (MC in %/100) gives rise to Eq. (2), and substituting w in Eq. (1) gives rise to Eq. (3) (Kollmann and Côté 1968).

$$w=m/(1+m) \qquad (2)$$

$$c=(c_{water}m+c_0)/(1+m) \qquad (3)$$

Eqs. (1) and (3) consider wet wood to be a mixture of two independent materials; however, this may be an oversimplification, and some authors have suggested that this relationship only holds true when the MC is >5% (Jia et al. 2010; Sonderegger et al. 2011). Table 1 summarizes the different relations between c and MC. As indicated, some authors propose an additional coefficient (A_c) to take into account the energy lost during the wetting of the cell wall due to the creation of H bonds between cellulose and water (Simpson and TenWolde 1999; Sonderegger et al. 2011). However, A_c values vary among authors and are only valid below FSP. Other authors modify the coefficients in the rule of mixtures as a function of MC (Siau 1995; Koumoutsakos et al. 2001). However, the correlation between specific heat c and $w/(1+w)$ was linear in case of beech and spruce (Sonderegger et al. 2011). Studies focusing on heat diffusion κ of wet and dry wood are scarce. According to Kollmann and Côté (1968), κ decreases slightly with MC, with a very low inclination (-0.01) (see Table 1).

Measurement methods of thermal properties

The guarded hot plate method has proven to be the most accurate procedure for measuring unidirectional thermal conductivity in all kind of materials under conditions of steady-state heat conduction (Speyer 1994; Bučar and Straže 2008). Establishing a steady-state heat flow, when a stable temperature gradient is developed (ISO 8302), takes ~10 min in the case of a 200-mm-thick wood sample. This condition can be achieved by maintaining MC values below the FSP (up to 20% MC) by controlling the relative humidity (Sonderegger et al. 2011). However, testing green wood under such conditions is impossible without risking the formation of a perturbing moisture gradient within the sample.

Meanwhile, the thermal properties of green wood can be measured using transient methods within a couple of

Predicting equations for the thermal properties indicated	Required conditions (literature[a])
λ (W m^{-1} K^{-1})	
$\lambda=G(0.2+0.4m)+0.02$	5%<MC<35% (1); MC<25% (2); MC<40% (3, 4)
$\lambda=G(0.2+0.5m)+0.02$	MC>40% (3, 4)
$\lambda R=0.086+0.108m$	MC<20%, spruce (1)
$\lambda T=0.092+0.235m$	
$\lambda R=0.120+0.193m$	MC<20%, beech (1)
$\lambda T=0.071+0.128m$	
$\lambda R/\lambda T$	
13%	fir (5)
11%	oak (5)
3%–20%	(1)
5%–10%	(3)
c (kJ kg^{-1} K^{-1})	
$c=((c_{water}m+c_0)/(1+m))+A_c$	MC<5%, A_c=0 (1, 6); 5%<MC<FSP, A_c<0 (1); MC<FSP, A_c=m(-6.191+2.36×10^{-2}T-1.33m) (2)
$c=(4.15m+1.260)/(1+m)$	MC<5% (7, 8)
$c=(5.859m+1.176)/(1+m)$	5%<MC<30% (7, 8)
$c=(4.185m+1.678)/(1+m)$	MC>30% (7, 8)
$c=(0.0364m)/(1+m)+1.245$	MC<17%, spruce (1)
$c=(0.0337m)/(1+m)+1.134$	MC<17%, beech (1)
$c_0=1350$	20°C (4)
$c_0=1590$	20°C (9)
$c_0=1250$	20°C (10)
$c_0=1176$	20°C (6)
κ (m^2 s^{-1})	
$\kappa=(-m+0.199)10^{-6}$	ρ=200 kg/m^3 (3)
$\kappa=(-m+0.167)10^{-6}$	ρ=400 kg/m^3 (3)
$\kappa=(-0.9m+0.153)10^{-6}$	ρ=600 kg/m^3 (3)
$\kappa=(-0.6m+0.143)10^{-6}$	ρ=800 kg/m^3 (3)

Table 1 Literature equations predicting the influence of MC, density, and transversal directions on λ, C, and κ.
[a]Literature: (1) Sonderegger et al. (2011), (2) Simpson and TenWolde (1999), (3) Kollmann and Côté (1968), (4) Siau (1971), (5) Incropera et al. (2011), (6) Jia et al. (2010), (7) Siau (1995), (8) Koumoutsakos et al. (2001), (9) Steinhagen (1977), (10) Harada et al. (1998); $G=(m_0/V_\mu)/\rho_{water}$=specific gravity based on the weight of the oven-dried wood, m_0, and volume at MC, V_μ (no dimension).

seconds. The transient hot wire (THW) and transient hot strip (THS) techniques can provide values for λ and κ from the temperature measured locally by a thermocouple sandwiched between two specimens and located next to the electrified wire or strip that dissipates heat to the surrounding material. The flash method is another transient technique that can provide κ values from the temperature change on the rear face of a sample exposed to a laser or a lamp that supplies heat through the front face. The temperature change can be measured locally by a thermocouple or an infrared camera to obtain the whole temperature field on the rear face of the sample.

The advantage of the TPS technique over the other transient methods cited above is that it is based on the measurement of the average temperature of the heated surface of the sample. It is particularly important in the case of anisotropic materials such as wood. Moreover, it permits the simultaneous characterization of κ, λ, and C. Table 2 compares the advantages and disadvantages of each method in measuring the thermal properties of green wood.

The general theory of TPS has been comprehensively described by Gustafsson (1991). The TPS technique entails recording the resistance change as a function of time of the heat source, in form of a disk, which serves as the measuring sensor. The TPS element is sandwiched between two specimens while an electrical current is passed through it with sufficient power to slightly increase its temperature (between 1 and 2 K). The temperature coefficient of the resistivity (TCR) of the sensor is known; thus, its resistance change gives information on its temperature variation. As with the THS and THW techniques, the solution of the equations involved in the TPS method relies on the assumption that the sensor is placed in an infinite medium. This assumption implies that the time of transient recording ends before heat reaches the outer boundaries of the sample to avoid edge effects and that the sample

size, which can be arbitrary, ensures that the distance from the sensor edges to the nearest sample boundary exceeds the probing depth Δ_p [Figure 1, Eq. (6)] (Gustavsson et al. 2000):

$$\Delta_p = 2(\kappa t_{max})^{1/2} \tag{6}$$

where t_{max} is the total time of experiment. The benefit of the TPS technique lies in its ability to combine both heat source and temperature sensor in the same TPS element, thereby ensuring a better accuracy of the thermal transport measurement compared with the THS or THW methods. The TPS technique consists of measuring λ and κ, whereas C is calculated from the relationship $\kappa = \lambda/C$. Fitting the TPS experimental results with the analytical models presented by Gustafsson (1991) leads to λ and κ values.

Specific objectives of the study

The aim of the work reported herein was to investigate the transverse (radial and tangential) thermal conductivity (λ), heat capacity (C), and thermal diffusivity (κ) of the green wood of the species beech, birch, Douglas fir, and spruce at MC above FSP. The TPS technique was in focus. The literature data with TPS are limited to dry wood (Suleiman et al. 1999); thus, the present article intends to deliver data above FSP. Empirical equations for predicting the relationship between λ, C, and κ and MC above the FSP should be calculated. The rationale for conducting this study was to render possible numerical models that simulate the transverse IR heating of green wood based on accurate thermal property data (Dupleix et al. 2012). For this reason, only the transverse directions will be tested because they are the main directions of heat flow. The lack of data in the literature on the thermal properties of green wood provided the main impetus for this study.

Measurement methods	Properties		Regime state		Advantages for solid green wood	Drawbacks for solid green wood
	λ	κ	trans. state	steady state		
Hot-guarded plate	X	X		X	Accuracy of the steady-state heat flow	Long time, perturbing moisture gradient
THW	X		X		Short time	Localized measurement
THS		X	X		Short time	Localized measurement
Flash		X	X		Short time	High-energy, localized measurement
TPS	X	X	X		Short time, λ, and κ results	Possibly thermal inertia of the sensor

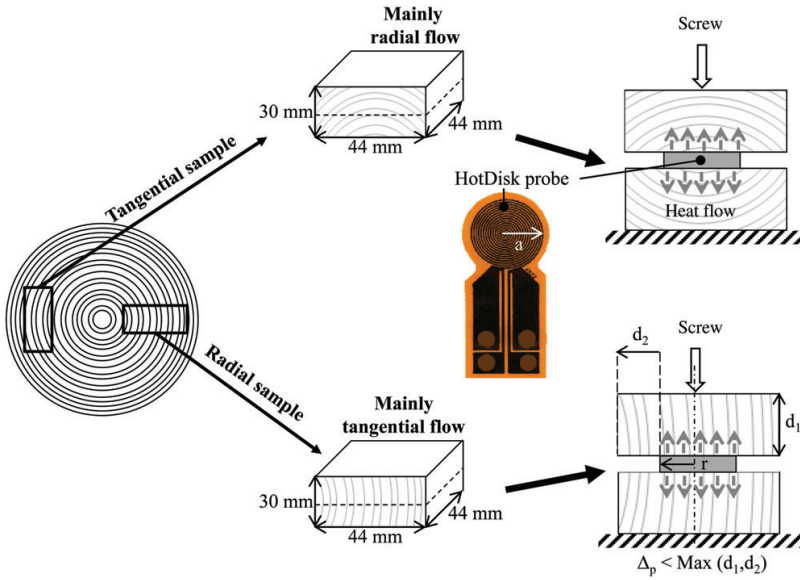**Table 2** Comparison of different measurement methods of green wood thermal properties.

Figure 1 Sampling identical samples and TPS measurement configuration showing probing depth Δ_p.

Materials and methods

List of symbols

c	Specific heat (kJ kg^{-1} K^{-1})
c_0	Specific heat of oven-dried wood (kJ kg^{-1} K^{-1})
$C=\rho c$	Heat capacity (J m^{-3} K^{-1})
CR	Radial heat capacity (J m^{-3} K^{-1})
CT	Tangential heat capacity (J m^{-3} K^{-1})
G	Specific gravity (no dimension)
$\kappa=\lambda/C$	Diffusivity (m^2 s^{-1})
κR	Radial diffusivity (m^2 s^{-1})
κT	Tangential diffusivity (m^2 s^{-1})
λ	Transverse conductivity (W m^{-1} K^{-1})
λR	Radial conductivity (W m^{-1} K^{-1})
λT	Tangential conductivity (W m^{-1} K^{-1})
m	MC in%/100 (no dimension)
r	Probe radius (mm)
ρ	Density (kg m^{-3})
t_{max}	Total time of experiment (s)
τ	Characteristic time (s)
w	Fraction of water in wet wood (no dimension)

Samples

Knot-free samples of beech [*Fagus sylvatica* (L)], birch [*Betula pendula* (Roth)], heartwood of Douglas fir [*Pseudotsuga menziesii* (Mull) Franco], and spruce [*Picea albies* (L.) Karst] were studied. The samples were split from the same freshly cut tree in the tangential (*T*) and radial (*R*) directions with respect to grain orientation and were sawn to the initial shape of a block with dimensions of 44×44×30 mm³. Each sample was then cut in two parts, giving rise to identical samples of 44×44×15 mm³ (Figure 1). Both top and bottom samples will have the same thermal transport behaviors because of their symmetrical growth ring geometry.

Method

The pretesting of each sample was performed to carefully adjust the parameters cited in Table 3 as a function of the chosen probe. This time-consuming process of adjusting the settings was, however, essential for the TPS measurement method because of its numerous parameters, which would distort the results, if inappropriately selected (Olek et al. 2003). Once values obtained are ensured to be representative of wood thermal properties, repetitions of the test were performed until hardly any change in the standard deviation (SD) was observable. Hence, each point plotted in the graphs in the Results and Discussion section represents the average of 30 individual measurements taken at five different locations of the sample. The TPS element sandwiched between two samples delivers a heat flow mainly radially for the sample cut in the *T* direction and vice versa.

Moisture content

The samples were maintained in the green state by vacuum packing until testing. Samples were subsequently placed in a hot and wet air flow for different durations to obtain a wide range of MCs above the

TPS parameters	Values and units
TCR	0.005 K^{-1}
Temperature increase	1–2 K
Measurement time τ	80–320 s
Probing depth Δ_p	~10 mm
Probe radius r	6.4 mm (model 5501)
Input power	0.01–0.05 W
External temperature	22°C

Table 3 Summary of the parameters used during the experiments with TPS.

FSP. The slow drying procedure should have ensured that the MC is homogeneous throughout the sample, thus minimizing any possible side-effects caused by moisture gradient. MC was measured with the double weighing method, where the initial weight was the weight at the time of the experiments. This limited the time of the measurements to a couple of seconds, and placing the sample underneath the cover of the TPS device ensured that heat transfer by convection was avoided, resulting in the drying of the samples during the experiment. This assumption was confirmed by measuring the MC at the start and at the end of the experiment. The MC difference never exceeded 1%, thus the effect of drying during the experiments is negligible. The MC values are the means of five determinations after the TPS measurement on each of the five locations tested for a sample (Table 4).

	Mainly tangential flow			Mainly radial flow		
MC (%)	(SD)	MC differences[a] (%)	MC (%)	(SD)	MC differences[a] (%)
Birch						
59.9	(0.3)	0.6	125.6	(0.3)	0.8
82.6	(0.3)	0.7	59.9	(0.3)	0.6
46.5	(0.4)	0.9	51.5	(0.2)	0.4
40.0	(0.4)	0.8	42.7	(0.4)	0.9
			33.6	(0.4)	0.6
Beech						
121.8	(0.1)	0.1	121.6	(0.4)	0.8
81.9	(0.2)	0.3	113.6	(0.4)	0.8
30.2	(0.2)	0.3	45.9	(0.5)	1.0
			30.7	(0.5)	0.9
Spruce						
151.8	(0.1)	0.2	147.4	(0.3)	0.6
149.6	(0.2)	0.3	76.3	(0.3)	0.7
83.9	(0.3)	0.6	52.1	(0.2)	0.3
67.2	(0.4)	0.9	28.8	(0.2)	0.4
44.5	(0.5)	0.9			
Douglas fir						
158.3	(0.4)	0.8	70.9	(0.3)	0.6
73.6	(0.5)	0.9	61.6	(0.1)	0.1
68.2	(0.4)	0.6	60.2	(0.2)	0.3
59.5	(0.5)	0.6	58.5	(0.3)	0.8
			55.8	(0.5)	0.7

Table 4 Mean MC, SD, and difference of MC between the start and the end of experiment calculated on five tested locations for the wood samples indicated.
[a]Between start and end of experiments.

TPS device

The HotDisk® Thermal Constants Analyser® was from I2M (Bordeaux, France). The 13-µm-thick, 6.403-mm-radius, spiral-shaped TPS element of known TCR was of nickel foil covered by a polymer Kapton, which is highly temperature-resistant and electrically insulating (Figure 1). Clamps were used to ensure good and reproducible thermal contact. Before the experiments, a Wheatstone bridge composed of the TPS element as one resistor was balanced to reset the TPS element resistance to 0. To enable the wood samples to recover isothermal conditions between measurements, a relaxation time was set on 36 times the duration of the transient recording, as recommended in the HotDisk® user's manual. The experiments were performed at constant room temperature. The parameters are listed in Table 3.

The probe size was chosen to be as large as possible to widen the probed area and obtain average values representative of the thermal properties with minimum disturbance induced by structural heterogeneities (e.g., annual growth rings, differences of densities between earlywood and latewood). However, the larger probe size, the longer characteristic time τ [Eq. (7), where r is the probe radius] and therefore the longer measurement time. Thus, a compromise had to be made between the largest possible probe size and the limited measurement time to avoid any edge effects and prevent the drying of the sample.

$$\tau = r^2/\kappa \qquad (7)$$

Results

Transverse conductivity (λ), heat capacity (C), and thermal diffusivity (κ) are presented in Figures 2–4, respectively, as calculated by the equations in Table 5. The repeatability of the experiments is demonstrated by moderate SDs (error bars). The predictive equations for λ, C, and κ are presented in Table 5 as obtained by the HotDisk® method in the present article and by the flash method according to Beluche (2011). As clearly visible, the relationships with MC above the FSP are good, as expressed by the high coefficients of determination (R^2). The equations are particularly useful for understanding heat transfer in wood in the green state (Table 5).

Figure 2 compares the λ values obtained in this work with those obtained by the steady-state guarded hot plate method (Sonderegger et al. 2011). Apart from spruce, the λ experimental values continuously match results from the literature (Sonderegger et al. 2011), but the values are slightly higher for all other species. There is no significant difference in λ between the radial and the tangential directions for wood in the green state – apart from spruce. It seems that the presence of free water in the cell overrides any effects arising from the anisotropy of the wood. The exception in the case of spruce might be explained by

Method, wood	Predictive equations for thermal conductivity (λ), thermal diffusivity (κ), and heat capacity (C)			
	Equations in radial direction	Equation number	Equations in tangential direction	Equation number
HotDisk®				
Beech	λR=0.003MC+0.172 (R^2 0.997)	(8)	λT=0.003MC+0.194 (R^2 0.974)	(9)
Birch	λR=0.003MC+0.191 (R^2 0.998)	(10)	λT=0.003MC+0.165 (R^2 0.983)	(11)
Spruce	λR=0.002MC+0.130 (R^2 0.960)	(12)	λT=0.001MC+0.137 (R^2 0.985)	(13)
Beech	CR=0.019MC+0.746 (R^2 0.940)	(14)	CT=0.024MC+0.600 (R^2 0.997)	(15)
Birch	CR=0.021MC+0.577 (R^2 0.999)	(16)	CT=0.032MC-0.170 (R^2 0.976)	(17)
Spruce	CR=0.032MC-0.311 (R^2 0.964)	(18)	CT=0.030MC-1.540 (R^2 0.992)	(19)
Beech	κR=-0.0005MC+0.2 (R^2 0.962)	(20)	κT=-0.0006MC+0.2 (R^2 0.990)	(21)
Birch	κR=-0.0005MC+0.2 (R^2 0.924)	(22)	κT=-0.002MC+0.4 (R^2 0.989)	(23)
Spruce	κR=-0.001MC+0.3 (R^2 0.938)	(24)	κT=-0.003MC+0.6 (R^2 0.998)	(25)
Flash				
Beech	κR=-0.001MC+0.2 (R^2 0.961)	(26)		
Douglas fir	κR=-0.0009MC+0.2 (R^2 0.947)	(27)		

Table 5 Equations and coefficients of determination of linear regressions plotted for λ, C, and κ in radial and tangential directions.

the presence of ray cells that promote heat transfer in the radial direction (λR>λT).

Figure 3 compares the C values obtained with the results of Sonderegger et al. (2011) and oven-dried values at 20°C referred to in the literature (Kollmann and Côté 1968; Steinhagen 1977; Jia et al. 2010). The gradients of the linear relationships between C and MC above FSP are steeper than below the FSP (results from literature),

most probably arising from the dominating effect of the free water. The scattered results for Douglas fir and spruce can be interpreted to mean that C in the green state is not unique for all wood species. There are probably two different ranges of C values for hardwoods and softwoods: the former in the green state would need more energy for heating than softwoods. This behavior is different from that described in the literature below the FSP.
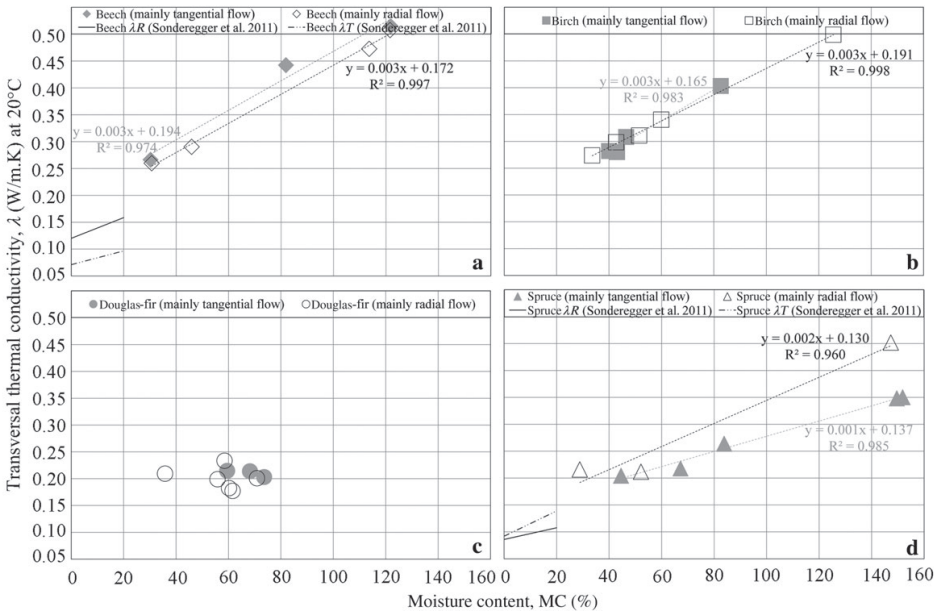

Figure 2 Thermal conductivity (λ, in W m^{-1} K^{-1}) at green state with HotDisk® of (a) beech, (b) birch, (c) Douglas fir, and (d) spruce.
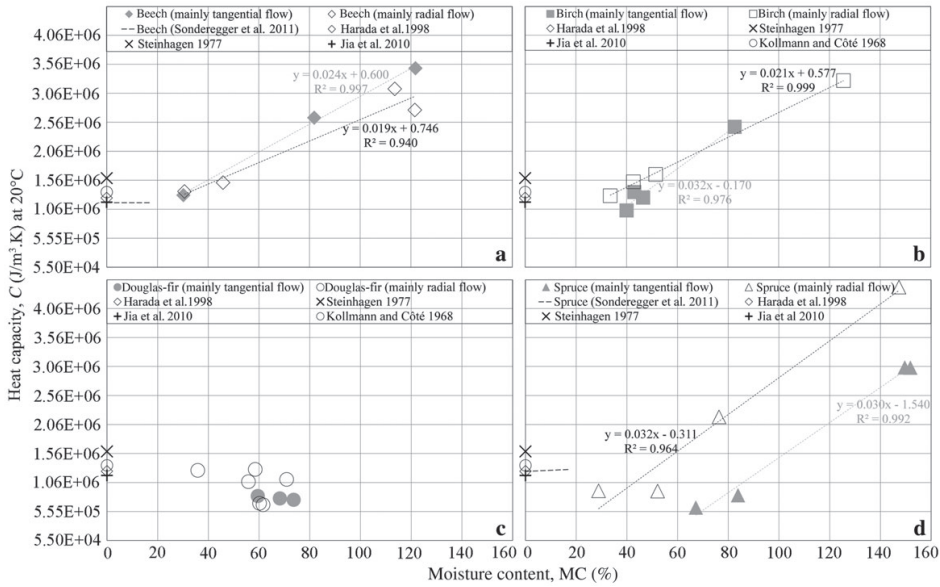
Figure 3 Heat capacity (C, in J m^{-3} K^{-1}) at green state with HotDisk® of (a) beech, (b) birch, (c) Douglas fir, and (d) spruce.

Figure 4 compares the κ values obtained with the TPS measurement with experimental results obtained with the flash method (Beluche 2011). The comparison is available only in the radial direction because samples for the flash method were obtained from veneers peeled tangentially. The results obtained with both methods are close to each other. The percentage differences between both methods are low (4% difference for Douglas fir at 56% MC and 7% difference for beech at 46% MC). The similarity of the data in Figure 4 is a sign of their reliability.
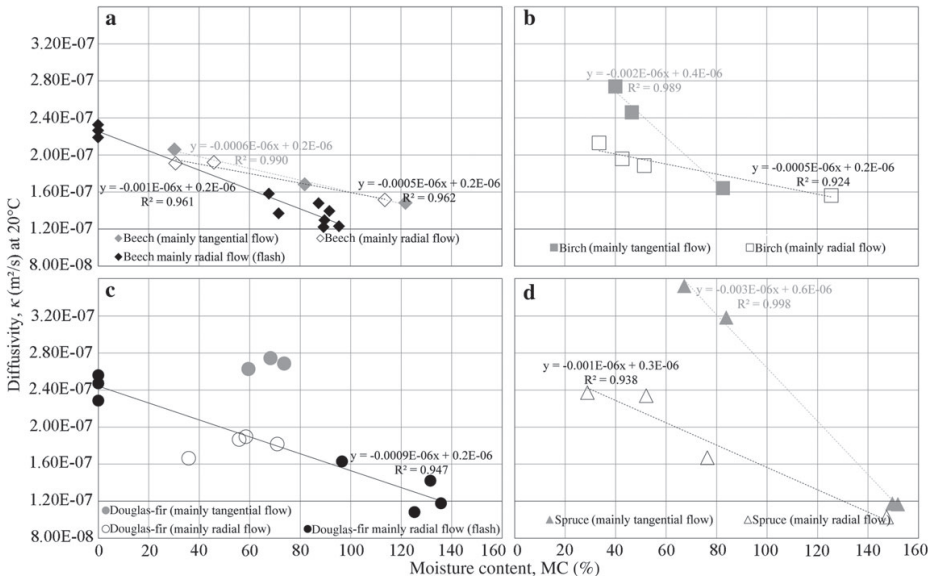

Figure 4 Thermal diffusivity (κ, in m^2 s^{-1}) at green state with HotDisk® of (a) beech, (b) birch, (c) Douglas fir, and (d) spruce.

Discussion and conclusions

The TPS technique was used to characterize the thermal behavior of green wood, providing values of the thermal conductivity (λ), heat capacity (C), and thermal diffusivity (κ) at the macroscopic level. The TPS technique is more universal than the THW of the THS methods, where temperature measurement is localized to the thermocouple hot junction. However, as explained earlier, the probe size is limited by the characteristic time and the size of the sample to avoid edge effects: the probe cannot encompass the whole sample. The influence of heterogeneities cannot be completely eliminated if the probe location is changed: the pattern of annual rings varies and the heat flows through different densities of earlywood and latewood.

The comparisons with proven older techniques such as the steady-state and flash methods have demonstrated similar results, establishing that the TPS technique offers new opportunities for characterizing the thermal properties of wood especially in the green state. The measurements in the present work did not take into account possible water transfer by capillarity within the sample and by evaporation. This type of water transport would affect the results because one part of the absorbed heat may contribute to water transfer instead of temperature increment, thereby leading to erroneously higher measured λ values. However, the small input power of the HotDisk® leads to a maximal temperature increase of 1–2 K, which is insufficient to bring about water mass transfer by evaporation. Moreover, the MC was nearly constant, with very limited changes during the short measurement time.

Results have shown that the thermal behavior of water, which is more conductive and has a higher heat capacity than wood, overrides that of wood: the greater the MC, the more similar the thermal behavior of green wood to that of water. However, the insulating properties of the wood material limit the thermal behavior of green wood, which never reaches that of water at any MC, even above 100%. The heat capacity and conductivity of wood increase with MC, but the diffusivity of wood is lower for wet wood than for dry wood. Therefore, the former requires more input energy in heating than the latter. It also takes more time for heat transfer within wet wood until the temperature is reached at a given depth. In the green state, the influence of anisotropy is frequently negated, with λ being the same in the radial and tangential directions, whereas C would be higher in hardwoods than in softwoods. In the present work, the behavior of these parameters has been formalized, and the equations obtained may increase the reliability of the input data for numerical models, which was the objective of this work. Further studies concerning thermal transfer in knots are needed to increase our knowledge of the thermal behavior of green wood.

References

Beluche, G. Modélisation numérique et développement d'un système expérimental de la diffusivité et de la transmission infrarouge. Arts et Metiers ParisTech, Cluny, France, 2011 (in French).

Bučar, B., Straže, A. (2008) Determination of the thermal conductivity of wood by the hot plate method: the influence of morphological properties of fir wood (*Abies alba* Mill.) to the contact thermal resistance. Holzforschung 62:362–367.

Dupleix, A., Ould Ahmedou, S.A., Bleron, L., Rossi, F., Hughes, M. (2012) Rational production of veneer by IR-heating of green wood during peeling: modeling experiments. Holzforschung, in press.

Gustafsson, S.E. (1991) Transient plane source techniques for thermal conductivity and thermal diffusivity measurements of solid materials. Rev. Sci. Instrum. 62:797–804.

Gustavsson, M., Gustavsson, J.S., Gustafsson, S.E., Halldahl, L. (2000) Recent developments and applications of the hot disk thermal constants analyser for measuring thermal transport properties of solids. High Temp. – High Press. 32:47–52.

Harada, T., Hata, T., Ishihara, S. (1998) Thermal constants of wood during the heating process measured with the laser flash method. J. Wood Sci. 44:425–431.

Incropera, F.P., Bergman, T.L., Lavine, A.S., DeWitt, D.P. Fundamentals of Heat and Mass Transfer. Wiley, 2011. p. 940.

ISO standard (1991) ISO 8302. Thermal insulation – determination of steady-state thermal resistance and related properties – guarded hot plate apparatus.

Jia, D., Afzal, M.T., Gongc, M., Bedane, A.H. (2010) Modeling of moisture diffusion and heat transfer during softening in wood densification. Int. J. Eng. 4:191–200.

Kollmann, F.F.P., Côté, W.A. Principles of Wood Science. I – Solid Wood. Springer-Verlag, New York, NY, 1968.

Koumoutsakos, A., Avramidis, S., Hatzikiriakos, S.G. (2001) Radio frequency vacuum drying of wood. I. Mathematical model. Dry. Technol. 19:65–84.

Olek, W., Weres, J., Guzenda, R. (2003) Effects of thermal conductivity data on accuracy of modeling heat transfer in wood. Holzforschung 57:317–325.

Rohsenow, W., Hartnett, J., Ganic, E. Handbook of Heat Transfer Fundamentals. McGraw-Hill Book Company, New York, NY, 1973.

Siau, J.F. Flow in Wood. Syracuse University Press, Syracuse, NY, 1971.

Siau, J.F. Wood: Influence of Moisture on Physical Properties. Virginia Polytechnic Institute and State University, Blacksburg, VA, 1995.

Simpson, W., TenWolde, A. (1999) Physical properties and moisture relations of wood. In: Wood Handbook – Wood as an Engineering Material, Chapter 3, Forest Products Laboratory, Madison, WI. pp. 15–20.

Sonderegger, W., Hering, S., Niemz, P. (2011) Thermal behaviour of Norway spruce and European beech in and between the principal anatomical directions. Holzforschung 65: 369–375.

Speyer, R.F. Thermal Analysis of Materials. Marcel Dekker, New York, NY, 1994.

Steinhagen, H.P. Thermal Conductive Properties of Wood, Green or Dry, from -40° to +100°C: A Literature Review. Forest Products Laboratory, Madison, WI, 1977.

Suleiman, B.M., Larfeldt, J., Leckner, B., Gustavsson, M. (1999) Thermal conductivity and diffusivity of wood. Wood Sci. Technol. 33:465–473.

IV

Rational production of veneer by IR-heating of green wood during peeling: Modeling experiments

Anna Dupleix[1,*], Sid' Ahmed Ould Ahmedou[1], Laurent Bleron[1], Frédéric Rossi[1] and Mark Hughes[2]

[1] Arts et Metiers ParisTech LaBoMaP, Rue Porte de Paris, F-71250 Cluny, France

[2] School of Chemical Technology, Department of Forest Products Technology, Aalto University, FI-00076 Aalto, Finland

*Corresponding author.
Arts et Metiers ParisTech LaBoMaP, Rue Porte de Paris, F-71250 Cluny, France
Phone: +33 (0)3 85 59 53 27
Fax: +33 (0)3 85 59 53 85
E-mail: anna.dupleix@ensam.eu

Abstract

Heating green wood logs by infrared (IR) radiation during peeling for veneer production has been numerically simulated, focusing on the heating kinetics of a green wood cylinder rotating with a decreasing radius. The results confirm those of previous experiments, that this kind of heating is a promising alternative to soaking wood prior to peeling. The model integrates the green wood parameters such as moisture content, density, distribution and ratios of earlywood and latewood, on the one hand, and the peeling conditions of veneer thickness and peeling speed, on the other. The following heat transfer processes were considered: conduction within the bolt, external heating by the IR source, and convection between the bolt surface and the external environment. The outputs were the temperatures of the bolt surface and of layers several millimeters deep. For maximal heat penetration, the bolt should turn in front of the IR source before cutting starts and the IR source should be positioned at the greatest angular distance ahead of the knife. Several heating scenarios could be simulated by the model, thus it is a useful decision-making tool for the design of an in-line IR heating system installed on the peeling lathe.

Keywords: green wood; heating; infrared; modeling; peeling for veneer production.

Introduction

For industrial veneer production, bolts are heated by soaking or steaming prior to peeling, which increases mechanical deformability of wood by softening the lignin moiety (Baldwin 1975; Matsunaga and Minato 1998; Bardet et al. 2003; Yamauchi et al. 2005). Water, as an integral part of wood, makes it an ideal medium for heat transfer into green wood. This kind of pretreatment also reduces the risk of lathe checking, ameliorates veneer surface quality, and lowers cutting forces and power consumption. Thermoforming of wood veneers was discussed by Srinivasan et al. (2007) and the complex interrelation between cutting forces in wood machining was reviewed by Marchal et al. (2009). In the same context, the properties of wood surfaces and the fracture behavior of wood was summarized by Sinn et al. (2009) and Stanzl-Tschegg and Navi (2009), respectively. The mechanical behavior of thin veneers is a special issue, as pointed out recently by Buchelt and Pfriem (2011) and Klüppel and Mai (2012).

The softening of knots contributes to preservation of cutting tool wear (Marchal et al. 2004). Heating alone is also utile, but soaking in water is beneficial because of the improvement of color homogeneity of decorative veneers. However, soaking is an empirical process performed between 32°C and 90°C (Baldwin 1975) and it has also some disadvantages, for example: (1) the long treatment time (12–72 h); (2) the washing out of extractable matter, which leads to water pollution and affects the natural durability of wood; (3) an increase in bolt-end splitting, which reduces bolt cohesion; and (4) the requirement for large soaking basins and sophisticated handling, i.e., the investment costs are high.

This is the reason why alternative heating solutions are sought for. Experiments with electric ohmic and microwave heating methods (Torgovnikov and Vinden 2010) have demonstrated that the "softening" effect does not depend on heating time, but only on the wood temperature attained, i.e., wood softening does not necessitate "cooking" for a long time as was thought before (Lutz 1960). A promising solution is a local heating of the surface just ahead of the knife, to a depth equal to the thickness of the veneer produced (Marchal and Collet 2000). An IR heating system may be the most suitable technology in terms of rapid heating rates and such a system is easy to install on the peeling lathe (Coste 2005).

Recently, it has been demonstrated that lower bolt surface temperatures of around 50°C for beech, birch, Douglas-fir, and spruce, were sufficient for acceptable peeling (Dupleix et al. 2011). It was established that IR radiation is suitable for heating green wood surfaces up to a depth of several millimetres (Gaudilliere 2003). A finite-difference method has demonstrated that living trees are heated via IR radiation (Potter and Andresen 2010). However, the promising experimental results of the quoted authors have not been confirmed by any numerical simulation under conditions of dynamic movement of the log in terms of IR induced heating rates.

The intention of the present paper is to fill this gap and to model IR heating of logs under industrial conditions of veneer production. The technical feasibility of an in-line IR heating system [Figure 1(a)] is a challenge. The principal issue is the
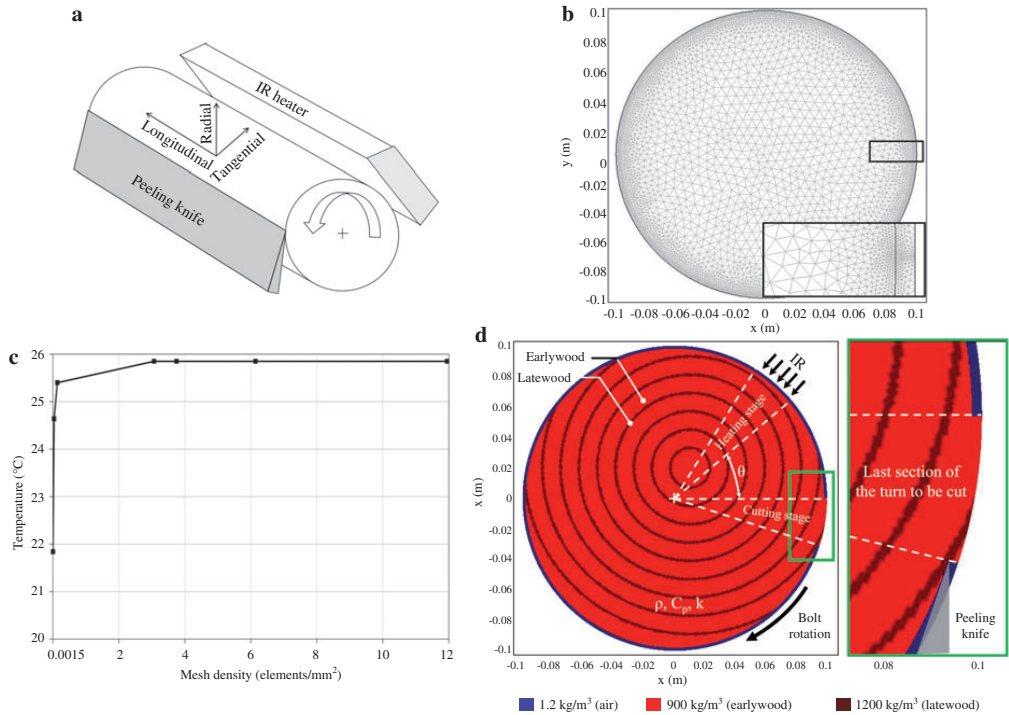
Figure 1 Modeling of IR on-line heating of logs for veneer production. (a) Principle of surface heating, (b) finer mesh close to the bolt surface, (c) influence of mesh-density refinement on results and (d) modeling the surface layer removal, when a peeling of a bolt is defined by subdomain parametric settings (case of off-centered pith) – densities on display.

ability of IR heating to raise the temperature of the surface of a rotating bolt to a certain value, within the shortest possible time (depending on the peeling speed) and to a deepness needed for peeling. On the other hand, overheating should be avoided, which would lead to quality defects on the surface. An open question is, whether sufficient heating of the cutting plane is achievable under industrial peeling conditions. In the industry, peeling speeds, depths and heating temperatures vary as a function of wood species and the end use of the veneers.

In the present study, the following parameters were considered as acceptable under industrial conditions: a minimum temperature of 50°C achieved on the cutting plane located up to 3 mm depth and peeling speeds between 1 to 10 ms^{-1}. The expectation is that modeling the heating of green wood by IR during peeling, will abbreviate the finding of the best process conditions in practice.

Materials and methods

Methodology

Software for equation solution: Comsol Multiphysics (Comsol Inc., Burlington, MA, USA), a partial differential equations solver based on the finite element (FE) method, with the overall procedure implemented under the flexible MatLab (MathWorks Inc.,

Natick, MA, USA). This approach offers the following advantages: (1) generating an appropriate and easy-to-modify FE geometry; (2) facilitating the implementation of intrinsic model properties (physical, optical, thermal, structural, etc.) to its geometrical parameters and mesh; and (3) solving partial differential equations with Comsol Multiphysics.

Configuration

The bolt was modeled in 2D, i.e., the cross-section (radial and transversal directions) whilst the bolt length (the longitudinal direction) can be varied and does not play any role in heat transfer. The IR source was applied locally to the surface of the bolt as depicted in Figure 1(a). The cross-section was meshed by Lagrange-quadratic elements with triangular shapes as the basic functions. To predict heat transfer accurately in the vicinity of the bolt surface, the non-uniform mesh is close to the bolt surface and the cutting plane [Figure 1(b)]. Meshing actually occurs on the whole bolt cross-section, but meshing limited only to the external ring of the bolt up to a sufficient depth might also be considered, if speeding up the calculations is necessary.

A sensitivity analysis indicated that with a minimum element size of 0.7 mm in the bolt cross-section, a mesh density >3 elements per mm^2 would be required to obtain a mesh-independent solution. This is illustrated through the evolution of temperature at a point located on the bolt surface according to mesh density [Figure 1(c)]. For mesh density >3 elements per mm^2, there is no influence of the refinement on the resulting temperatures.

Equations

The temperature distribution within the bolt cross-section is governed by the transient heat transfer equation for conduction according to Eq. (1) derived from Fourier's law. This equation only considers IR radiation absorbed by wood surface, and it does not integrate IR penetrated to deeper wood layers (volumetric absorption). The boundary conditions for temperature at the bolt surface are given by Neumann conditions $(-n\,(-\lambda\nabla T)=Q_{rad})$ with **n** normal vector to the boundary. Eq. (2) takes into account heat losses due to convection and external input heat due to radiation from the IR source Q_{rad} and adiabatic conditions elsewhere:

$$\rho C_p \frac{\partial T}{\partial t} = \nabla(\lambda \nabla T) \qquad (1)$$

$$Q_{rad} = h(T_{ext} - T) + \varepsilon\sigma(T_{ext}^4 - T^4) \qquad (2)$$

where C_p is the heat capacity of the wood (in $J\,kg^{-1}\,K^{-1}$), T_{ext} the external IR source temperature (in K), T is the bolt temperature (in K), λ the conductivity of wood (in $W\,m^{-1}\,K^{-1}$), ε is the wood emissivity and σ is Stefan-Boltzmann's constant (in $W\,m^{-2}\,K^{-4}$). The heat transfer coefficient, h, is fixed at $5\,W\,m^{-2}\,K^{-1}$ (Quéméner et al. 2003). The mean value $\varepsilon=0.85$ is chosen because unplaned wood emissivity is said to vary from 0.70 to 0.98 for temperatures ranging from 17 to 70°C (Flir Systems 2004). However, moisture content (MC) is not detailed in these values, and the emissivity of green wood would need to be characterized more carefully. Wood emissivity here is independent of the IR wavelength (total emissivity) because the whole emission spectrum of the IR source determined by T_{ext} is taken into account (Planck's law).

Subdomain settings

The cross-section of the bolt is divided into subdomains, with specific initial settings in terms of structural properties – earlywood (EW), latewood (LW) – physical properties (density ρ in $kg\,m^{-3}$) and thermal properties (C_p, λ). All parameters considered to describe the bolt structure, such as bolt diameter, annual ring width, heartwood ring width, latewood ring width, and pith eccentricity, are defined by modifiable input values. Different physical and thermal properties of wood, ρ, C_p, and λ, are then applied to the different wood substructures concerning EW and LW and as functions of their MC conditions [Figure 1(d)]. Structural properties such as heartwood/sapwood, wood rays, and knots have not been taken into account in this model. It is likely that structural properties influence heat transfer into wood, because of their variations in densities and therefore in thermal characteristics. Distinguishing heartwood from sapwood could be integrated in the present mesh, contrary to inserting wood rays and knots, which would necessitate modifying the geometry and the mesh of the model. But given the lack of data concerning their variations in thermal characteristics, definitions of wood structural properties are limited to variations of densities. For this reason, only the influence of MC at 12%, 40%, and 72% on IR heating of green wood is considered in this study. However, thermal properties of wood above the fiber saturation point (FSP) are not available in the literature and are considered as constant at MCs higher than FSP, but a precise characterization of thermal properties of wood above the FSP would be necessary. In all other simulations, MC is set to 72% (saturated state) with corresponding physical and thermal properties for wood (Table 1).

Table 1 Thermal and physical properties concerning density (ρ), conductivity (λ), and heat capacity (C_p) of earlywood (EW) and latewood (LW) as a function of their moisture content (MC) according to Glass and Zelinka (2010) for wood species with specific densities for earlywood of 0.60 and for latewood of 0.70.

Parameter	EW	LW
ρ (kg cm^{-3})		
at 12% MC	672	784
at 40% MC	840	980
at 72% MC	1066	1204
λ (W m^{-1} K^{-1})		
at 12% MC	0.164	0.189
at 40% MC	0.196	0.226
at 72% MC	0.196	0.226
C_p (kJ kg^{-1} K^{-1})		
at 12% MC	2000	3000
at 40% MC	2700	3500
at 72% MC	2700	3500

Boundary setting

The bolt surface is divided into 360 sections with uniform boundary settings. Only the IR source external input Q_{rad} (in $W\,m^{-2}$) defined with the external IR source temperature T_{ext} [Eq. (2)] is successively activated with a Boolean operator for each section, with S_i of the bolt surface being radiated. Q_{rad} is applied on a constant number of segments during the whole cutting process. Technical solutions on the peeling lathe are: (1) either the IR source is kept at a constant distance from the bolt and equipped with a deflector able to concentrate radiation with a varying angle on specific bolt segments, or (2) the IR source with a fixed spectrum width adapts its distance to the bolt surface according to the bolt's decreasing radius. The distance between the peeling knife and the IR source is defined by the angle θ [Figure 1(d)].

Modeling

For geometric convenience, the real situation was converted by supposing an immobile bolt with an IR heat source turning around it. The relative movement of the IR source and wood to each other is important. On the one hand, the model can simulate only heating of a bolt rotating in front of an IR source without cutting it [Figure 2(a), right path]. In that case, no removal of material is induced and subdomain settings are constant with time. On the other hand, left path in Figure 2(a) simulates IR heating of a rotating bolt while peeling. The continuous removal of a wood surface layer by peeling is modeled by turning the physical properties of each cut segment from wood to air. In Figure 1(d), segments in blue featuring 1.2 kg m^{-3} density represent air, i.e., segments that have been cut from the bolt. In that case, subdomain settings are functions of time and are automatically modified with Boolean functions. At each angular step, each element of the angular section S_i reaches a new temperature achieved, due to the input of the external IR source and calculated with Eqs. (1) and (2). After each angular step, the IR is moved (by modifying boundary settings) and the last heated section is removed (by turning its density to air density). After each turn, the final calculated temperature of each element is used as the initial temperature of the new meshing element at the bolt surface. In contrast to a real peeling process, where the cutting knife trajectory draws spirals, the model is simplified to the removal of a cylinder of veneer upon every complete rotation. This approximation
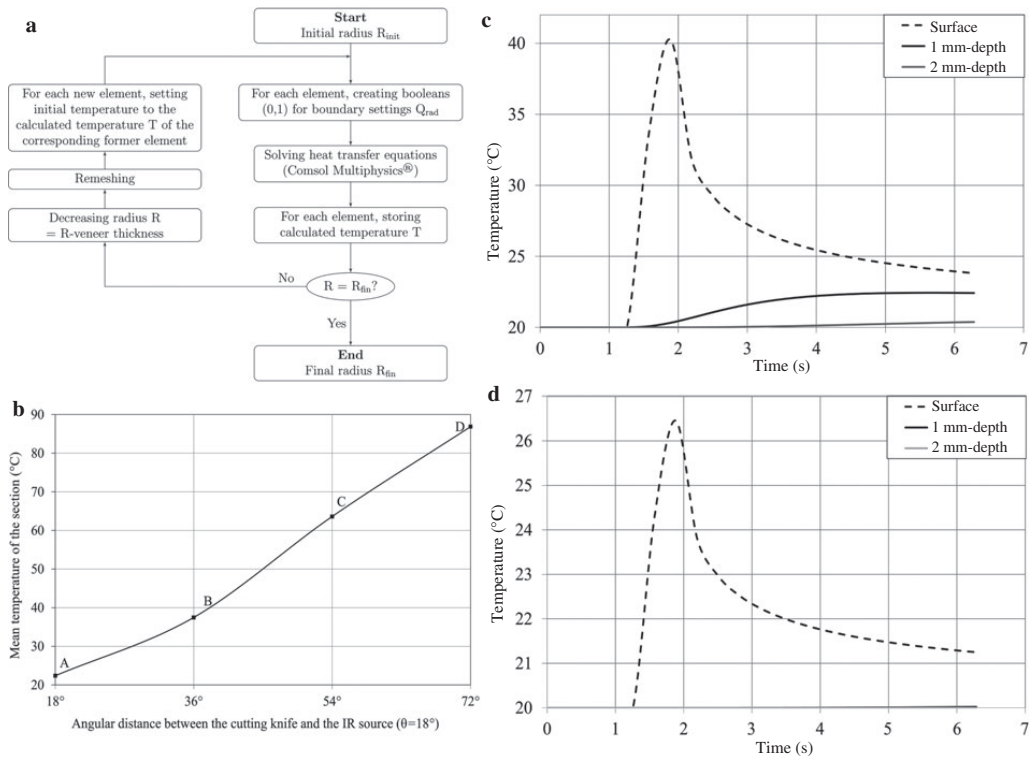
Figure 2 Details of modeling the IR heating during peeling. (a) flow chart of the numerical procedure, (b) influence of the angular distance θ between knife and IR source (T_{ext}=2500°C, v=0.3 ms^{-1}, bolt diameter=20 cm, MC=72%, θ=18°), (c) and (d) temporal evolution of temperature within the bolt during one turn of external heating for T_{ext}=500°C, bolt diameter=20 cm, and MC=72%; however for (c) v=0.1 ms^{-1} and for (d) v=1 ms^{-1}.

only affects the distance between the IR source and the bolt surface to a negligible extent – to that of the veneer thickness – without a significant influence on the numerical simulation of heat transfer.

Results and discussion

Figures 2(c) and 2(d) show the temporal evolution of temperature during one turn of a rotating bolt initially at 20°C and heated by external IR radiation at a source temperature T_{ext}=500°C and for cutting speeds of 0.1 ms^{-1} and 1 ms^{-1}, respectively. The results provide information on the heat transfer behavior deep within the bolt and support 2-step heating kinetics (Bedard and Laganiere 2009). Firstly, the IR energy is absorbed at the wood surface to a negligible penetration depth [dashed curve in Figure 2(c)]. Considering the hypothesis of surface absorption (see Equations), IR heat is then partly lost to the surroundings by convection and partly transferred towards the interior of the bolt by conduction to the deeper layers [black and gray curves in Figure 2(c)]. However, the 2 mm-deep layers never benefit from heat by conduction. This delay in temperature rise corresponds to the

time-lapse that must necessarily occur between the heating and cutting stages and can be interpreted geometrically to determine the optimum angular position of the IR source as a function of the bolt diameter. In the present setting [Figure 2(c)], 3 s are necessary to raise the temperature of a 1 mm-deep layer to the maximum value achievable by conduction of heat from the surface (from t=1.5 s to t=4.5 s). In the present case, for a cutting speed of 0.1 ms^{-1} and a bolt of 20 cm diameter, these 3 s would be achieved if the IR source is located at an angle of 170° ahead of the cutting knife.

Distance between knife and IR source

Figure 2(b) confirms the influence of the angular distance θ between the cutting knife and the IR source (in the present case, θ=18°). Clearly, the further the knife is from the IR source, the more time is needed for heat penetration into the bolt, and therefore, the higher must be the temperature. Temperatures in Figure 2(b) are mean values within each segment A, B, C, and D for source temperature T_{ext}=2500°C and peeling speed v=0.3 ms^{-1}.

Peeling speeds and source temperatures

Varying peeling speeds (0.1, 0.5, and 1 ms^{-1}) and source temperatures (500, 1500, and 2500°C) lead to the same 2-step heat transfer behavior as shown in Figures 2(c) and 2(d) [Figures 3(a) and 3(b)]. The high amount of energy absorbed at the bolt surface is transferred by conduction to the adjacent layers beneath. Logically, heating rates decrease with higher peeling speed, thicker veneer thickness and lower IR source temperature [Figures 2(c), 2(d), 3(a) and 3(b)]. Approaching industrial peeling speeds at around 1 ms^{-1}, the time is too short to enable heat transfer by conduction from the surface to deeper layers. For peeling speeds above 0.5 ms^{-1}, the temperature rise in the 2 mm-deep layer becomes effectively insignificant as shown in Figure 3b. Increasing the source temperature from 500 to 2500°C does not improve this situation; it only leads to the risk of the bolt surface burning with the maximum of curves reaching temperatures above 300°C.

Rotation without cutting

For the above-mentioned reasons, a possibility was investigated, in which the bolt was left turning in front of the IR source before cutting starts. This would allow more time for heat transfer into deeper layers. Figures 3a and 3b illustrate the temperature evolution within the bolt as a function of the number of rotations for peeling speeds of 0.1, 0.5, 1 ms^{-1} and source temperature T_{ext}=500°C. At depths of 1 mm [Figure 3(a)] and 2 mm [Figure 3(b)], the temperature rise is perceptible.

Figure 3(c) illustrates this situation (continuous curve) before cutting starts on the 6th turn (dashed curve). The temperature evolution as a function of the number of turns is given for a "floating" layer always located at 2 mm deep from the cutting plane, therefore, at varying bolt diameters detailed in the data labels. These simulations provide information about the temperatures achievable at the cutting plane, where cutting is interrupted by heating stages. This solution could only be considered for slicing (non-continuous cutting process) but not for the continuous peeling process. However, the configuration of the heating system should be optimized to adapt it to realistic slicing speeds (approx. 1 ms^{-1}) with heating source temperatures, which would not lead to burning of the surface.

Influence of MC

Figure 3(d) illustrates the influence of MC on temperature elevation at local points of the bolt surface, for a source temperature of 2500°C. Firstly, for the same amount of energy from the IR source, the final temperature reached at the bolt surface

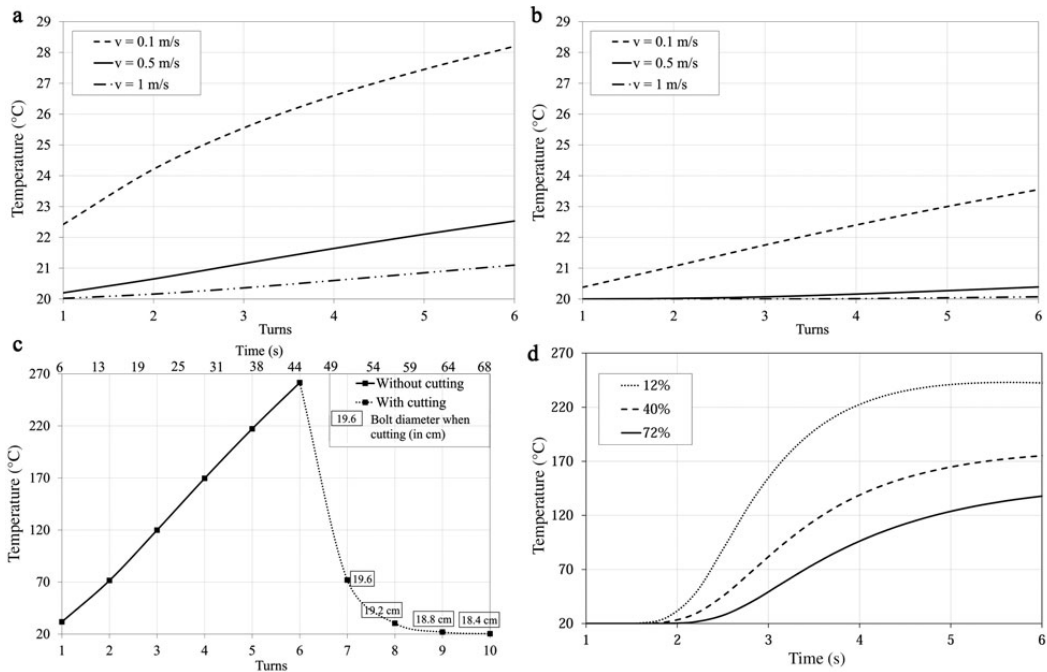**Figure 3** Temperature evolution as a function of turn number for bolts with 20 cm diameter. (a) T_{ext}=500°C, e=1 mm, variable cutting speeds, (b) T_{ext}=500°C, e=2 mm, variable cutting speeds, (c) constant 2 mm depth, T_{ext}=2500°C, v=0.1 ms^{-1}, (d) temperature elevation at the bolt surface as a function of MC and time, if T_{ext}=2500°C, v=0.1 ms^{-1}.

is lower when the MC is higher. Then, the time required to reach the maximum surface temperature is longer when the MC is higher. Figure 3(d) illustrates that the influence of MC on wood heating can be predicted by means of parametric definitions of the physical properties of wood. Given the significant influence of MC, it might be of interest, in the future, to integrate mass transfer equations in the model to take into account the effect of drying during heating. Although the presented model does not take into account the heterogeneity of wood, it clearly shows the roles that various parameters play in influencing heat transfer. It is particularly the case concerning the influence of MC on wood heat transfer.

Conclusions

The simulation provides information on the optimum configuration of the IR heating system, to achieve the temperatures required on the cutting plane. Firstly, to ensure heat penetration up to the cutting plane, it is necessary to let the bolt turn in front of the IR source before cutting starts. The model enables calculation of the number of turns before cutting commences, according to the peeling settings. Then, the position of the IR source can be geometrically determined as a function of the time calculated by the model for heat transfer from the bolt surface to adjacent layers. Given the significant losses due to convection to the exterior environment and the relatively slow conduction process, the IR source should be located as far as possible from the knife. The presented model could be a part of an essential decision-making tool, prior to the design of in-line IR heating system directly embedded on the cutting machine. The results support the utilization of IR heating for slicing processes. Experimental data are needed for validating the presented calculations. The flexibility of this model permits the modification of input parameters, if necessary, in the course of matching data of simulation and experiments. In the future, the model should integrate the thermal properties of wood (C_p, λ) also above the fiber saturation point. Moreover, the optical properties of green wood in terms of emissivity, transmissivity, and absorptivity must be taken into account for situations when IR should penetrate into deeper layers. Last but not least, the presence of wood radial elements, such as knots and rays, whose high densities play a significant role in heat transfer, must be included into future models.

References

Baldwin, R.F. (1975) Plywood Manufacturing Practices. Miller Freeman Publications Inc., San Fransisco, California, pp. 62–78.

Bardet, S., Beauchêne, J., Thibaut, B. (2003) Influence of basic density and temperature on mechanical properties perpendicular to grain of ten wood tropical species. Ann. Forest Sci. 60:49–59.

Bedard, N., Laganiere, B. (2009) Debarking enhancement of frozen logs. Part II: infrared system for heating logs prior to debarking. Forest Prod. J. 59:25–30.

Buchelt, B., Pfriem, A. (2011) Influence of wood specimen thickness on its mechanical properties by tensile testing: solid wood versus veneer. Holzforschung 65:249–252.

Coste, N. (2005) Interest of radiant energy for wood peeling and slicing process. Master's thesis, University of Melbourne.

Dupleix, A., Marchal, R., Bléron, L., Rossi, F., Hughes, M. (2011) On-line heating temperatures of green-wood prior to peeling. Joint International Symposium on Wood Composites and Veneer Processing and Products Proceedings.

Flir Systems (2004) ThermaCAM User's Manual.

Gaudilliere, C. (2003) Contribution au développement d'une chauffe électrique rapide de bois vert de Douglas en vue de son déroulage. Master's thesis, Arts et Métiers ParisTech.

Glass, S.V., Zelinka, S.L. (2010) Wood handbook, Chapter 03: Moisture relations and physical properties of wood. General Technical Report FPL-GTR-190 Department of Agriculture, Forest Service, Forest Products Laboratory, Madison, WI, USA. 3-1–3-19.

Klüppel, A., Mai, C. (2012) Effect of lignin and hemicelluloses on the tensile strength of micro-veneers determined at finite span and zero span. Holzforschung 66:493–496.

Lutz, J.F. (1960) Heating veneer bolts to improve quality of douglas-fir plywood. Technical report USDA Forest Service General FPL-2182, Forest Products Laboratory, Madison, WI, USA.

Marchal, R., Collet, R. (2000) Contribution au développement d'une chauffe électrique rapide de bois vert de douglas en vue de son déroulage. Technical report, Arts et Métiers ParisTech.

Marchal, R., Gaudilliere, C., Collet, R. (2004) Technical feasibility of an embedded wood heating device on the slicer or the peeling lathe. International Symposium Veneer Processing and Products Proceedings. pp. 29–44.

Marchal, R., Mothe, F., Denaud, L.-E., Thibaut, B., Bleron, L. (2009) Cutting forces in wood machining – Basics and applications in industrial processes. A review COST Action E35 2004–2008: Wood machining – micromechanics and fracture. Holzforschung 63:157–167.

Matsunaga, M., Minato, K. (1998) Physical and mechanical properties required for violin bow materials II: Comparison of the processing properties and durability between pernambuco and substitutable wood species. J. Wood Sci. 44:142–146.

Potter, B.E., Andresen, J.A. (2010) A finite-difference model of temperatures and heat flow within a tree stem. Revue Canadienne de Recherche Forestière 32:548–555.

Quéméner, O., Battaglia, J.L., Neveu, A. (2003) Résolution d'un problème inverse par utilisation d'un modèle réduit modal. Application au frottement d'un pion sur un disque en rotation. Int. J. Thermal Sci. 42:361–378.

Sinn, G., Sandak, J., Ramananantoandro, T. (2009) Properties of wood surfaces – characterisation and measurement. A review COST Action E35 2004–2008: Wood machining – micromechanics and fracture. Holzforschung 63:196–203.

Srinivasan, N., Bhattacharyya, D., Jayaraman, K. (2007) Thermoforming of wood veneer composite sheets. Holzforschung 61:558–562.

Stanzl-Tschegg, S., Navi, P. (2009) Fracture behaviour of wood and its composites. A review COST Action E35 2004–2008: Wood machining – micromechanics and fracture. Holzforschung 63:139–149.

Torgovnikov, G., Vinden, P. (2010) Microwave wood modification technology and its applications. Forest Prod. J. 60:173.

Yamauchi, S., Iijima, Y., Doi, S. (2005) Spectrochemical characterization by FT-Raman spectroscopy of wood heat-treated at low temperatures: Japanese larch and beech. J. Wood Sci. 51:498–506.

V
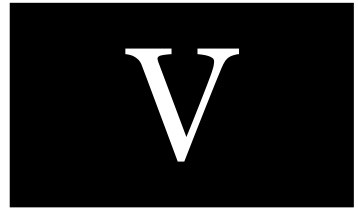
Dupleix A., Batsale J.C., Kusiak A., Hughes M., Denaud L. (2013) Experimental validation of green wood peeling assisted by IR heating – some analytical considerations for system design.

Submitted.

Experimental validation of green wood peeling assisted by IR heating – some analytical considerations for system design

Anna Dupleix (corresponding author)
Arts et Metiers ParisTech LaBoMaP, Rue Porte de Paris, F-71250 Cluny, France
School of Chemical Technology, Department of Forest Products Technology, Aalto University, FI-00076 Aalto, Finland
Phone: +33 (0)3 85 59 53 27
Fax: +33 (0)3 85 59 53 85
Email : anna.dupleix@ensam.eu

Jean-Christophe Batsale
Arts et Metiers ParisTech I2M, Esplanade des Arts et Metiers, F-33405 Talence Cedex, France

Andrzej Kusiak
Universite Bordeaux 1, I2M, Esplanade des Arts et Metiers, F-33405 Talence Cedex, France

Mark Hughes
School of Chemical Technology, Department of Forest Products Technology, Aalto University, FI-00076 Aalto, Finland

Louis-Etienne Denaud
Arts et Metiers ParisTech LaBoMaP, Rue Porte de Paris, F-71250 Cluny, France

Abstract

Experimental results have been used to validate a 2D simulation model in order to check its reliability in predicting the heating of a green log rotating under an IR heating source. For the purpose of validation, it was assumed that this experimental situation could be described by simplified analytical solutions for thermal transfer in a semi-infinite body in 1D Cartesian coordinates. This assumption has been confirmed. Knowing the thermal and physical characteristics of green wood, two methods are now available to rapidly calculate the temperature within the wood and the maximum surface temperature reached by a green log rotating under an IR heating

source: (1) by numerical simulation and (2) by analytical equations which dispense with the computationally intensive finite element method. Experimental results validated by both methods show that an IR heating system embedded on an industrial peeling machine would not warm-up green wood to the required peeling temperature at current peeling speeds.

Keywords

green wood, on-line infrared heating, numerical model, temperature field

Introduction

For certain species, the veneer peeling process requires the prior heating of round green wood to temperatures ranging from 30 to 90°C. This treatment is necessary to increase the deformability of wood, to reduce the severity of lathe checking in the veneers and to reduce cutting forces. This heating is usually done by immersing the logs in hot water (soaking); however the soaking currently used in industry to soften wood prior to peeling has a number of disadvantages. These include the duration of the process, water pollution, the need for sophisticated handling, stock downtimes and a loss of the cohesion and durability of the wood itself (Dupleix et al. 2011). Recent research on beech, birch and spruce (Dupleix et al. 2012b) has demonstrated that conventional soaking temperatures can be lowered to 50°C at the wood cutting plane, whilst still retaining acceptable peeling characteristics in terms of veneer quality (thickness variation, lathe check depth and distribution). As demonstrated by Grimhall and Hoel (1983) a possible alternative to the traditional log soaking employed in the manufacture of veneer, is the use of infrared radiation (IR) to heat green wood. This alternative technology would employ IR heaters, integrated into the peeling machine, to heat the round green wood before peeling in a manner similar to that of the laser heating sources used in the metal

machining industry to soften the work-piece ahead of the cutting tool (Braham-Bouchnak et al. 2013, Rahman Rashid et al. 2012). IR heating could feasibly be used to heat the wood to the requited temperature because 70 to 90% of incident IR radiation is absorbed at the surface to a depth of around 0.3mm (Dupleix 2012c). Heat then penetrates by conduction within the green wood, with diffusivities (decreasing with increasing moisture content) of between 0.12 and 0.32 $mm^2.s^{-1}$ (Dupleix et al. 2012d). The choice of IR technology was also motivated by the potential ease with which IR heaters could be integrated into peeling machines and by the power it offers, enabling the required heating temperatures to be achieved quickly, in line with the highly demanding peeling speeds (from 1 to 5 $m.s^{-1}$) in use in the industry.

Previous studies have demonstrated the ability of IR radiation to raise both the surface temperature and the temperature below the surface in green wood, either for the purpose of heating the wood (Makoviny and Zemiar 2004) or for drying it (Cserta et al. 2012). With heating source flux densities of 126 $kW.m^{-2}$, it has been shown that with IR heating it is possible to achieve surface temperatures of 50°C in green logs of beech, Douglas-fir and okoumé rotating at speeds corresponding to peeling speeds of 0.25 – 0.5 $m.s^{-1}$ (Coste and De Bevy 2005). Similar results have also been obtained in spruce logs rotating at speeds equivalent to peeling at 0.1 $m.s^{-1}$ using relatively low IR flux densities of 4-20 $kW.m^{-2}$ for the purpose of defreezing the logs (Bédard and Laganière 2009). As might be expected, the greater the input power of the IR source, the faster the target temperature of 50°C is achieved at a particular depth. However, the input power of the IR source must be limited in order to avoid overheating and eventual burning of the surface (Makoviny and Zemiar 2004, Marchal et al. 2004).

The aim of the work reported in this paper was to validate experimentally a 2D numerical model of the heating kinetics in a green wood cylinder

rotating under an IR heating source. This model developed by Dupleix et al. (2012a) can predict the heating temperatures within wood and could potentially be used to set up the parameters of an IR heating system embedded on a peeling lathe. The validation consisted of comparing the surface and sub-surface temperatures, measured experimentally in green wood samples conveyed under an external IR heating source by thermocouples, with the numerically simulated curves of the heating rates. During this validation process, it has been demonstrated that simple analytical equations can be used to compute the heating rates and the maximum temperatures achievable at the surface and below the surface.

Material and methods

In comparing experimental data to numerical results, the difficulty of assessing the effective real flux density received by the sample, which is necessary input data for the numerical simulation, was faced. Since it was not possible to reliably measure the absolute value of the flux density experimentally, the following alternative approach was adopted. If the experimental situation could be reduced to semi-infinite behaviour in 1D Cartesian coordinates described by simple analytical considerations, the surface temperatures could be used to derive the flux density received by the sample.

   Thus, experimentally validating the numerical simulation of heating rates necessitated the following steps: 1) testing the ability of the analytical equations (based on the hypothesis of semi-infinite behaviour in 1D Cartesian coordinates) to describe the IR heating of a green bolt, then 2) based on the inverse method of deconvolution proposed by Beck et al. (1985), use these analytical equations to determine the real flux density received by the sample using experimental surface temperature and 3) to

integrate the real flux density received by the sample into the numerical simulation in order to compare experimental to numerical curves.

Samples and experiments

Knot free samples of wood were sawn (either quarter, rift or flat sawn) from the same freshly-cut tree into blocks having the following dimensions: 0.044×0.035×0.020 m3 (Fig.1 for a rift sawn sample). Four species of wood were used: two hardwoods - beech (*Fagus sylvatica* (L)) and birch (*Betula pendula* (Roth)) – and two softwoods - Douglas-fir (*Pseudotsuga menziesii* (Mull) Franco) and spruce (*Picea albies* (L.) Karst). The physical experiments consisted of conveying the samples of green wood at a speed, s, of 0.0032 m.s-1 under an electric infrared lamp composed of a quartz tube delivering a heat flux density, q, onto a surface approximately 0.03 m wide (the gridded surface shown in Fig.1). The samples were shaped in the form of rectangular prisms because (1) it is easier to record internal temperature rises in a block in motion than in a rotating cylinder, (2) the numerical simulation mentioned below has demonstrated that, with characteristics of
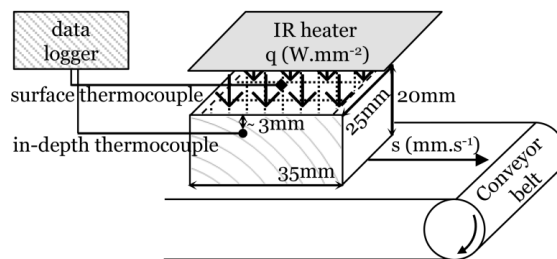

Figure 1 The experimental set-up for measuring the surface temperature of a rift sawn sample under IR heating

the IR source used in the model, blocks behave in a similar manner to cylinders. The increase in surface temperature over time was recorded using a surface thermocouple, tightly stapled to the surface in order to

minimize thermal contact resistance. Holes were drilled into the samples to insert the thermocouples which were used to measure the temperatures within the block. The holes were drilled at a distance of 3 mm millimeters beneath the exposed tangential surface (Fig.1). A tight fit and filling the drilled holes with wood dust after inserting the thermocouples ensured minimal heat losses and thermal contact resistance. The thermocouples were connected to a data acquisition system which recorded the temperature every second. The samples were initially in the green state and at least 3 replicate tests were performed with different samples (termed 'replicates' in Figs 5 to 7) of each species (both sapwood and heartwood). Drying out of the samples during heating was determined by calculating the moisture contents before heating MC_i and after heating MC_f, gravimetrically using Eqs.1 and 2.

$$MC_i(\%) = \frac{m_i(g) - m_{od}(g)}{m_{od}(g)} \qquad (1)$$

$$MC_f(\%) = \frac{m_f(g) - m_{od}(g)}{m_{od}(g)} \qquad (2)$$

Changes in moisture content during heating, ΔMC, were calculated using Eq.3.

$$\Delta MC(\%) = (1 - \frac{MC_f}{MC_i}) \times 100 \qquad (3)$$

Numerical simulation

Comsol Multiphysics (Comsol Inc., Burlington, MA, USA) and MatLab (MathWorks Inc., Natick, MA, USA) were used to simulate the development of log surface and sub-surface temperatures over time (Dupleix et al. 2012a). The model meshes the log cross-section with 2D finite elements since heat transfer in the longitudinal direction can be neglected. An external input heat flux density, q, was applied to a selected number of surface elements to simulate the rotation of the log in front of the IR source.

The temperature distribution was calculated by solving the transient equation for conduction derived from Fourier's law (Eq.4).

$$\rho c \frac{\partial T}{\partial t} = \nabla(\lambda \nabla T) \tag{4}$$

where T is the bolt temperature (in K), ρ, the density of wood (in $kg.m^{-3}$), c, the specific heat capacity of wood (in $J.kg^{-1}.K^{-1}$) and, λ, the thermal conductivity of the wood (in $W.m^{-1}.K^{-1}$). The three latter parameters, varying with wood moisture content, were determined according to the empirical equations developed by Dupleix et al. (2012d). The influence of temperature on c and λ was neglected because according to Suleiman (1999) a 40°C temperature increase (observed experimentally) leads to a variation in thermal characteristics of between 7 and 12%. The initial condition is given by the initial temperature of the bolt, T_{init} = 293 K. The boundary conditions at the bolt surface are defined by Eqs. 5a and 5b with, n, the vector normal to the boundary.

$$-\text{on the arc surface } x: -n.(\lambda \nabla T) = \varepsilon.q.H(x) \tag{5a}$$

$$-\text{on the rest of the surface: } -n.(-\lambda \nabla T) = h\,(T - T_{ext}) \tag{5b}$$

where H is the Heaviside function (Fig.2), ε, the emissivity of the wood surface, taken to be 0.85 (Dupleix et al. 2012a), T_{ext}, the external temperature (in K), h, the heat transfer coefficient (in $W.m^{-2}.K^{-1}$) and, q, flux density (in $W.m^{-2}$).

Analytical equations

Firstly, given the large dimension of the bolt diameter, D, compared to x, the arc surface of the green log subjected to external infrared heating (x = D/20), it is possible to reduce the situation to one dimension in Cartesian coordinates (Fig.2). Secondly, in view of the very low thermal diffusivity of green wood (Dupleix et al. 2012d), the behaviour can be assumed to be that of a semi-infinite body with a spatially uniform step heat flux diffusing

normal to the surface, x, applied during a heating time, t_h, where $t_h = x/s$ and s is the peeling speed (i.e. the constant linear speed at which veneer is generated at the output of the peeling lathe).
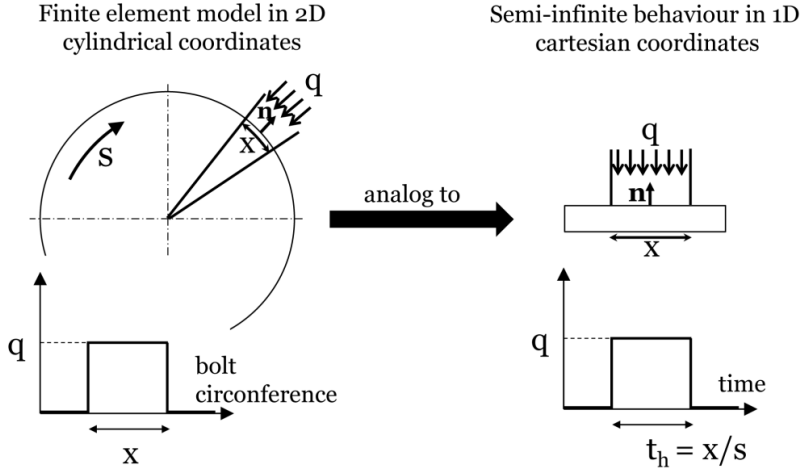

Figure 2 Analogy of finite element model in 2D to semi-infinite behavior in 1D Cartesian coordinates

The problem therefore becomes analogous to a 1D-transient problem where the spatial variable, x, is replaced by the temporal variable t_h. With these assumptions, the evolution of the sample surface temperature, T_{surf}, with the square root of time is linear according to Eq.6 (Taler and Duda 2006).

$$T_{surf} = \frac{2q}{\sqrt{\pi}\sqrt{\lambda\rho c}}\sqrt{\frac{x}{s}} \qquad \text{or} \qquad T_{surf} = \frac{2q}{\sqrt{\pi}\sqrt{\lambda\rho c}}\sqrt{t} \qquad (6)$$

The exact solution of the temperature, T_d, attained at depth, d, within the sample is then given by Eq.7 (with the diffusivity of wood, $\kappa = \lambda/(\rho c)$) (Taler and Duda 2006).

$$T_d = \frac{2q}{\sqrt{\pi}\sqrt{\lambda\rho c}}e^{-d^2/4\kappa t} - \frac{d}{\lambda}q\,\text{erfc}\frac{d}{2\sqrt{\kappa t}} \qquad (7)$$

where erfc is the complementary error function which tends to 1 when time tends to infinity. Therefore, the long-term behaviour of T_d is given by

the asymptotic solution obtained when time tends to infinity (Eq.8). It can be seen that at extended heating times the temperature at depth, d, also evolves at a rate proportional to the square root of time.

$$T_d = \frac{2\,q}{\sqrt{\pi}\sqrt{\lambda\rho c}}\sqrt{t} - \frac{d}{\lambda}q \tag{8}$$

Results and Discussion

Validating the hypothesis of semi-infinite behaviour in 1D Cartesian coordinates (step 1)

This hypothesis would be validated if the surface temperatures plotted as a function of the square root of time $T_{surf} = f(\sqrt{t})$ showed the same linear behaviour as predicted by the simplified analytical equation, Eq.6. In view of the variability of the experimental measurements of $T_{surf} = f(t)$ on the different replicate samples (due to the natural heterogeneity of wood) it is more reliable to check this hypothesis on the results of $T_{surf} = f(\sqrt{t})$ obtained by numerical simulation. Fig.3 shows the results for beech in the early stages of heating (up to $3\sqrt{s}$). The table inserted in Fig.3 summarises the corresponding results obtained in the cases of birch, Douglas-fir and spruce. In order to keep in close touch with the reality of the experimental cases and further to re-use these numerical simulation results when comparing them to the experimental results (see step 3), the values of the simulation parameters (rotation speed, s, flux density, q and sample MC) and green log thermal parameters (thermal conductivity, λ, and specific heat capacity, ρc) were the same as those employed in the physical experiments (Table 1).
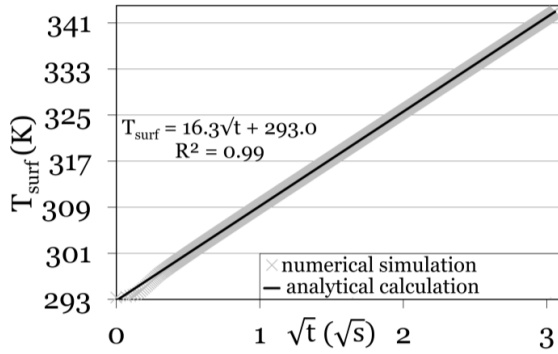
	$R^2(*)$	α_{surf}^{simul}	α_{surf}^{anal}
Beech	0.99	16.3	16.3
Birch	1	15.4	15.4
Douglas-fir	1	24.4	24.3
Spruce	0.99	19.6	19.5

(*) calculated on 80 values

Figure 3 Comparison of Finite Element simulated surface temperatures of rotating log and analytically calculated surface temperature response of half space. The temperatures are represented as a function of the square root of time for beech. Table: Comparison of numerical and analytical values of the slopes α_{surf}^{simul} and α_{surf}^{anal} of $T_{surf} = f(\sqrt{t})$ with their corresponding coefficients of determination, R^2, in the case of beech, birch, Douglas-fir and spruce

Parameters	Values	
Rotating speed s	0.0032 m.s^{-1}	
Density of flux q	10 000 W.m^{-2}	
	Beech	**Birch**
Moisture Content MC (%)	43	85
Thermal conductivity λ (W.m^{-1}.K^{-1})	0.30 (0.003MC+0.172) (1)	0.45 (0.003MC+0.191) (1)
Heat capacity ρc (J.m^{-3}.K^{-1})	1.6E+06 (0.019MC+0.746)+06 (1)	1.2E+06 (0.021MC+0.577)+06 (1)
	Douglas-fir	**Spruce**
Moisture Content MC (%)	115	55
Thermal conductivity λ (W.m^{-1}.K^{-1})	0.23 (1)	0.24 (0.002MC+0.130) (1)
Heat capacity ρc (J.m^{-3}.K^{-1})	9.4E+05 (1)	1.4E+06 (0.032MC-0.311)+06 (1)

(1) Dupleix et al. 2012d

Table 1 Thermophysical parameters and their corresponding values used in numerical and analytical simulations

From the results presented in Fig.3, two conclusions can be drawn. Firstly, the linearity of the relationship $T_{surf} = f(\sqrt{t})$, confirmed by the high coefficients of determination, validates the assumption that the log can be treated as a semi-infinite body with a step increase in surface temperature of a half-space. Secondly, for the four species, the near equivalence of α_{surf}^{simul} (calculated by linear regression analysis of numerical simulation curves) and $\alpha_{surf}^{anal} = \dfrac{2\,q}{\sqrt{\pi}\sqrt{\lambda\rho c}}$ (calculated with the simulation parameters) confirms the suitability of a 1D analytical equation in Cartesian coordinates (Eq.6) to be used to evaluate the surface temperature increase of a green rotating log under external IR heating. The slight difference between α_{surf}^{simul} and α_{surf}^{anal} in the case of spruce and Douglas-fir can be explained by the lack of linearity at the beginning of the curve (which is also visible in the other species) due to a perturbation at the early stages attributable to the numerical simulation.

Determining the effective flux density, q, received by the sample (step 2)

From the results above, that confirm the 1D semi-infinite behaviour of a half space of the wood bolt, it is easy to estimate the effective flux density, q, received by the sample by the inverse method of deconvolution proposed by Beck et al. (1985). This method uses the recorded surface temperature data, T_{surf}, to recover the signal q as it existed before it has been convolved by the impulse response of the half-space. The result of the deconvolution gives the maximum value (found to be around 10 000 W.m^{-2}) of the estimated heat flux density, q_{est}.

It is possible to check the reliability of the deconvolution by measuring the spatial profile of the incident radiative heat flux received by the sample surface, q_{mes}, which corresponds directly to the electric signal produced by an IR sensitive sensor placed on the sample surface. For one sample, Fig.4

compares the normalised values of the estimated heat flux density, q_{est}, with the measured IR sensor signal (which is proportional to the received heat flux density, q_{mes}) and shows a reliable agreement between estimation and measurement. This comparison provides further confirmation (with the results presented in the first paragraph) of the ability of analytical equations (Eqs.6, 7 and 8) to describe the temperature increase in a green log rotating under external IR heating. Fig.4 shows the spatial profile of the effective real flux density received by the sample which is necessary data for input into the model in order to compare the simulation to the experimental results.
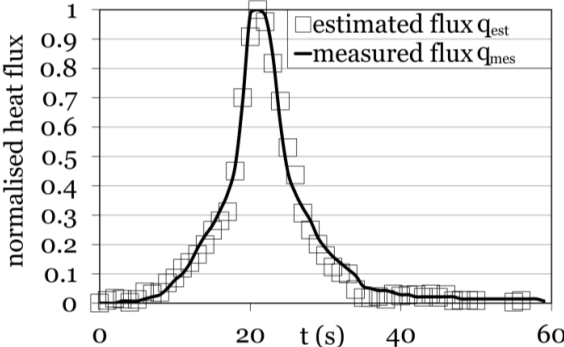

Figure 4 Comparison of the estimated heat flux density and the measured IR sensor signal on one sample surface (normalised values are represented)

Comparison of experimental and numerical simulation results (step 3)

In Figs.5 to 7, the residuals are calculated with the difference between experimental and modelled results and are plotted below each graph. Fig.5a compares the surface temperatures $T_{surf} = f(t)$ of beech at 43% MC, obtained experimentally from surface thermocouples, with the numerical simulation results modelled using similar parameters (Table 1).
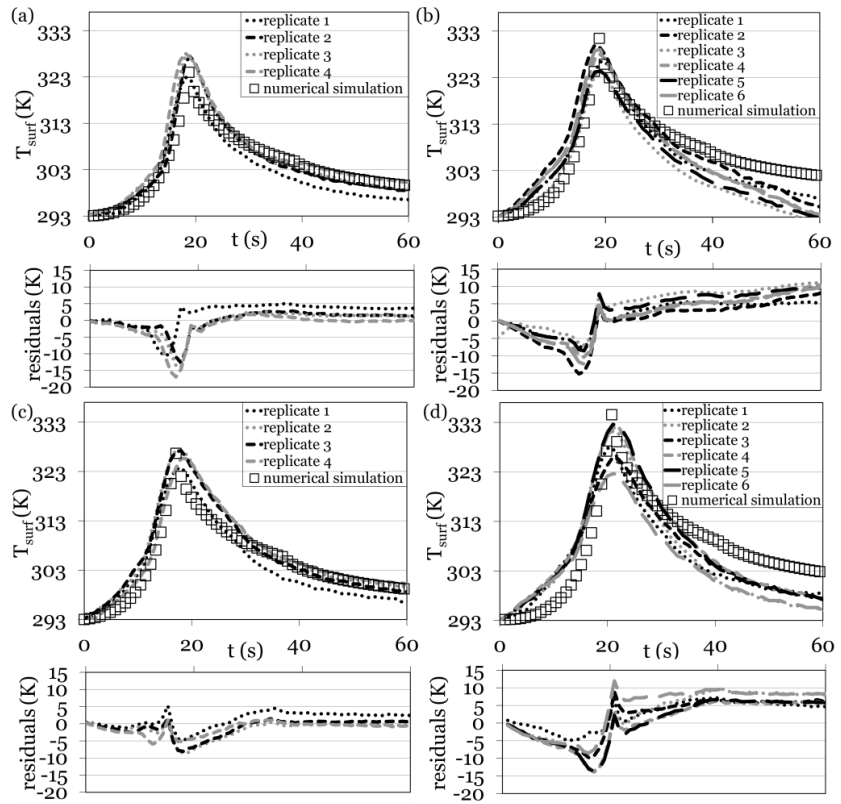
Figure 5 Comparison of numerical simulation curves of surface temperatures $T_{surf} = f(t)$ to experimental results obtained on different replicates of (a) beech at 43% MC, (b) birch at 85% MC, (c) Douglas-fir at 115% MC and (d) spruce at 55% MC (residuals are plotted below each graph)

Similar results were also obtained for birch at 85% MC (Fig.5b), Douglas-fir at 115% MC (Fig.5c) and spruce at 55% MC (Fig.5d). In the 20 first seconds, the increasing slopes of the experimental curves are steeper than simulated (the residuals drop consequently below 0). This difference might be explained by some eventual moisture gradient within the wood created when drying and responsible for heterogeneities in the thermal properties of wood which are impossible to evaluate accurately and to implement in the model. Moreover variations in the surface emissivities of different wood samples can lead to some errors in the heat flux received by the samples.

But apart from this difference, these results show a reliable agreement between the numerical estimation and measurement (as can be seen by residuals which balance around 0).

For several replicates of birch at 85% MC (Fig.6a), beech at 43% MC (Fig. 7a), Douglas-fir at 115% MC (Fig. 6b) and spruce at 55% MC (Fig.7b) compare temperatures T_{3mm} = f(t) obtained experimentally from the thermocouples embedded 3mm below the wood surface, with numerical simulation results modelled using similar parameters (Table 1). These results show good agreement between numerical estimation and measurement with low residuals relatively close to 0. However, around the maximum temperature, the residuals increase: the difficulty of fitting the numerical simulation to the experimental data may arise from three side-effects: (1) the imprecise insertion depth of the thermocouples; the margin of error in the insertion depth of the thermocouples was estimated to be ±0.5mm, which clearly might have had an effect, (2) the effect of drying during heating; the difference in the block moisture content before and after heating, ΔMC_S, remained low (never exceeding 5%), however, even though it could not be reliably measured, this change was attributed to water evaporating from the surface layers of the samples, (3) the influence of sawing; the differences in densities (and thus in thermal properties) between earlywood and latewood may have a greater influence in quarter sawn samples where annual rings are parallel to the IR flux. In order to take the effect of drying on thermal properties of wood into account, it is possible to estimate to 50% the margin of error on the MC.
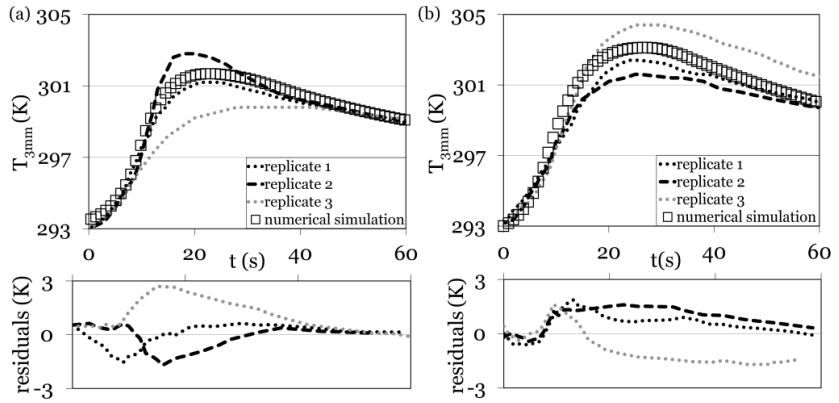
Figure 6 Comparison of numerical simulation curves of temperatures measured at 3 mm depth T_{3mm} = f(t) to experimental results obtained on different replicates of (a) birch at 85% MC, (b) Douglas-fir at 115% MC (residuals are plotted below each graph)
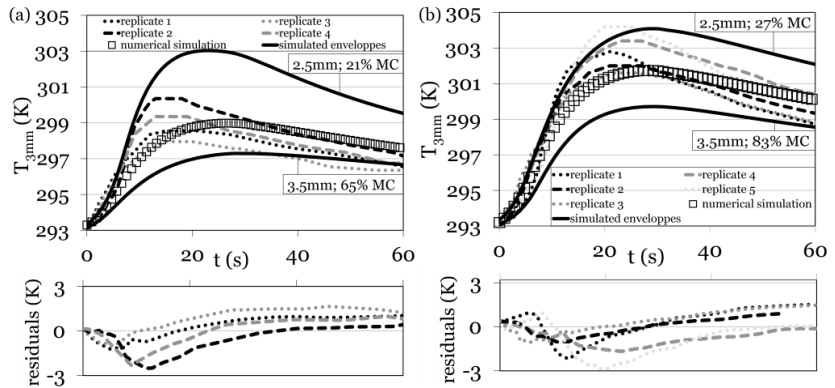

Figure 7 Comparison of experimental results measured at a depth of 3 mm with numerical simulation curves of temperatures T_{3mm} = f(t) and their envelopes $T_{3\pm0.5mm}$ = f(t) (dotted lines) obtained on different replicates of (a) beech at 43±22% MC, (b) spruce at 55±28% MC (residuals are plotted below each graph)

Assuming both effects (1) and (2), Fig.7 plots the envelope curves (in dotted lines) of temperatures below the wood surface, T_{3mm} = f(t), simulated numerically in the most favourable case, where both insertion depth and MC are underestimated (Fig.7a plots $T_{2.5mm}$ =f(t) at 21% MC and $T_{3.5mm}$ = f(t) at 65% MC for birch) and in the least favourable case when insertion depth and MC are overestimated (Fig.7b plots $T_{2.5mm}$ = f(t) at 27% MC and

$T_{3.5mm}$ = f(t) at 83% MC for spruce). When plotting these envelope curves, the effect of drying (2) dominates over the effect of the imprecise insertion of the thermocouples (1). The envelope curves surround all the experimental curves, which demonstrate that taking into account these two effects is more representative of the reality of the experiments.

Conclusion

By comparing experimental to numerical simulation results, this paper validates the ability of the numerical model developed by Dupleix et al. (2012a), using finite elements to simulate in 2D, heat transfer within a log and to output the temporal evolution of surface and below surface temperatures. During this validation process, it has been demonstrated that simple analytical equations, that assume the behaviour to be that of a semi-infinite body in 1D Cartesian coordinates, can estimate the heating rates and the maximum temperatures achievable at the surface and below the surface (Eqs. 6 and 7). With both methods, the inputs are the thermal and physical properties of green wood and the heat flux density of the infrared source. With the analytical equations provided in this article, it is possible to rapidly calculate the temperature at a certain depth below the surface and the maximum surface temperature reached by a green log with thermal characteristics, λ, and, ρc, rotating at a peeling speed, s, under an IR heating source (heat flux density q, width x).

Being able to calculate the temperature below the surface would be particularly useful in setting up the parameters for an IR heating system. This approach was developed in order to know, for a given peeling speed, s, the heating flux density, q, required to reach the 'minimum-optimum' heating temperature at the cutting plane - located several millimeters beneath the surface (Dupleix et al. 2012b). Conversely, for a given heat flux density, q, the temperature at a given depth can be used to determine the

appropriate peeling speed, s. Unfortunately, the heating rate that can be achieved is insufficient for most of today's industrial peeling speeds, but consideration should also be given to the fact that the use of an IR heating source obviates the need for lengthy soaking times and the associated infrastructure requirements, and so overall may be a worthwhile approach to log heating for veneer peeling.

Acknowledgements

References

Beck, J.V., St Clair, C.R., Blackwell, B. (1985) Inverse heat conduction. John Wiley and Sons Inc., New York

Bédard, N., Laganière, B. (2009) Debarking enhancement of frozen logs. Part II: infrared system for heating logs prior to debarking. *Forest Prod J, 59:25-30*.

Braham-Bouchnak, T., Germain, G., Morel, A., Lebrun, J.L. (2013) The influence of laser assistance on the machinability of the titanium alloy Ti555-3. *Int J Adv Manuf Tech, 68 (9-12):2471-2481*.

Cserta E., Hegedus G., Nemeth R. (2012) Evolution of temperature and moisture profiles of wood exposed to infrared radiation. *Bioresources, 7(4):5304-5311*.

Coste N., De Bevy T. (2005) Interest of radiant energy for wood peeling and slicing process. Master's thesis, Arts et Metiers ParisTech.

Dupleix, A., Marchal, R., Bléron, L., Rossi, F., Hughes, M. (2011) On-line heating temperatures of green-wood prior to peeling. *Joint International*

Symposium on Wood Composites and Veneer Processing and Products Proceedings.

Dupleix, A., Ahmedou, S.A.O., Bléron, L., Rossi, F., Hughes, M. (2012a) Rational production of veneer by IR-heating of green wood during peeling: Modeling experiments. *Holzforschung, 67(1):53-58, DOI 10.1515/hf-2012-0005.*

Dupleix, A., Denaud, L., Bléron, L., Marchal, R., Hughes, M. (2012b) The effect of log heating temperature on the peeling process and veneer quality: beech, birch and spruce case studies. *Eur J Wood Prod, 71(2):163-171, DOI 10.1007/s00107-012-0656-1.*

Dupleix, A., De Sousa Meneses, D., Hughes, M., Marchal, R. (2012c) Mid infrared absorption properties of green wood. *Wood Sci Technol, DOI 10.1007/s00226-013-0572-5.*

Dupleix, A., Kusiak, A., Hughes, M., Rossi, F. (2012d) Measuring the thermal properties of green wood by the transient plane source (TPS) technique. *Holzforschung, 67(4): 437-445, DOI 10.1515/hf-2012-0125*

Grimhall, C.G., Hoel, O. (1983) Method of slicing veneer *U.S. Patent No. 4,516,614. Filed June 3, 1983, and issued May 14, 1985.*

Marchal, R., Gaudillière, C., Collet, R. (2004) Technical feasibility of an embedded wood heating device on the slicer or the peeling lathe. *1st International Symposium Veneer Processing and Products Proceedings, 29-44*

Makoviny, I., Zemiar, J. (2004) Heating of wood surface layers by infrared and microwave radiation. *Wood research, 49(4):33-40.*

Rahman Rashid, R.A., Sun S., Wang G., Dargusch M.S. (2012) The effect of laser power on the machinability of the Ti-6Cr-5Mo-5V-4Al beta titanium alloy during laser assisted machining. *Int J Mach Tool Manu, 63:41-43.*

Suleiman, B.M., Larfeldt, J., Leckner, B., Gustavsson, M. (1999) Thermal conductivity and diffusivity of wood. *Wood Sci Technol, 33:465-473.*

Taler, J., Duda P. (2006) Solving direct and inverse heat conduction problems. Springer, Berlin

FAISABILITÉ DU DÉROULAGE DU BOIS ASSISTÉ PAR INFRAROUGE

RESUME : Le déroulage permet de transformer un billon en un ruban continu de bois vert (de 0.6 à plus de 3 mm d'épaisseur) appelé 'placage' dont la production joue un rôle important dans l'industrie du bois. Pour certaines essences, ce procédé exige un prétraitement, appelé « étuvage » qui consiste à chauffer au préalable le bois vert (saturé en eau) par immersion dans l'eau ou dans la vapeur d'eau chaude (de 30 à 90°C) afin de lui conférer une déformabilité remarquable et faciliter la coupe. Cette pratique présente cependant de nombreux inconvénients industriels et environnementaux. L'objectif de cette étude est de développer une innovation majeure pour les industries du déroulage et du tranchage, visant à remplacer les pratiques d'étuvage par une technologie de chauffe par rayonnement infrarouge embarquée sur les machines de production.

Mots clés : bois vert, bouleau, chauffe, déroulage, Douglas; épicéa, hêtre, infrarouge.

FEASIBILITY OF WOOD PEELING ASSISTED BY INFRARED

ABSTRACT: In the wood-products industry "peeling" is the process of converting a log into a continuous thin ribbon of green wood (from 0.6 to more than 3 mm thickness) termed "veneer". Veneers are mainly used for manufacturing light weight packaging and Engineer Wood Products (EWP) such as plywood, Laminated Veneer Lumber (LVL) and Parallel Strand Lumbers (PSL). These three latter EWPs manufactured from veneers glued and pressed together, are amongst the most used wood products. That is the reason why the production of veneer plays an important role in the wood-products industry. For certain species, the peeling process requires the prior heating of round green-wood to temperatures ranging from 30 to 90°C. This treatment is necessary to increase wood deformability, to reduce the severity of lathe checking in the veneers and to reduce cutting forces. It is usually done by immersion in hot water or by steam treatment. However it has many disadvantages amongst which are the duration of treatment (12 to 72 hours), the washing out of polyphenolic extractives - which causes water pollution and can affect wood's natural durability - low yield and energy losses. The goal of this PhD thesis was to develop a heating system embedded on the peeling lathe to circumvent many of these disadvantages. Infrared technology appears to be the most promising solution because of the ease of integration into the peeling process and of the power it offers, enabling the required heating temperatures to be achieved quickly and follow the highly demanding peeling speeds in use in the industry (from 1 to 5 m.s^{-1}). This new technology, using radiant energy to heat green-wood prior to peeling, would be a major innovation for the industries involved in the production of plywood, Laminated Veneer Lumber (LVL), etc.

Keywords : beech; birch, Douglas-fir, green wood, heating, infrared, peeling, spruce.

Aalto University
School of Chemical
Technology

ARTS ET MÉTIERS
ParisTech

ParisTech
INSTITUT DES SCIENCES ET TECHNOLOGIES
PARIS INSTITUTE OF TECHNOLOGY